Bone Morphogenetic Protein Receptor Mutation and Heritable Pulmonary Arterial Hypertension

By

Andrea Lee Frump

Dissertation

Submitted to the Faculty of the

Graduate School of Vanderbilt University

in partial fulfillment of the requirements

for the degree of

DOCTOR OF PHILOSOPHY

In

Cell and Developmental Biology

May, 2014

Nashville, Tennessee

Approved:

Christopher Wright, Ph.D.

Kevin Ess, M.D., Ph.D.

Scott Baldwin, M.D.

Maureen Gannon, Ph.D.

Mark de Caestecker, M.B., B.S., Ph.D.

To my family, friends, labmates, and mentors. This journey has been long.

I never would have made it to the end without your support.

ACKNOWLEDGEMENTS

This research was supported by the NIH/NIHLBI grants HL093057 and HL095797. I am especially grateful to the offices of the Vanderbilt University School of Medicine Division of Nephrology and the Department of Cell and Developmental Biology for their help, and for the Vanderbilt University Graduate School for giving me the opportunity to finish my degree.

I am grateful to Dr. Rekha Patel and Indhira Handy for introducing me to the world of research, to Dr. Josiane Eid for beginning my training, and especially to Dr. Mark de Caestecker for taking me in as a stray graduate student and giving me the chance to finish my Ph.D. I wouldn't be who I am today as a scientist or as a person without his mentorship. I would like to thank my friends and colleagues in the Pulmonary Hypertension research group at Vanderbilt, for providing patient samples, reagents, expertise, advice, or just being there to bounce ideas off of. I'd like to thank Dr. Kevin Ess and Dr. Aaron Bowman and their labs for their help, time, reagents, and general hand-holding while I tried to generate iPS cells. I'd like to thank my labmates, who have been amazing friends, and a great support system to my many freakouts.

Most importantly, I'd like to thank my family, who have never understood what I'm doing, but supported me anyway. Who have only wanted the best for me. Whose love and guidance are why I am who I am, and who I want to be. I never would have persevered without you in my corner.

TABLE OF CONTENTS

Page

LIST OF TABLES

LIST OF FIGURES

LIST OF ABBREVIATIONS

BMPR2	Bone morphogenetic protein receptor 2
HPAH	Heritable pulmonary arterial hypertension
BMP	Bone morphogenetic protein
NMD	nonsense mediated mRNA decay
4-PBA	sodium phenylbutyrate
TUDCA	sodium taurourdeoxycholic acid
PEC	pulmonary endothelial cell
ciPEC	conditionally immortalized endothelial cell
ER	endoplasmic reticulum
PH	pulmonary hypertension
FBS	fetal bovine serum
EGM-2MV	endothelial growth media
PBS	phosphate buffered saline
TBST	Tris-buffered Saline and Tween-20
LB	lysis buffer
EBM-2	endothelial basal media
BSA	bovine serum albumin
α-SMA	alpha-Smooth muscle actin
ANOVA	analysis of variance
Bp	base pair
DAPI	4.6-diamindino-2-phenylindole
PCNA	proliferating cell nuclear antigen

eNOS	endothelial nitric oxide synthase
Id1	inhibitor of differentiation1
iPSc	induced pluripotent stem cells
kDa	kilodaltons
NO	nitric oxide
PAH	pulmonary arterial hypertension
RV	right ventricle
RVSP	right ventricle systolic pressure
SEM	standard error of mean
VEGR2	vascular endothelial growth receptor 2
VSMC	vascular smooth muscle cell
mPAP	mean pulmonary arterial pressure

CHAPTER I

INTRODUCTION

Part I. Pulmonary Hypertension

Definition of Pulmonary Hypertension

Pulmonary hypertension (PH) is most simply defined as an increase in mean pulmonary artery pressure (mPAP) greater than or equal to 25 mm Hg at rest using right heart catheterization. Resting mPAPs in heritable pulmonary arterial hypertension (HPAH) patients with *BMPR2* mutations, can be as high as 61 mm Hg compared to 56 mm Hg in pulmonary arterial hypertension (PAH) patients without *BMPR2* mutation [1,2]. This is in contrast to a normal mPAP, which is defined as 14 +/- 3.3 mm Hg at rest with the upper most mPAP that is still considered clinically normal at 20.6 mm Hg [3,4]. Interestingly, patients with mPAPs that are between 21-24 mm Hg remain undefined clinically [3].

Previously, a mPAP of greater than 30 mm Hg during exercise has been used to help diagnose patients with PH. However, it has been increasingly shown that clinically normal patients can also reach mPAPs of greater than 30 mm Hg during exercise. Because of this, meausurement of mPAP during exercise is no longer as widely accepted as a clinical assessment of PH [3-5].

Table 1.WHO Current Clinical Classification of Pulmonary Hypertension Adapted from [6]

Group 1. Pulmonary arterial hypertension
- 1.1 Idiopathic pulmonary arterial hypertension
- 1.2 Heritable pulmonary arterial hypertension
  - 1.2.1 *BMPR2*
  - 1.2.2 *ALK1, Endoglin*
  - 1.2.3 Unknown
- 1.3 Drug and toxin-induced pulmonary arterial hypertension
- 1.4 Associated with
  - 1.4.1 Connective tissue diseases
  - 1.4.2 HIV infection
  - 1.4.3 Portal hypertension
  - 1.4.4 Congenital heart diseases
  - 1.4.5 Schistosomiasis
  - 1.4.6 Chronic hemolytic anemia
- 1.5 Persistent Pulmonary Hypertension of the newborn
- 1' Pulmonary veno-occulusive disease and/or pulmonary capillary hemangiomatosis

Group 2. Pulmonary Hypertension as a result of left heart diseases
- 2.1 Systolic dysfunction
- 2.2 Diastolic dysfunction
- 2.3 Valvular disease

Group 3. Pulmonary Hypertension associated with lung diseases and/or hypoxia
- 3.1 Chronic obstructive pulmonary disease
- 3.2 Interstitial lung disease
- 3.3 Other pulmonary diseases with mixed restrictive and obstructive pattern
- 3.4 Sleep-disordered breathing
- 3.5 Aveolar hypoventilation disorders
- 3.6 Chronic exposure to high altitude
- 3.7 Developmental abnormalities

Group 4. Chronic thromboembolic pulmonary hypertension (CTEPH)

Group 5. Pulmonary hypertension with unclear multifactorial mechanisms
- 5.1 Hematologic disorders
- 5.2 Systemic disorders
- 5.3 Metabolic disorders
- 5.4 Others: tumor obstruction, chronic renal failure

More recently, measurements of pulmonary vascular resistance (PVR), cardiac output (CO), and pulmonary wedge pressure (PWP) have been used in combination as a way to hemodynamically assess patients with PH. PWP in particular has been used to classify patients with pre-capillary PH (PWP less than or equal to 15 mm Hg) or post-capillary PH (PWP greater than 15 mm Hg). This provides a way to distinguish between clinical groups of patients; those patients with pre-capillary PH fall within clinical groups 1, 3, 4, and 5. Patients with post-capillary PH fall within clinical group 2 (PH due to left heart disease) [3,6].

Classification of Pulmonary Hypertension

The first classification system for PH was developed in 1973 and had only two groups; patients could be categorized with prim-ary or secondary PH [3,7]. The current World Health Organization (WHO) classification system, developed in 2008, incorporates current research and clinical assessment. Patients can be categorized into one of five groups, and further classified into subgroups based on hemodynamics, similar disease pathogenesis and characteristics, and response to therapeutics (Table 1)[3,6].

Group 1 of the classification system is comprised of patients that develop pulmonary arterial hypertension (PAH) and include multiple causalities of PAH ranging from sporadic cases to disease-associated cases. It is important to note that PAH is distinct from other forms of PH, and is a group in the classification system for PH. It consists of idiopathic and heritable pulmonary arterial hypertension, drug-induced pulmonary hypertension (most notably the diet drug fenfluramine) [8,9], connective tissue disease-associated hypertension [10-13], pulmonary hypertension of newborns [14], and pulmonary hypertension associated with pulmonary veno-occlusive disease [15] [3,6].

Of interest, idiopathic pulmonary arterial hypertension (IPAH), which is defined as sporadic pulmonary hypertension occurring in patients with no family history or identified risk factors, occurs at an incidence of 2-3 new cases per million people a year [3,6,16]. The heritable pulmonary arterial hypertension (HPAH) subgroup includes germline mutations in genes *BMPR2*, *ACVRL1*, *CAV1*, or *ENDOGLIN* in patients with or without a family history [6,17-19]. Interestingly, germline mutations in *BMPR2* occur in 10-40% of all new incidences of pulmonary arterial hypertension [17,20]. Additionally, the HPAH group includes patients with a family history but no identified germline mutation. Together, IPAH and HPAH account for roughly 1500 new cases a year in the USA [21]. In contrast, the remaining PAH patients account for 3000 new cases a year [6,21].

Group 2 of the PH classification system are made up of patients with left heart disease (systolic, diastolic dysfunction or valvular disease). This group develops PH due to increased left atrial pressure. This increase in pressure in the atrium leads to a backward transmission of pressure causing a gradual increase in pulmonary arterial pressure, increase in vascular tone, and remodeling [22]. Patients have a PWP of greater than 15 mm Hg, making this form of PH post-capillary in contrast to every other group. This group makes up the majority of cases of PH, however treatment options are limited, and currently the efficacy of PAH treatments on this population of PH patients is unknown [3,6].

Group 3 develop PH due to lung diseases and/or hypoxia. The most dominant cause of PH in this group is due to COPD but its prevalence is largely unknown [23,24]. Patients classified in Group 4 develop chronic thromboembolic PH. On average, 4% of patients with an acute pulmonary embolism develop PH [25]. Group 5 consists of patients that develop PH from unclear or multifactorial mechanisms. This includes patients that develop PH after hematologic

disorders, systemic disorders, metabolic disorders, thyroid disorders, and other causes including chronic renal failure [26-30].

Pathobiology of Pulmonary Hypertension

Patients with PH have progressive obliteration of small pulmonary arteries, abnormal vasoreactivity, right ventricle hypertrophy and eventual right heart failure (cor pulmonale) [3,31]. PH is characterized by remodeling of the distal pulmonary arteries, intimal thickening, proliferation of vascular smooth muscle cells and apoptosis-resistance pulmonary artery endothelial cells, increased fibrosis, and in the most severe cases the formation of plexiform lesions which are a unique feature to severe PH and are complex lesions containing capillary-like channels [32-34].

Incidence and treatment

There are 2.4-7.6 new cases of HPAH (the focus of this dissertation) per million people annually [35]. Although rare, current available therapies are largely ineffective, resulting in a 5 year survival rate of just 60% in patients with PAH and just 48% in patients with HPAH [36]. The most common treatment for PH, including patients with PAH, is currently prostacyclin (epoprostenol), a vasodilator. PH patients receiving prostacylins have an 84% 2 year survival rate [37]. Calcium channel-blockers are also used. Calcium channel-blockers inhibit calcium influx into smooth muscle cells leading to vasodilation of the pulmonary vasculature. Calcium channel blockers have been shown to improve 5 year survival to 97%. However, only a subset of PH patients responds to vasodilator therapy, and in PAH just 10% of IPAH patients and even fewer HPAH patients are responsive [2,38]. Endothelin receptor antagonists, which function by inhibiting the vasoconstrictive activity of Endothelin-1 [39], and Phosphodiesterase-5 inhibitors,

which inhibit the degradation of cGMP (activated in response to vasodilator Nitric Oxide) by Phosphodiesterase-5 leading to vasodilation of the pulmonary vasculature [40], are

also currently used with 91% and 72% 2 year survival rates respectively [41]. Although current therapies target vasodilatory pathways to improve quality of life, they do not reverse vascular remodeling and do not help maintain normal hemodynamics in the long term.

Heritable Pulmonary Arterial Hypertension and BMPR2 mutations

Mutations in the *BMPR2* receptor have been identified in 70% of HPAH patients, including 10% of patients who have had no prior family history of PAH [20,42,43]. There is also evidence of BMPR2 dysregulation as a contributor to other forms of PH [44,45]. Patients with a mutation in *BMPR2* clinically present symptoms on average 10 years earlier than PAH patients without mutation, have more severe hemodynamics, mortality at an earlier age [1,17], and are less likely to respond to vasodilator therapy [1,2]. To date, over 200 different *BMPR2* mutations have been identified in HPAH patients [31,45-47], and the exact role of *BMPR2* mutation in disease pathogenesis is an area of active investigation. This dissertation investigates the role of *BMPR2* mutation type and its effect on experimental PH.

Part II. Signaling and function of the BMPR2 receptor

The Bone Morphogenetic Protein (BMP) family

BMPs make up the largest subset of the TGF-β superfamily of proteins, which in addition to BMPs include Growth differentiation factors (GDFs), activins, and nodal (reviewed in [48-

51]). They were first identified by, and subsequently named for inducing the ectopic bone formation [52]. Members of the TGF-β family are grouped due to similarities in structure, receptor binding, and signaling function. Members of this superfamily control a diverse range of developmental and cellular processes including embryonic patterning, formation of the mesoderm, development of the kidney, lung, heart, amnion, eye, lung, and in embryonic and adult stem cell self-renewal and differentiation pathways, to name a few [53-56]. Currently, there are 15 identified mammalian BMP ligands that bind and signal through two distinct types of receptors. Type I receptors include Activin-like kinase (Alk) 1,2,3,and 6. Type II receptors include BMPR2, Activin like kinase receptor 2 (ActR2A) and ActR2B [50,55].

BMP receptor structure and signaling complex formation

Type I and Type II BMP receptors are made up of an extracellular domain containing the ligand binding domain, a single pass transmembrane domain, and an intracellular kinase domain. Both types of receptors are serine/threonine kinases, however the Type II receptors are constitutively active while the Type I receptors are inhibited due to the interaction of repressor protein FKBP12, which prevents phosphorylation of the G/S box, a glycine/serine rich region unique to Type I receptors [48,57,58]. Of note, the BMPR2 receptor has an additional 530 amino acid cytoplasmic tail that is unique among other receptor family members [59].

To initiate signaling responses, BMP ligand binds preferentially to Type I receptors, which in turn recruits Type II receptors to form a hetero-tetrameric complex [60,61]. BMPs 5-8 are exceptions to this, these ligands preferentially bind to the Type II receptor and subsequently recruit the Type I receptor to the complex [49]. Once in proximity to the Type I receptor, the Type II receptor is able to initiate a conformational change in the Type I receptor leading to the

dissociation of the repressor protein FKBP12 from the G/S box, and then phosphorylate the Type I receptor and initiate downstream signaling pathways. Signaling through the Smad pathway has been identified as the canonical BMP-mediated pathway. Once activated by phosphorylation of the c-terminus by the Type I receptor, regulatory Smads, Smad 1, Smad 5, and Smad 8, with the aid of co-Smad 4, translocate to the nucleus where they regulate transcription of target genes. Inhibitory Smads 6 and Smad 7 regulate the amount and duration of signal of the regulatory Smads.

Non-canonical signaling responses ERK1/2, p38MAPK, JNK, PI3K, and Rho kinase have also been shown to be activated in response to BMP stimulation [62]. Type I and Type II receptors have distinct binding affinities for different BMP ligands, however receptors and ligands are promiscuous and are able to activate downstream signaling responses after stimulation from different combinations of ligand and receptor (Table 2)[51].

Complexes between Type I and particularly Type II receptors are able to form in the absence of BMP ligand, however stimulation with BMP results in a 2-3 fold increase in complex formation. There is increasing evidence that the preformed complexes preferentially activate canonical signaling pathways while the BMP-mediated receptor complexes preferentially stimulate noncanonical pathways [60,61].

Although the heteromeric complex formation between Type I and Type II receptors is necessary and sufficient to induce downstream canonical and non-canonical signaling pathways, a number of co-receptors have been identified to further modulate BMP signaling responses. These co-receptors, including Endoglin, TGFβR3, RGMa, DRAGON, and Bambi, have been

Table 2. Known BMP ligand and BMP receptor interactions, adapted from [51]

Ligand	Type I Receptor	Type II Receptor	Reference
Bmp2	Alk3, Alk6	Bmpr2, Actr2, Actr2B	[63,64]
Bmp4	Alk3, Alk6	Bmpr2, Actr2, Actr2B	[63-65]
Bmp6	Alk2, Alk3, Alk6	Bmpr2, Actr2, Actr2B	[66]
Bmp7	Alk2, Alk3, Alk6	Bmpr2, Actr2	[65,67]
Bmp9	Alk1, Alk2	Bmpr2, Actr2, Actr2B	[68,69]
Bmp10	Alk1, Alk3, Alk6	Bmpr2	[69]
Gdf5	Alk3, Alk6	Bmpr2	[70,71]
Gdf6	Alk3, Alk6	Bmpr2, Actr2B	[71]
Gdf9	Alk3, Alk6	Bmpr2, Actr2	[72]
Gdf9B	Alk6	Bmpr2	[73]

shown to regulate BMP receptor-ligand interactions providing another level of regulation to the BMP-signaling response [48,50].

BMP signaling and vascular disease

In addition to the identification of *BMPR2* mutants, mutations in other BMP signaling pathway proteins including *Endoglin*, *ALK1*, *SMAD4* and *8* have been identified in HPAH patients without *BMPR2* mutations [51,74,75]. Additionally, these proteins have been implicated in other vascular diseases. Over 80% of patients with Hereditary Hemorrhagic Telangiectasia (HTT), characterized by arteriovenous malformations, have mutations in *ALK1* or *ENG*. A small percentage of HHT patients may have mutations in *SMAD4*. Interestingly, HHT patients may develop PAH in addition to HTT [51,76,77].

BMPR2 signaling responses in HPAH

BMP signaling in the pulmonary vasculature is cell-type and ligand dependent [2,51,78]. Expression of BMP receptors and ligands is tightly regulated by the pulmonary vasculature (Table 3) [51,79]. However, the pulmonary vasculature is made up of a heterogenic population of cells, even amongst cells of the same type-for example endothelial cells, therefore, it is not uncommon to observe opposing signaling responses in the same cell type in distinct regions of the pulmonary vasculature [80,81]. This is likely due to the different developmental origins of the endothelium making up the macro-and micro pulmonary vasculature. The macro-vascular endothelium (greater than 100 μm) is developed through angiogenesis of the pulmonary truncus, whereas the endothelium comprising the pulmonary micro-vasculature is developed *via* vasculogenesis of blood islands [82,83]. The different developmental origin of the macro- and micro-pulmonary vascular endothelium causes distinct expression and phenotypic differences

Table 3. Expression of BMP signaling components in the human pulmonary vasculature modified from RT-PCR data [84]

BMP family member	Human pulmonary artery endothelial cells	Human vascular smooth muscle cells
BMP Type I receptors	ALK1, ALK2, ALK5, ALK6	ALK2, ALK3, ALK5, ALK6
BMP Type II receptors	ACTR2, ACTR2B, BMPR2	ACTR2, ACTR2B, BMPR2
BMP ligands	BMP2	BMP2
BMP co-receptor	ENDOGLIN, BETAGLYCAN	ENDOGLIN, BETAGLYCAN
SMAD	SMAD1, SMAD2, SMAD3, SMAD4, SMAD5	SMAD1, SMAD2, SMAD3, SMAD4, SMAD5
TGF-β	TβR-II, TGF-β1	TβR-II, TGF-β1

between regions of the pulmonary vasculature. The heterogeneity of the endothelium comprising the pulmonary vasculature leads to different integration of signaling pathways, including the BMP pathway, in response to stimuli. For example, BMPs are pro-apoptotic in smooth muscle cells from the main artery, but are pro-proliferative in smooth muscle cells from more distal arteries [85-87]. In general, studies have shown BMP2, BMP4, BMP6, and BMP7 are largely expressed by the pulmonary vasculature and play a variety of cell-type dependent functions including vascular homeostasis, regulation of vasoreactivity, and endothelial cell function [80,81,88].

BMPR2 is predominately expressed in the pulmonary endothelium, but to a lesser extent is also expressed in vascular smooth muscle cells [44,89]. BMP2 and BMP4 stimulate phosphorylation of eNOS in pulmonary artery endothelial cells (PAECs) which lead to endothelial cell migration via BMPR2 and PKA dependent mechanisms [80,90]. Endothelial cell migration is necessary for the repair of pulmonary arteries in response to vascular injury. Lack of endothelial cell migration and initiation of repair pathways is thought to contribute to HPAH pathogenesis by exposing SMCs to growth factors and inflammatory proteins in the circulation, which could in turn contribute to the vascular remodeling observed in disease [91]. In fact in PAECs with *BMPR2* mutations, there is decreased phosphorylation of eNOS, providing a possible mechanism for vascular remodeling [90]. Additionally, BMP4 stimulates reactive oxygen species production in endothelial cells, and in some endothelial cell types, initiate apoptosis. BMPR2 expression in PAECs also induces the formation of a complex between PPARγ and β-catenin [92]. This protein complex upregulates the expression of apelin, which is required to modulate normal responses to vascular injury, resulting in another vascular injury

repair pathway that is impaired with the loss of expression and function of BMPR2 in HPAH [92].

BMPs are expressed in, and secreted by, endothelial cells. This in turn influences smooth muscle cell (SMC) function in the pulmonary vasculature. BMP2, 4, and 7 inhibit vascular SMC proliferation [44,81,85,93,94]. Additionally, BMP4 decreases the expression of anti-apoptotic protein Bcl-2, leading to increased apoptotic sensitivity in SMCs. In SMCs isolated from HPAH patients with mutations in *BMPR2*, BMP2 and BMP7 stimulation increased SMC proliferation [95]. SMCs isolated from patients with IPAH (no mutation in *BMPR2*) had decreased Smad1/5/8 activation and an increase in p38 activation[95]. Proliferation in these cells was inhibited by stimulation with BMP4. Overall levels of *BMPR2* expression were reduced in these cells isolated from IPAH and HPAH patients, but unlike the IPAH SMCs, SMCs isolated from HPAH patients did not have reduced proliferative responses due to BMP4 stimulation [95].

Increasingly, *in vivo* models have been used to determine the role of BMP signaling in vascular disease. Heterozygous Bmpr2 null mice, $Bmpr2^{+/-}$, have slightly elevated pulmonary vascular resistance and increased susceptibility to PH with the addition of chronic hypoxia + serotonin or inflammatory stress [96-98]. These mice do not display increased vascular remodeling in response to hypoxia [96]. Mice carrying an hpyomorphic allele, $Bmpr2^{\Delta Ex2/+}$, have increased susceptibility to chronic hypoxia PH [99]. $Bmpr^{2+/-}$ and $Bmpr2^{\Delta Ex2/+}$ mice have increased pulmonary vasoconstriction [98,99], but the $Bmpr2^{\Delta Ex2/+}$ mice also have defects in endothelial cell-dependent and independent vasodilation [99]. The $Bmpr2^{\Delta Ex2/+}$ mice also have reduced eNOS expression, suggesting defects in eNOS pathway are responsible for the endothelial cell-dependent vasodilatory defects [99]. Mice with an endothelial cell-specific

deletion of *Bmpr2* spontaneously develop PH in a subset of mice [100]. Interestingly, mice overexpressing a dominant negative Bmpr2 mutation in SMCs also develop spontaneous PH [101]. These studies show that Bmpr2 signaling influences both SMCs and ECs to help regulate vascular homeostasis.

Part III. *BMPR2* mutation type and experimental PH

BMPR2 mutation type and disease

50-80% of HPAH patients have a germline mutation in *BMPR2* [20,42,43]. Patients with a *BMPR2* mutation are less likely to react to vasodilator therapy, more likely to present clinical symptoms at a younger age, and have a shorter time to death or lung transplantation compared to IPAH patients without a *BMPR2* mutation [1,2,17]. Despite this, disease severity among patients with a *BMPR2* mutation is not uniform. Differences of penetrance, age of onset, and age of death vary widely between mutation carriers [102]. This is likely due in part to the large number of identified *BMPR2* mutations, over 200, and spread of mutations throughout the *BMPR2* gene [45-47,103]. It is likely the location of the *BMPR2* mutation affects the resulting protein production differently and leads to different phenotypic responses. 60% of *BMPR2* mutations are identified as nonsense, or frameshift mutations [45]. This type of mutation is degraded by the nonsense-mediated mRNA decay pathway (NMD) [104]. NMD is an RNA surveillance pathway that recognizes mutated RNA that would otherwise be translated into a potentially detrimental mutant protein (reviewed in [105]). *BMPR2* mutations that are positive for the NMD pathway (NMD+) are degraded and result in a haploinsufficient phenotype [104]. Conversely, 40% of identified *BMPR2* mutations are missense mutations, and are unlikely to be recognized

by the NMD machinery. The result from this type of mutation (NMD-) is likely the production of a mutant BMPR2 protein. Though not without controversy [106], clinical data indicates that HPAH patients with NMD- *BMPR2* mutations have more severe disease, a shorter time to lung transplant, and earlier age of diagnosis compared to patients with an NMD+ *BMPR2* mutation [104]. In Chapter II of this dissertation we utilize two different mouse models with germline *Bmpr2* mutations, one NMD+ and one NMD- and three experimental models of PH to determine if we could recapitulate the clinical data, that NMD- *Bmpr2* mutants have more severe PH, in vivo. We also attempt to characterize the impact of *Bmpr2* mutation type on the progression and severity of experimental PH. We demonstrate that NMD- mutants have a higher right ventricular systolic pressure (RVSP), have an increase in vascular obstructive lesions, and impaired phospho-eNOS signaling.

To further characterize the NMD- *Bmpr2* mutant, we wanted to determine if the predicted NMD- mutant protein product was endogenously expressed. To do this we isolated pulmonary endothelial cells (PECs) and used lymphocytes from an HPAH family expressing the same NMD- mutation in which *EXON2* is deleted. Once we were able to establish that the mutant Bmpr2ΔEx protein was expressed, we next wanted to determine if the mutant protein was able to reach the cell surface. We found that the NMD- product was mis-trafficked and retained in the endoplasmic reticulum and that PECs had impaird phospho-Smad1/5/8 signaling function and reduced expression of the Smad1/5/8 target gene, *Id1*. We show that trafficking to the cell surface and signaling function can be restored in the NMD- *Bmpr2* mutant with the addition of chemical chaperones 4-PBA and TUDCA, providing possible therapeutic application for certain types of mutations.

HPAH-patient cells are difficult to obtain, requiring a lung biopsy, are often of end-stage disease, and have limited capacity to propagate. In chapter 4 we establish several induced Pluripotent Stem Cell lines (iPSCs) from HPAH patient fibroblasts with known NMD+ and NMD- *BMPR2* mutations with the aim to further examine the link between NMD *BMPR2* mutation status and disease severity using HPAH patient-derived iPS cells that have been differentiated into endothelial cells. Additionally, we plan to expand our *in vitro* findings to other NMD- *BMPR2* mutations. We report preliminary findings with an endothelial differentiation protocol in control IPS cells. The creation of these lines would provide a source of patient-derived cells that could be utilized to dissect the role of BMPR2 mutation type and signaling function in endothelial and smooth muscle cells. The studies presented in chapter 4 are preliminary, and require further validation and characterization.

Collectively, these studies describe how *Bmpr2* mutations contribute to HPAH. We determine if different types of *BMPR2* mutation result in different phenotypic outcomes. We utilize in vivo and in vitro methods using mouse models and patient samples to try to characterize the function of NMD- and NMD+ mutations on the severity of experimental PH. We further evaluate the expression, localization, and signaling capacity of a *Bmpr2* NMD- mutation predicted to express a mutant protein in vivo. Together, our data show that NMD- and NMD+ *Bmpr2* mutations alter different signaling pathways and lead to experimental PH likely through different mechanisms.

CHAPTER II

EFFECT OF NMD STATUS IN *BMPR2* HETERZYGOUS MUTANTS IN CHRONIC HYPOXIA, SEROTONIN, AND SU5416 MODELS OF PH

Introduction

HPAH patients with mutations in *BMPR2* have more severe disease as characterized by decreased responsiveness to vasodilator drugs [1,2], younger age at diagnosis and worse hemodynamics [1,17], and shorter time to death or lung transplant [17] compared to PAH patients. Recently, two clinical groups published conflicting results from two different patient cohorts linking *BMPR2* mutation NMD status and severity of disease. The first group found patients with BMPR2 NMD- mutations (making up 40% of identified *BMPR2* mutations) had an increase in disease severity [104]. HPAH patients with NMD- *BMPR2* mutations had an even earlier age of onset compared to *BMPR2* NMD+ mutants and shorter time to lung transplant [104]. Conversely, the second group, using a different patient cohort, showed that there were no significant differences in disease severity between *BMPR2* mutation types.

Based on this controversy, we set out to characterize biologically how BMPR2 mutation status might affect disease severity. To do this we evaluated the effects of three different models of experimental PH (chronic hypoxia, serotonin + hypoxia, and VEGFR2 inhibitor SU5416 + hypoxia) on a mouse model of an NMD+ mutation ($Bmpr2^{+/-}$) and a mouse model of an NMD- mutation ($Bmpr2^{\Delta Ex2/+}$) to determine *in vitro* if we could reproduce the clinical data.

Studies from our laboratory have shown that mice carrying a heterozygous mutation at the *Bmpr2* locus, *Bmpr2*$^{\Delta Ex2/+}$, which is indistinguishable from the NMD- HPAH Family 108 mutation, described in chapter 3, develop more severe hypoxic PH [99]. This is in contrast to reported findings showing mice carrying a heterozygous null *Bmpr2*$^{+/-}$ mutation, similar to an NMD+ HPAH Family 20 mutation, which are only more slightly susceptible to hypoxic PH [96]. However, until recently direct assessment of the role of different *Bmpr2* mutation type in experimental PH was not possible, mainly owing to the fact that the *Bmpr2* mutant mice were on different genetic backgrounds [107,108].

Here we report, for the first time, a direct comparison between an NMD- *Bmpr2* mutation and an NMD+ *Bmpr2* mutation in three different models of experimental PH. We evaluated the effects on disease progression by assessing hemodynamic and molecular parameters and found that the NMD- *Bmpr2* mice (Bmpr2$^{\Delta Ex2/+}$) have basal signaling defects in phospho-eNOS, an increase in RVSP (the equivalent of mPAP in mice), and an increase in the number of obstructive vascular lesions. Taken together, these data show that NMD- and NMD+ *Bmpr2* mutations likely have different mechanisms of disease pathogenesis, likely due to the expression of a mutant *Bmpr2* protein product in the NMD- *Bmpr2* mutants and a haploinsufficient effect in the NMD+ *Bmpr2* mutants.

Materials and Methods

Ethics Statement

Mice used in studies were approved by the Vanderbilt University Institutional Animal Care and Use Committee (Dr. Ron Emeson, IACUC chair) under protocol number M/11/015 and

were adherent with the National Institutes of Health guidelines for care and use of laboratory animals under Vanderbilt animal welfare assurance licence number A3227-01.

Mouse lines

Bmpr2$^{\Delta Ex2/+}$ mice were described previously [108]. Studies were approved by the Vanderbilt University Institutional Animal Care and Use Committee (see above for ethics statement). Mice were backcrossed onto a C57Bl/6J background for more than 9 generations. Genotyping was performed by PCR from ear punch DNA using the following primers: Common forward CCATGCTCTTTTGAAGATGG; Wild type reverse: GTCCCCTTTTGATTTCTCCCA (producing a 1kB WT product); and mutant reverse: GGCCGCTTTTCTGGATTCATC (producing a 700bp mutant product).

Bmpr2$^{+/-}$ mice were described previously in [107]. Genotyping was performed by PCR from ear punch DNA using three primers: Common forward GCTAAAGCGCATGCTCCAGA CTGCCTTG; Wild type reverse TCACAGCATGAACATGATGGAGGCG G (producing a 200 bp product); and mutant reverse AGGTTGGCCTGGAACCTGAGGAAATC (producing a 260 bp product).

Experimental models of PH

Mice were exposed to chronic hypoxia (10% O_2) for three weeks. RVSP was evaluated as a parameter of cardiac function. The serotonin and chronic hypoxia model of PH was adapted from [98]. Briefly, adult male and female (because there were no sex differences in this model of experimental PH [98]) *WT*, *Bmpr2*$^{+/-}$, or *Bmpr2*$^{\Delta Ex2/+}$ mice, 8-12 weeks of age weighing 20 g +/- 5 g, received serotonin (Sigma) via intraperitoneal osmotic minipumps (Model 1002, Alzet) at a rate of 5 nmol/h over 2 weeks, or saline vehicle. At 2 weeks the pumps were

replaced. After recovery, animals were maintained in room air (21% O_2) or in a hypoxic chamber (10% O_2) for 5 weeks.

First characterized in rats [109], the VEGFR2 inhibitor Sugen 5416 and chronic hypoxia model has recently been adapted to mice [110]. Adult male *WT*, *Bmpr2*$^{+/-}$, or *Bmpr2*$^{\Delta Ex2/+}$ mice, 8-12 weeks of age weighing 20 g +/- 5 g, were injected subcutaneously with SU5416 (Tocris) suspended in CMC (0.5% [w/v] carboxymethylcellulose sodium (Sigma), 0.9% [w/v] sodium chloride (Sigma), 0.4% [v/v] polysorbate 80 (Sigma), 0.9% [v/v] benzyl alcohol (Sigma) in deionized water) once per week at 20 mg/kg for 3 weeks. The animals were maintained in room air (21% O_2) or in a hypoxia chamber (10% O_2) for the duration of the 3 weeks. Hemodynamics were assessed 1 week after the last injection of SU5416, at 4 weeks.

Hemodynamic assessment of experimental PH

Mice were anesthetized with tribromoethanol (Avertin, Sigma) at 375 mg/kg body weight. To evaluate PAP, right ventricular systolic pressure was measured directly by right heart catheterization with a PVR-1035 pressure/volume catheter (Millar Instruments) through the surgically exposed right jugular vein. Pressure data was recorded for 10-20 seconds using the MPVS-300 System (Millar Instruments) and analyzed using LabChart Pro7 software (ADI instruments). The left lung was clamped and removed then snap frozen for later use in protein expression analysis. The right lung was inflated with 10% formalin, fixed overnight, and then used for immunohistochemical analysis. The heart was removed for later analysis of right ventricle hypertrophy.

Assessment of RV hypertrophy

The right ventricle was dissected from the left ventricle and septum, dried for 2 days at 55^{o}C, and then weighed. Right ventricle hypertrophy was measured by dividing the weight of the right ventricle by the weight of the left ventricle and septum.

Assessment of vascular remodeling

Peripheral muscularization assessment was performed while blinded to genotype. Sections were stained by co-immunofluorescence using mouse anti-α-Smooth Muscle actin (SMA) at a dilution of 1:50 (Sigma) and rabbit anti-von-Willebrand Factor (Dako) at a dilution of 1:400. Peripheral vessels were defined as small vessels less than 100 μM, distal to muscularized bronchioles. Vessels were classified as non-muscularized, partially muscularized, or fully muscularized.

Assessment of vascular cell proliferation

Assessment was made while blinded to genotype. Co-immunofluorescence using rabbit anti-PCNA (Santa Cruz) and anti-α-SMA were used to identify actively proliferating vascular cells. If PCNA fluorescence was internal to α-SMA expressing cells, it was counted as a PCNA positive endothelial cell.

Assessment of obstructive lesions

H&E staining of lung tissue was performed in the Translational Pathology Shared Resource. Assessment of lesions was performed while blinded to genotype. Lesions were defined as a greater than 25% blockage or obstruction of the pulmonary vessel lumen by cells other than red blood cells.

Western blot analysis

Lung tissue was homogenized using a Fisherbrand motorized tissue homogenizer. Homogenized tissue was lysed in ice cold lysis buffer (LB) made up of 25mM HEPES, 150mM NaCl, 5mM EDTA, 1% Triton X-100, 10% glycerol containing proteinase inhibitor cocktail and phosphatase inhibitor cocktails 2 and 3 (Sigma). Protein concentration was measured using the DC Protein Assay (Bio-Rad). Mouse monoclonal anti-BMPR2 (clone 18, BD Biosciences) anti-phospho-eNOS (Tyr 495), anti-eNOS (BD Biosciences) and anti-β-actin (Sigma-Aldrich); rabbit polyclonal anti-phospho-Smad1 (Ser463, Ser 465) /5(Ser 463, 465) /8(Ser 426, 428), anti-phospho-p38 and anti-phospho-Erk1/2 (Thr 202, Tyr 204), phospho-eNOS (Ser 1177) (Cell Signaling), anti-Id1 (BioCheck) were used in signaling analysis. All primary antibodies were used at a dilution of 1:1000 in 5% nonfat dry milk in TBST (25 mM Tris, 1 M NaCl, 1% Tween 20), excepting phospho-specific antibodies which were diluted 1:1000 in 5% BSA in TBST. Secondary antibodies were diluted 1:2000 in 5% nonfat dry milk in TBST.

Statistics

Statistical analyses were performed using one-way ANOVA with Multiple comparisons between groups and Bonferroni Comparison test correction post hoc with Graphpad Prism 5 software. Significance is indicated if $p<0.05$.

Results

Serotonin and chronic hypoxia causes an increase in right ventricular systolic pressure in mice expressing Bmpr2 mutations

To assess if NMD+ and NMD- *Bmpr2* mutations mitigated different effects we used 3 experimental models of PH , chronic hypoxia [96,99], chronic infusion of serotonin and 5 weeks of hypoxia [98], and chronic hypoxia +SU5416. We measured RVSP, a parameter in mice that is similar to the mPAP in humans and indicative of PH. Mice that have RVSPs greater than 25 mm Hg have PH. Our findings revealed a modest increase in RVSP between mice in normoxia and chronic hypoxia but no significant differences between *WT*, *Bmpr2*$^{+/-}$*, and Bmpr2*$^{\Delta Ex2/+}$ mice (Figure 1 and 2). *Bmpr2*$^{+/-}$*and Bmpr2*$^{\Delta Ex2/+}$ mutant mice infused with serotonin and placed in hypoxia had significant differences in RVSP compared to normoxic controls, but the NMD- and NMD+ Bmpr2 mice were not significantly different from each other or form WT mice.

Bmpr2$^{\Delta Ex2/+}$ *mutants have increased RVSP in the SU5416 and hypoxia model of PH.*

The VEGFR2 inhibitor SU5416 and hypoxia model of PH, in addition to having more robust hemodynamic responses, undergoes extensive pulmonary vasculature remodeling similar to observed characteristics of human PH [110,111]. Unlike the serotonin model, we found that mice injected with CMC vehicle control and placed in hypoxia had a significant increase in RVSP compared to normoxic CMC vehicle control *Bmpr2* mutant mice (Figure 2). This is likely due to gender differences between models. Female mice were used in combination with male mice in the serotonin and hypoxia model whereas only male mice were used in the SU5416 and hypoxia model. Females are more susceptible to PH than males [3,112] and are often left out in experimental models of PH. Similarly to the serotonin model, mice treated with SU5416 and placed in hypoxia had significantly increased RVSPs compared to normoxic controls-but with much higher pressures. We found that *Bmpr2*$^{\Delta Ex2/+}$ mice had significantly higher pressures compared to the *Bmpr2*$^{+/-}$ mice. These findings indicate that there is a significant difference in

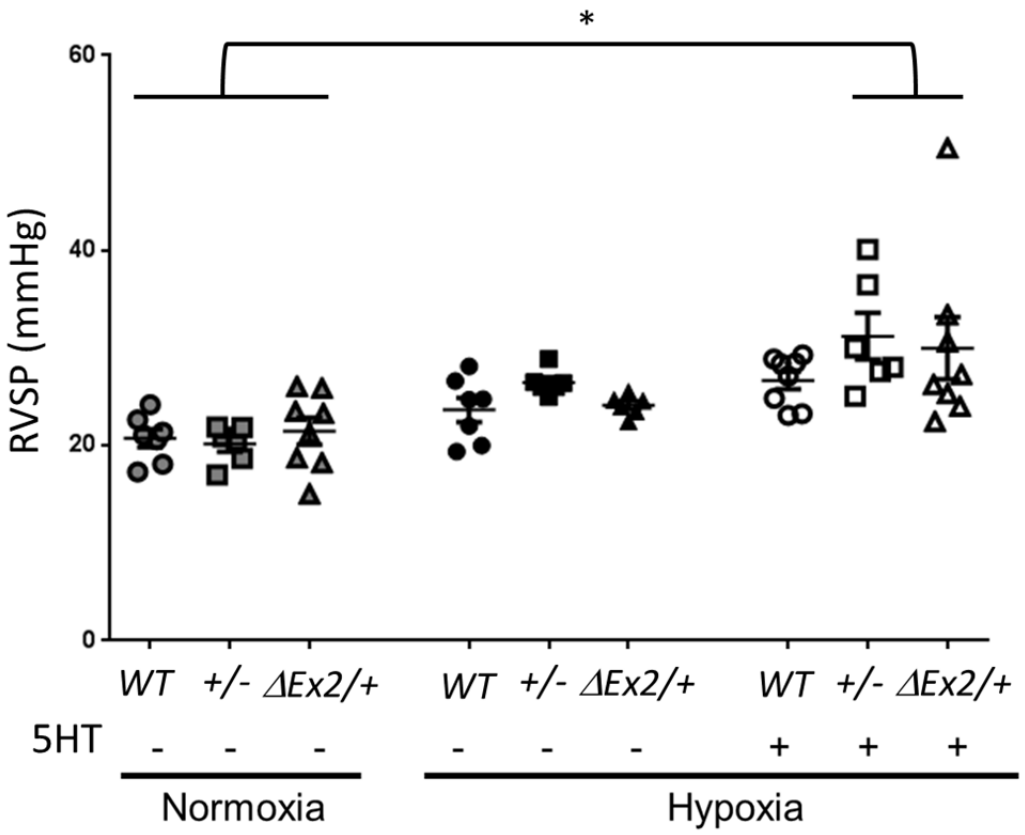

Figure 1. RVSP in *WT*, *Bmpr2*$^{+/-}$, and *Bmpr2*$^{\Delta Ex2/+}$ mice exposed to serotonin (5HT) and hypoxia. Data are means+/- SEM. *WT normoxia* n=7, *Bmpr2*$^{+/-}$*normoxia* n=6*, and Bmpr2*$^{\Delta Ex2/+}$*normoxia* n=8, *WT hypoxia* n=7, *Bmpr2*$^{+/-}$*hypoxia* n=6*, and Bmpr2*$^{\Delta Ex2/+}$*hypoxia* n=5, *WT hypoxia+ 5HT* n=8, *Bmpr2*$^{+/-}$*hypoxia + 5HT* n=6*, and Bmpr2*$^{\Delta Ex2}$*hypoxia +5HT* n=8. One-way ANOVA with post hoc Bonferroni correction for between group comparisons. *p<0.05.

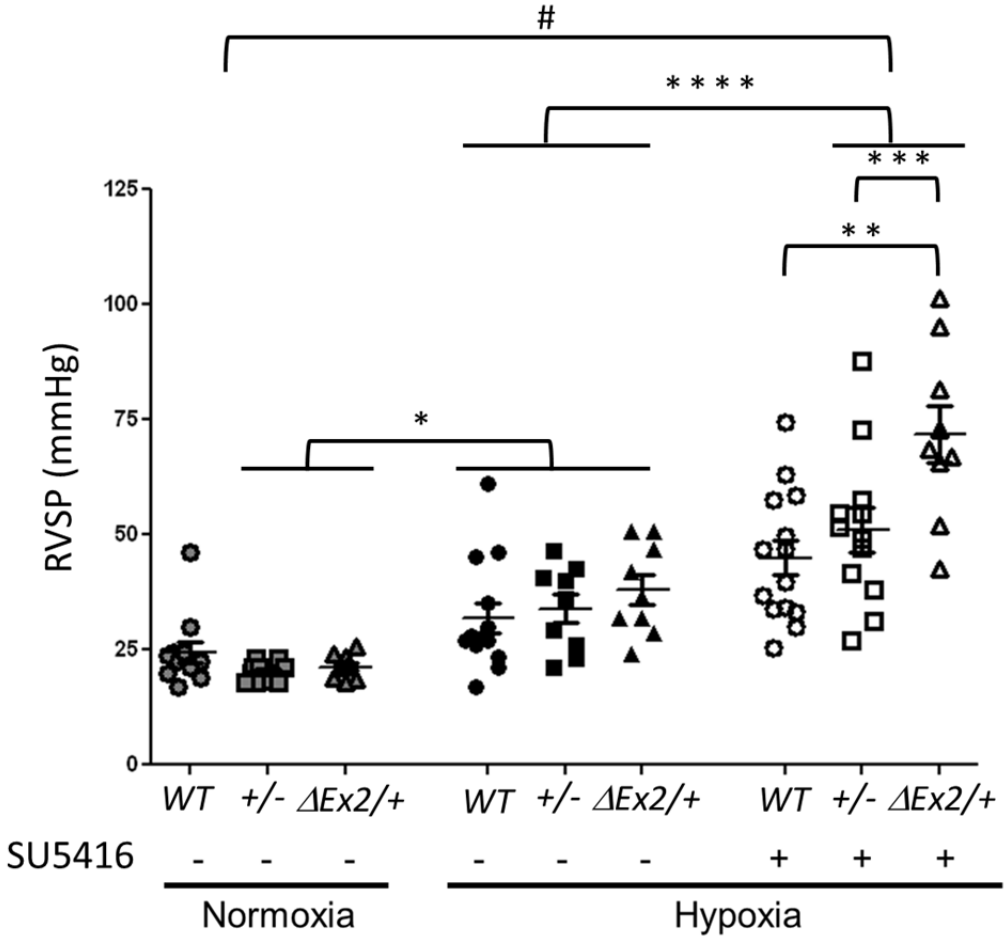

Figure 2. RVSP in *WT, Bmpr2*$^{+/-}$, and *Bmpr2*$^{\Delta Ex2/+}$ mice exposed to SU5416 and hypoxia. Data are means+/- SEM. *WT* normoxia n=9, *Bmpr2*$^{+/-}$ *normoxia* n=9, and *Bmpr2*$^{\Delta Ex2/+}$normoxia n=8, *WT* hypoxia n=10, *Bmpr2*$^{+/-}$hypoxia n=8, *and Bmpr2*$^{\Delta Ex2/+}$hypoxia n=9, *WT* hypoxia+ SU5416 n=14, *Bmpr2*$^{+/-}$hypoxia + SU5416 n=13, and *Bmpr2*$^{\Delta Ex2/+}$ hypoxia +SU5416 n=9. One-way ANOVA with post hoc Bonferroni correction for between group comparisons. *p<0.05 *Bmpr2*$^{+/-}$ and *Bmpr2*$^{\Delta Ex2/+}$normoxia vs. *WT, Bmpr2*$^{+/-}$, and *Bmpr2*$^{\Delta Ex2/+}$hypoxia. **p<0.05 *WT* hypoxia +SU5416 vs. *Bmpr2*$^{\Delta Ex2/+}$hypoxia + SU5416, ***p<0.05 vs. *Bmpr2*$^{+/-}$ hypoxia + SU5416vs. *Bmpr2*$^{\Delta Ex2/+}$hypoxia+ SU5416. ****p<0.05 *Bmpr2*$^{+/-}$ *and Bmpr2*$^{\Delta Ex2/+}$ hypoxia+SU5416 vs. hypoxia, and #p<0.05 normoxia vs. hypoxia+ SU5416

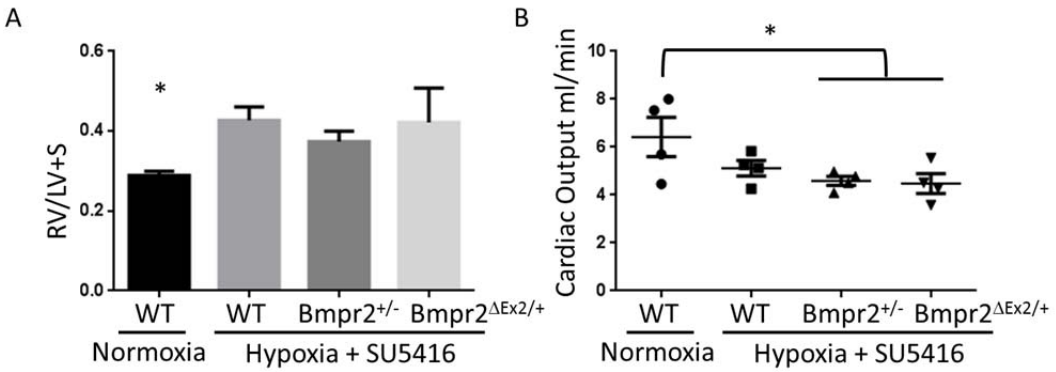

Figure 3. Hemodynamics of *WT*, *Bmpr2*$^{+/-}$, and *Bmpr2*$^{\Delta Ex2/+}$ Su5416+ hypoxia model of PH. A. RV/LV+S and B. Cardiac Output in *WT*, *Bmpr2*$^{+/-}$, and *Bmpr2*$^{\Delta Ex2/+}$ mice exposed to SU5416 and hypoxia. Data are means+/- SEM. For RV/LV+S *WT* normoxia n=9, *WT* hypoxia+ SU5416 n=14, *Bmpr2*$^{+/-}$hypoxia + SU5416 n=13, and *Bmpr2*$^{\Delta Ex2/+}$ hypoxia +SU5416 n=9. For CO n=4. One-way ANOVA with post hoc Bonferroni correction for between group comparisons. *p<0.05 *WT* normoxia *vs. hypoxia + SU5416.*

disease pathogenesis between all three models, and that each affects the *Bmpr2* mutants differently. Further characterization of experimental PH was carried out using the SU5416 and hypoxia model.

SU5416 and hypoxia mice have worse hemodynamics compared to normoxic controls

RV hypertrophy is an assessment of right heart muscularization in response to increased pulmonary pressure caused by the constriction of the pulmonary vessels. It is a way to assess a failing heart, and dysfunctional pulmonary circuit [113]. SU5416 and hypoxia *WT, Bmpr2*$^{+/-}$, and *Bmpr2*$^{\Delta Ex2/+}$ mice had significantly increased RV hypertrophy compared to *WT* normoxic controls, but not from each other (Figure 3A). We next assessed the cardiac output in these mice using a pressure/volume catheter (Millar). Mice treated with SU5416 and hypoxia showed a slight decrease in cardiac output (Figure 3B). Taken together, this assessment of hemodynamics shows that the SU5416 and hypoxia model of PH causes severe PH, but there are no significant differences in RV hypertrophy or cardiac output between *WT*, *Bmpr2*$^{+/-}$, *and Bmpr2*$^{\Delta Ex2/+}$mice.

Bmpr2$^{+/-}$ *mice have increased vascular remodeling*

To assess changes in vascular remodeling, we evaluated muscularization of the peripheral vessels (vessels under 100 μm) (Figure 4A). The *WT*, *Bmpr2*$^{+/-}$, and *Bmpr2*$^{\Delta Ex2/+}$ SU5416 and hypoxia mice had significant loss of non-muscularized peripheral vessels compared to *WT* normoxia control mice (Figure 4B). Conversely, *WT*, *Bmpr2*$^{+/-}$, and *Bmpr2*$^{\Delta Ex2/+}$ SU5416 and hypoxia mice had a significant increase in muscularized vessels compared to *WT* controls. There was no difference in muscularlized or nonmuscularized vessels between *Bmpr2*$^{+/-}$and *Bmpr2*$^{\Delta Ex2/+}$mice. When muscularized vessels are further categorized as fully or partially

muscularized, SU5416 and hypoxia *Bmpr2*$^{+/-}$mice have a significant increase in fully muscularized vessels in comparison to *WT* and *Bmpr2*$^{\Delta Ex2/+}$mice.

Increased vascular cell proliferation in SU5416 and hypoxia mice

Vascular cell proliferation is a key characteristic of PH. Uncontrolled proliferation leads to obstruction of the vessels as well as to a decrease in the surface area of the vessels leading to increased RVSP [3]. Previous studies showed that 1 week after SU5416 injection and placement in hypoxia resulted in the highest expression of PCNA in pulmonary vascular cells [110]. Based on this, we evaluated proliferative responses in *Bmpr2* mutant mice at 1 week. PCNA co-immunofluorescence with α-SMA was used to identify proliferating cells [80,99,114]. PCNA positive cells were internal to the a-SMA stain and were identified as endothelial cells (Figure 5A, arrows). PCNA positive cells co-localized with α-SMA, were identified as SMCs (Figure 5B, arrowheads). *WT*, *Bmpr2*$^{+/-}$, and *Bmpr2*$^{\Delta Ex2/+}$ SU5416 and hypoxia mice have a significant increase in the percentage of PCNA positive cells in the pulmonary vasculature (PCNA positive cells/total cells in vessel stained with DAPI) (Figure 5B). Interestingly, the *WT* SU5416 and hypoxia mice have the largest increase in proliferating cells. *WT* normoxia control mice have the lowest percentage of proliferating cells (Figure 5B) but most of the PCNA positive cells are SMCs (Figure 5C). This is in contrast to the SU5416 and hypoxia mice, all of which have a higher percentage of proliferating ECs (Figure 5D).

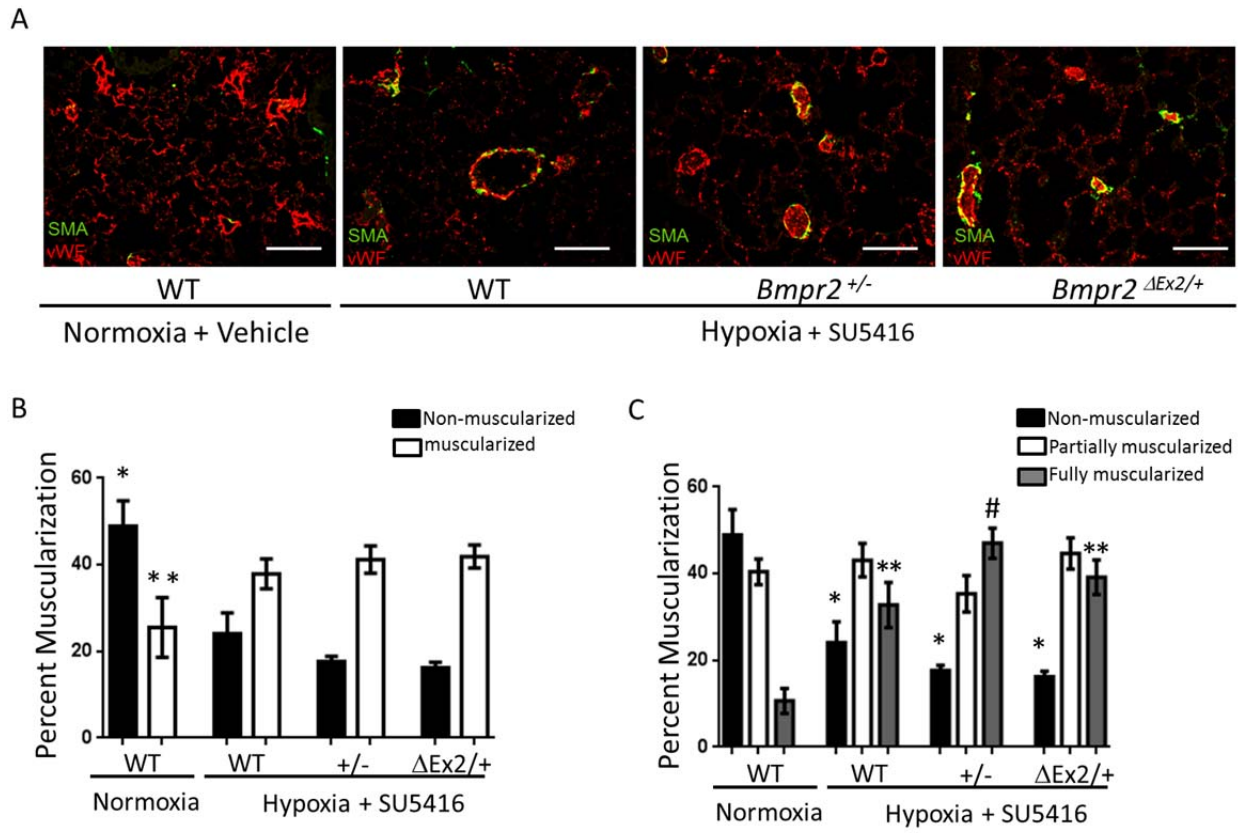

Figure 4. Peripheral vessel muscularization. The lungs were isolated, pressure perfused, fixed, and 5-µm sections stained with antibodies for α-smooth muscle actin (SMA) and von Willebrand factor (vWF). One hundred pulmonary arterioles (<100 µm) per section were analyzed blinded to the source of tissue. A. 40x representative picture for *WT Normoxia, WT, Bmpr2*$^{+/-}$, and *Bmpr2*$^{\Delta Ex2/+}$mice exposed to SU5416 and hypoxia, n=5 per group. B. Each vessel was assigned as either nonmuscularized (no α-SMA staining) or muscularized (α-SMA staining) C. Each vessel was assigned as either nonmuscularized (no α-SMA staining), partially muscularized, or fully muscularized (thick unbroken wall of smooth muscle), and then the percentage distribution of each calculated per group. Data are means+/- SEM. One-way ANOVA with post hoc Bonferroni correction for between group comparisons. *p<0.05 *WT* normoxia *vs.* hypoxia + SU5416, **p<0.05 *WT* normoxia *vs.* hypoxia + SU5416, #p<0.05 *Bmpr2*$^{+/-}$ hypoxia + SU5416 vs. *WT and Bmpr2*$^{\Delta Ex2/+}$ hypoxia + SU5416. Scale bar=50µM.

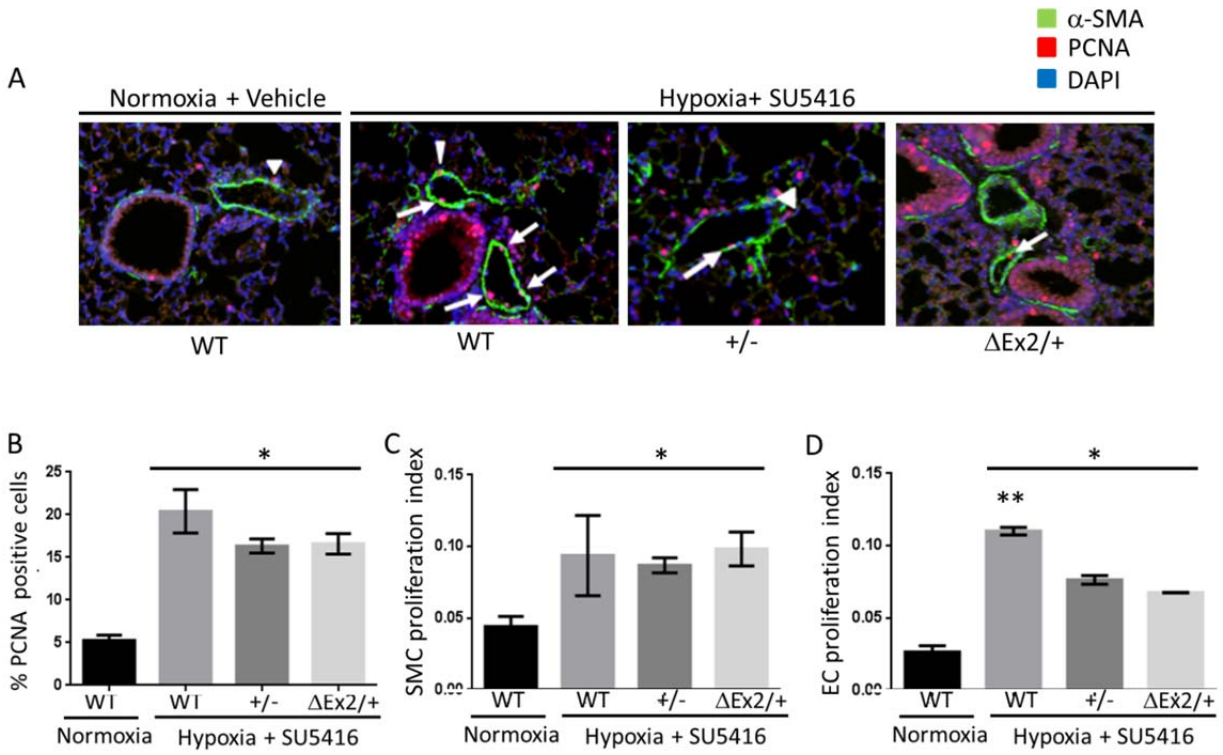

Figure 5. Evaluation of proliferation in pulmonary vasculature from mice treated with 1wk of SU5416 and hypoxia. The lungs were isolated, pressure perfused, fixed, and 5-μm sections stained with antibodies for α-smooth muscle actin (SMA) and proliferating cell nuclear antigen (PCNA). One hundred pulmonary arterioles (<100 μm) per section were analyzed blinded to the source of tissue. A. 40x representative picture for *WT Normoxia, WT, Bmpr2*$^{+/-}$, and *Bmpr2*$^{\Delta Ex2/+}$mice exposed to SU5416 and hypoxia, n=5 per group. B. Percent cells proliferating in vessels. Total PCNA positive cells divided by total nuclei per vessel (DAPI). C. SMC were stained with α-SMA. Number of SMC-PCNA positive cells per total PCNA positive cells D. EC (cells interior to α-SMA stain). Number of EC-PCNA positive cells per total PCNA positive cells. Data are means+/- SEM. One-way ANOVA with post hoc Bonferroni correction for between group comparisons. $p<0.05$ *WT* normoxia *vs.* hypoxia + SU5416. Scale bar = 100μm. White arrows=PCNA+ ECs, White arrowheads=PCNA+SMC.

$Bmpr2^{\Delta Ex2/+}$ SU5416 and hypoxia mice an increased number of obstructive vascular lesions

WT, $Bmpr2^{+/-}$ and *$Bmpr2^{\Delta Ex2/+}$* SU5416 and hypoxia mice have an increased number of vascular obstructions compared to WT normoxic controls (Figure 6A, B). Vascular obstructions were defined as blockage or obstruction of greater than 25% of the pulmonary vessel lumen by cells other than red blood cells. The *$Bmpr2^{\Delta Ex2/+}$* SU5416 and hypoxia treated mice also have significantly more obstructions than *WT* SU5416 and hypoxia mice (Figure 6B). The decreased surface area and blood flow due to the vascular lesions could provide one explanation for the increased RVSP observed in the *$Bmpr2^{\Delta Ex2/+}$* SU5416 and hypoxia mice, and is suggestive of a more severe form of PH. Evaluation of vessels per aveoli reveal no significant differences between *WT, $Bmpr2^{+/-}$* and *$Bmpr2^{\Delta Ex2/+}$* SU5416 and hypoxia mice (6C).

Basal signaling abnormalities in $Bmpr2^{\Delta Ex2/+}$ mice

To evaluate the effects of different Bmpr2 mutants on signaling pathways, we homogenized lungs from 4 mice of each genotype. The most striking difference was the significant reduction of phospho-S1177eNOS, phospho-T495eNOS, phospho-Erk1/2, and phospho-p38 in *$Bmpr2^{\Delta Ex2/+}$*mice (Figure 7). The *$Bmpr2^{+/-}$* mice also have a significant reduction of phospho-S1177eNOS expression compared to *WT* mice. Phospho-Smad1/5/8 is upregulated, although not significantly, in *Bmpr2* mutant mice.

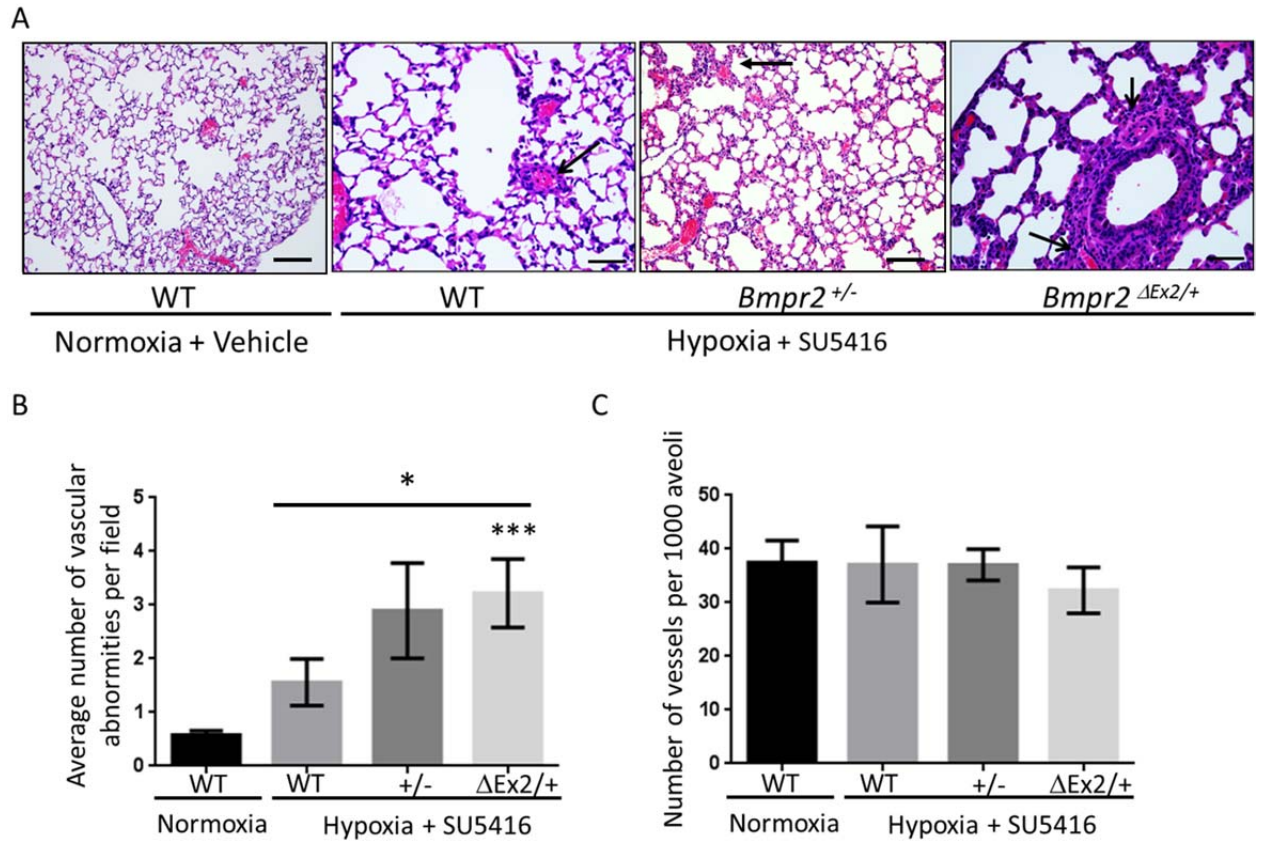

Figure 6. Evaluation of vascular obstructions in SU5416 and hypoxia. The lungs were isolated, pressure perfused, fixed, and 5-µm sections stained with H&E. Each section was analyzed blinded to the source of tissue. A. 20x representative picture for *WT Normoxia, WT, Bmpr2*$^{+/-}$, and *Bmpr2*$^{\Delta Ex2/+}$ mice exposed to SU5416 and hypoxia, n=5 per group. Black arrows indicate areas of vascular lesions. B. Average number of abnormalities per field. 50 fields per mouse were scored. C. Number of vessels per 1000 aveoli. Peripheral vessels and aveoli were counted until approximately 1000 aveoli was reached and expressed as vessels/aveoli. Data are means+/- SEM. One-way ANOVA with post hoc Bonferroni correction for between group comparisons. *p<0.05 and **p<0.05 *WT* normoxia *vs.* hypoxia + SU5416. ***p<0.05 *Bmpr2*$^{\Delta Ex2/+}$ hypoxia + SU5416 vs. *WT* hypoxia + SU5416. Scale bar = 100µm.

$Bmpr2^{\Delta Ex2/+}$ mice have decreased phospho-Smad1/5/8 expression after 1 week of SU5416 and hypoxia

Bmpr2 mediates signaling responses to regulate vascular homeostasis [51]. We wanted to evaluate Bmpr2 signaling responses to 1) determine which pathways were altered in the SU5416 + hypoxia model, and 2) determine if the *Bmpr2* mutants had similar signaling responses. At 1 week after the initiation of SU5416 injections and hypoxia, although basally reduced in $Bmpr2^{\Delta Ex2/+}$ mice (Figure 7), phospho-1177eNOS, phospho-T495eNOS, phospho-Erk1/2, and phospho-p38 expression are increased to levels similar to or greater than WT expression levels (Figure 8). Phospho-Smad1/5/8, upregulated in basal conditions, is significantly downregulated in $Bmpr2^{\Delta Ex2/+}$ mice after 1 week of SU5416 and hypoxia. The WT and *Bmpr2*+/- mice were not different from each other. This reduction in Smad and elevation in eNOS was interesting because it showed that these pathways are fluctuating, but not in the same ways-suggesting that the protein product of $Bmpr2^{\Delta Ex2/+}$ and $Bmpr2^{+/-}$ respond to different stimuli.

Evaluation of signaling responses in WT, $Bmpr2^{+/-}$ and $Bmpr2^{\Delta Ex2/+}$ mice after 3weeks of SU5416 and hypoxia and 1wk of hypoxia

We next wanted to evaluate signaling pathways after 3 weeks of SU5416 and hypoxia treatment with an additional 1 week of hypoxia to determine if *Bmpr2* mutation type elicits different signaling effects in mice. We found greater variability in signaling responses in *WT,* $Bmpr2^{+/-}$ and $Bmpr2^{\Delta Ex2/+}$ mice. We found no significant differences between WT and Bmpr2 mutants (Figure 9). Taken together, Figures 7, 8, and 9 illustrate the dynamic and unique signaling responses in different *Bmpr2* mutations over time.

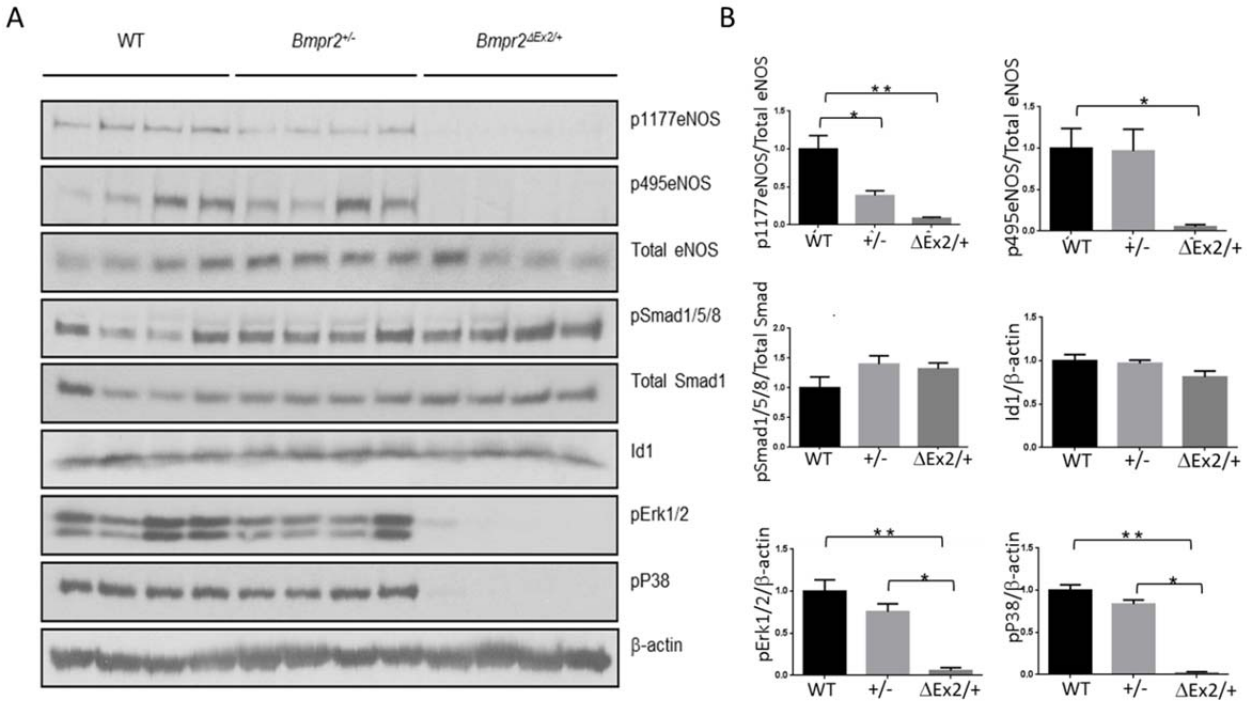

Figure 7. Aberrant signaling activity in whole lungs isolated from normoxic controls. The lungs were isolated, homogenized, and lysed. A. Western blots showing signaling pathway expression of common Bmp-mediated pathways. B. Densitometry of western blots. Data are means+/- SEM. One-way ANOVA with post hoc Bonferroni correction for between group comparisons. *p<0.05 *WT vs. Bmpr2*$^{+/-}$, **p<0.05 vs. *Bmpr2*$^{\Delta Ex2/+}$

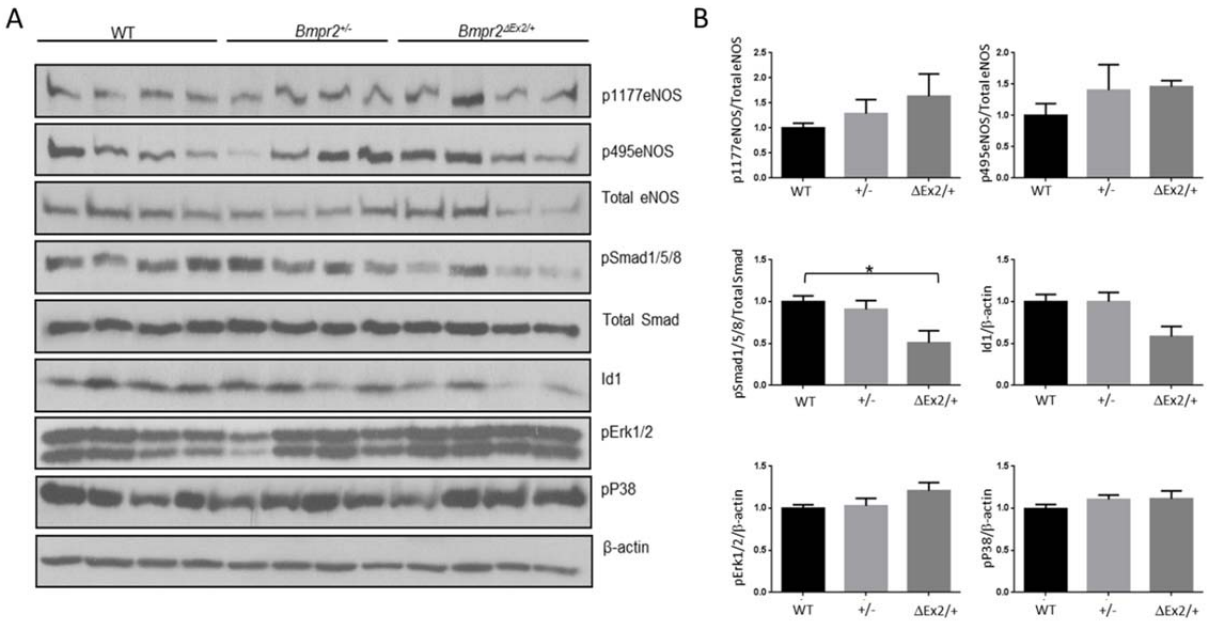

Figure 8. Aberrant signaling activity in whole lungs isolated after 1 week SU5416 and hypoxia. The lungs were isolated, homogenized, and lysed. A. Western blots show expression of common Bmp-mediated pathways. B. Densitometry of western blots. Data are means+/- SEM. One-way ANOVA with post hoc Bonferroni correction for between group comparisons. *p<0.05 *WT vs. Bmpr2*$^{\Delta Ex2/+}$

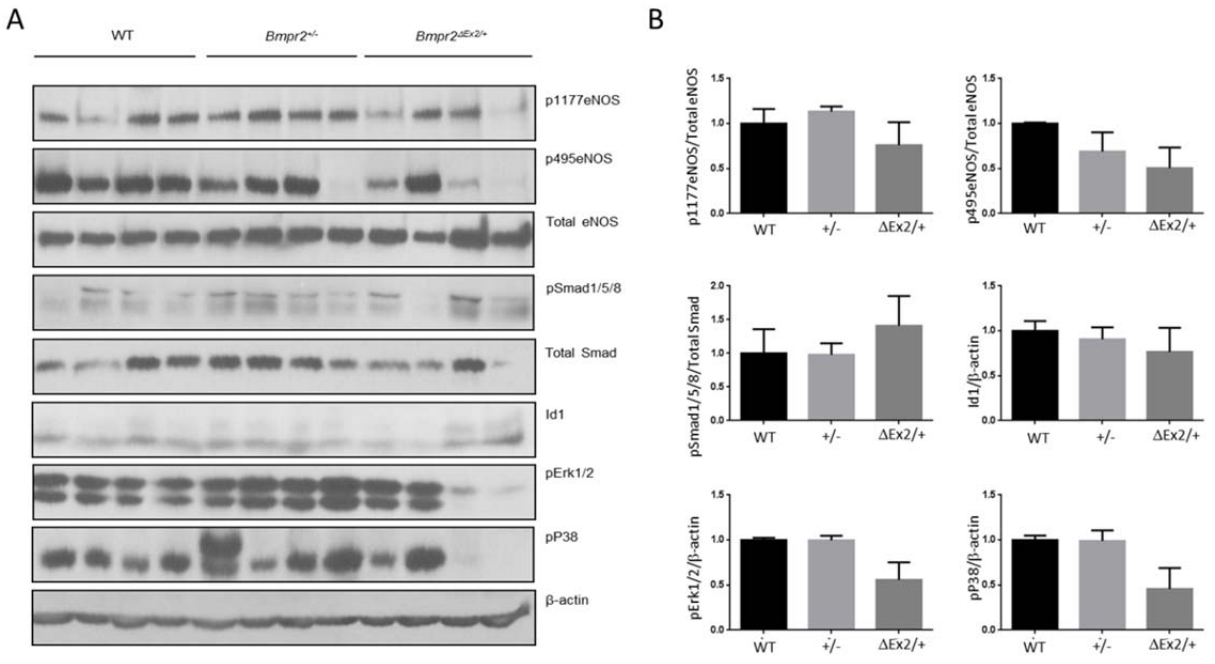

Figure 9. Aberrant signaling activity in whole lungs isolated from mice after treatment with 3 weeks SU5416 and hypoxia. The lungs were isolated, homogenized, and lysed. A. Western blots showing signaling pathway expression of common Bmp-mediated pathways. B. Densitometry of western blots. Data are means+/- SEM. One-way ANOVA with post hoc Bonferroni correction for between group comparisons.

Discussion

We report for the first time the *in vivo* analysis of an NMD- and an NMD+ *Bmpr2* mutation on the same genetic background. Using the chronic hypoxia and serotonin+hypoxia experimental models of PH we show that serotonin and hypoxia modestly, but significantly, increase the RVSP in $Bmpr2^{+/-}$and $Bmpr2^{\Delta Ex2/+}$mice compared to Normoxia controls. This finding indicates that serotonin-mediated responses in $Bmpr2^{+/-}$and $Bmpr2^{\Delta Ex2/+}$mice are not differentially effected by mutation type. The $Bmpr2^{\Delta Ex2/+}$mice do not show increased susceptibility to this model compared to $Bmpr2^{+/-}$ mice, indicating that the deletion of *Exon2* likely does not interface with pathways regulating serotonin.

However, in contrast to the serotonin model, $Bmpr2^{+/-}$ mice $Bmpr2^{\Delta Ex2/+}$mice have significant differences in the SU5416 and hypoxia model of PH. $Bmpr2^{\Delta Ex2/+}$ mice had significantly increased RVSPs compared to the $Bmpr2^{+/-}$ mice. Furthermore, $Bmpr2^{\Delta Ex2/+}$mice have more vascular lesions in response to SU5416 and hypoxia. This indicates that the functional consequences of the deletion of *Exon2* in the $Bmpr2^{\Delta Ex2/+}$ mice, is exacerbated with VEGFR2 inhibition.

Basal evaluation of signaling responses showed several key differences between mutants. $Bmpr2^{\Delta Ex2/+}$mice have decreased expression of phospho-s1177eNOS and phospho-T495eNOS, phospho-Erk1/2, and phospho-p38Mapk and increased phospho-Smad1/5/8. These results provide intriguing data about the signaling pathways in the $Bmpr2^{\Delta Ex2/+}$mice that are already altered without added environmental stimuli. Week 1 signaling data provides an interesting glimpse into the initial response capabilities of the $Bmpr2^{\Delta Ex2/+}$ mutant to stimuli (SU5416 and hypoxia) as PH is developing *in vivo*. In fact, phospho-Smad1/5/8, the canonical BMP-mediated

pathway, is reduced at this timepoint and phospho-eNOS, phospho-Erk1/2, and phospho-p38 that were significantly reduced basally, here are increased. This suggests the impairment of the *Bmpr2*$^{\Delta Ex2/+}$ mutant in regulating those signaling pathways, either because it is sequestered in the ER [84,115,116], is sequestering an interacting protein [116], or it is unable to provide or respond to biological feedback in response to VEGFR inhibition. This is interesting because it indicates that not all Bmpr2 mutations respond in the same ways to the same stimuli. This is significant because it provides a molecular basis to begin to understand what is observed in HPAH patients, that not all BMPR2 mutations lead to disease, and not all mutations affect patients in the same ways. The exacerbated response to VEGFR2 inhibitor also provides an insight into what pathways the Bmpr2ΔEx2 mutant product might be involved in and affecting.

Interestingly, the SU5416 and hypoxia model showed significant increases compared to normoxia controls but not between *Wt, Bmpr2*$^{+/-}$, *Bmpr2*$^{\Delta Ex2/+}$ in RV hypertrophy and cardiac output. It is important to note that the cardiac output measurement may be skewed. Due to poor pressure/volume loop quality, only 4 of 8 mice per group produced sufficient data to determine cardiac output. The mice that produced usable volume loops tended to have lower RVSPs, so the cardiac functions of mice with the most extreme RVSPs were unable to be used. This may not give an accurate assessment of cardiac output in experimental PH. One alternative would be to use echocardiography to assess the cardiac output of mice.

WT SU5416 and hypoxia mice have a significant increase in proliferating vascular cells. This data, in combination with the differences in RVSP in response to serotonin or SU5416 by the two *Bmpr2* mutants, the increase in remodeling observed in *Bmpr2*$^{+/-}$, and the differences in vascular abnormalities and signaling function in the *Bmpr2*$^{\Delta Ex2/+}$ provide compelling evidence

that the WT, *Bmpr2*$^{+/-}$, *Bmpr2*$^{\Delta Ex2/+}$mice are responding to/have increased sensitivity to different mechanisms leading to the development of experimental PH. In fact, this is observed in PAH patients [2,17,35,95,117]. Additionally, because of the number of *BMPR2* mutations in HPAH patients, it is not unreasonable for mutations to present different phenotypes, dependent on if the mutant is able to produce a protein, and where in the protein the mutation occurs [104]. This comparison of Bmpr2 mutation types in a SU5416 hypoxia model of PH offers an exciting, novel, and initial step to understand the HPAH clinical data and the role of *BMPR2* mutation in disease pathogenesis.

CHAPTER III

ABNORMAL TRAFFICKING OF ENDOGENOUSLY EXPRESSED *BMPR2* MUTANT ALLELIC PRODUCTS IN PATIENTS WITH HERITABLE PULMONARY ARTERIAL HYPERTENSION

Introduction

Over 200 unique mutation sites have been identified throughout the open reading frame of the *BMPR2* gene in HPAH patients [45,47]. The majority of these mutations are non-sense or frame-shift mutations, leading to degradation of an unstable mRNA by nonsense mediated mRNA decay (NMD positive mutation), ultimately leading to haploinsufficiency [104]. However, 40% of HPAH-associated *BMPR2* mutations are mis-sense or in-frame deletion mutations, predicted to produce stable mRNA transcripts and express mutant protein products. Clinical data indicate that HPAH patients with these mutations have a more severe form of HPAH with reduced time until lung transplant and an earlier age of diagnosis[104], suggesting that these mutant protein products are expressed and may have dominant negative effects on BMPR2 function. Previous studies have characterized NMD negative *BMPR2* mutations using heterologous over-expression systems. These data suggest that HPAH-associated missense mutations in the ligand binding and kinase domains of BMPR2 are unable to traffic to the cell surface [79,118], and that trafficking and signaling can be restored using chemical chaperones

[116]. These findings suggest that chemical chaperones, which correct folding and restore function of mutant protein products in a variety of heritable diseases including cystic fibrosis [119,120], might be used as disease modifying agents by restoring signaling function to some NMD negative *BMPR2* mutations in patients with HPAH. However there is no documented evidence that NMD negative *BMPR2* mutant proteins products are actually expressed endogenously in patients with HPAH, and no data to indicate whether chemical chaperones restore function in pulmonary vascular cells.

In these studies, we evaluate endogenous expression and intracellular trafficking of *BMPR2* mutant products in lymphocytes from an HPAH patient with an NMD negative *BMPR2* mutation expressing an in-frame deletion of *BMPR2 EXON 2*, and in pulmonary endothelial cells (PECs) from mice carrying the same mutation. We show that these mutant receptor products are expressed, abnormally trafficked to the cell surface and that these defects are corrected by treatment with chemical chaperones.

Materials and Methods

Ethics statement

Mice used in endothelial cell studies were approved by the Vanderbilt University Institutional Animal Care and Use Committee (Dr. Ron Emeson, IACUC chair) under protocol number M/11/015 and were adherent with the National Institutes of Health guidelines for care and use of laboratory animals under Vanderbilt animal welfare assurance licence number A3227-01.

The Vanderbilt University Medical Center Institutional Review Boards approved use of control and HPAH patient-derived lymphocytes and participants gave informed written consent

for use of their lymphocyte cultures for study (IRB #9401"Genetic and Environmental Pathogenesis of PPH" RFA-HL-04-019, Dr. James A.S. Muldowney, chair, Institutional Review Board Health Sciences Committee #3).

Mouse lines

Endothelial cell lines were isolated from *Bmpr2*$^{\Delta Ex2/+}$ mice (mice described previously [108]). Studies were approved by the Vanderbilt University Institutional Animal Care and Use Committee (see above for ethics statement). Mice were backcrossed onto a C57Bl/6J background for more than 9 generations. Genotyping was performed by PCR from ear punch DNA using the following primers: Common forward CCATGCTCTTTTGAAGATGG; Wild type reverse: GTCCCCTTTTGATTTCTCCCA (producing a 1kB WT product); and mutant reverse: GGCCGCTTTTCTGGATTCATC (producing a 700bp mutant product). To create the ciEC lines, *Bmpr2*$^{\Delta Ex2/+}$ mice were bred with H-2Kb-tsA58 immorto mice (immorto mice described previously [121]). Genotyping was performed as described above with the additional PCR primers for the immorto mice: forward: AGCGCTTGTGTCGCCATTGTATTC and reverse: GTCACACCACAGAAGTAAGGTTCC, producing a 1kb band.

Chemicals and Reagents

Sulfo-NHS-LC-Biotin and Streptavidin agarose conjugated beads (Pierce/Thermo Scientific); Dio-Ac-LDL (Biomedical Technologies Inc.); Endo-H and PNGase-F glycosidases (New England Biolabs); Human recombinant BMP-2 (R&D Systems); chemical chaperones sodium phenylbutyrate (4-PBA) and Sodium taurourdeoxycholic acid (TUDCA) (Sigma-Aldrich). The following antibodies were used for western blots: mouse monoclonal anti-BMPR2 (clone 18, BD Biosciences) and anti-β-actin (Sigma-Aldrich); rabbit polyclonal anti-phospho-

Smad1 (Ser463, Ser 465) /5(Ser 463, 465) /8(Ser 426, 428), anti-phospho-Akt(Ser 473), and anti-phospho-Erk1/2 (Thr 202, Tyr 204) (Cell Signaling). Affinity purified rabbit polyclonal anti-BMPR2 antibodies were generated in house by immunizing rabbits with keyhole limpet hemocyanin conjugated peptide ASQNQERLCAFKDP (ASQ). Secondary antibodies were anti-mouse horseradish peroxidase (HRP) and anti-rabbit-HRP from KPL and Cell Signaling, respectively.

Cell Culture

Conditionally immortalized pulmonary endothelial cells (ciPECs) were isolated, passaged and maintained as previously described [80,81,99]. Briefly, cells were grown at 33^{o}C in complete EGM-2MV media (LONZA) containing 10units/ml of interferon-γ (Peprotech). Prior to experimental use, interferon-γ was removed and cells shifted from 33^{o}C to 37^{o}C for 2 days. HPAH patient-derived and normal control immortalized lymphocytes were isolated as previously described [46,122]. Cells were passaged and maintained in 1640 RPMI media (Gibco/Life Technologies) containing 20% fetal bovine serum (FBS) (Sigma).

Isolation of Primary Pulmonary Endothelial Cells (PECs)

Mouse pulmonary vasculature was perfused with phosphate buffered saline (PBS) containing 2mM EDTA followed by 0.25% Trypsin-EDTA through the right ventricle. The lungs were excised, minced, placed in a 60mm dish with 0.25% Trypsin-EDTA and moved to a 37^{o} degree incubator for 20-30 minutes. The lung block was removed and complete EGM-2MV containing 5% FBS was then added to the dish to neutralize trypsin. Cells were centrifuged and re-suspended in fresh complete EGM-2MV with normacin (Invivogen). The cell suspension was plated on 35mm dishes coated in 0.1% gelatin and grown for 2-3 days before media was

replaced. The cells were identified as endothelial in origin based on morphology and Dio-AC-LDL staining. Functional studies were carried out in the cells by passage 2.

Western Blotting

Cells were lysed in ice cold lysis buffer (LB) made up of 25mM HEPES, 150mM NaCl, 5mM EDTA, 1% Triton X-100, 10% glycerol containing proteinase inhibitor cocktail and phosphatase inhibitor cocktails 2 and 3 (Sigma). Protein concentration was measured using the DC Protein Assay (Bio-Rad). Western blots were performed as previously described [114]. All primary antibodies were used at a dilution of 1:1000 in 5% nonfat dry milk in TBST (25mM Tris, 1M NaCl, 1% Tween 20), excepting phospho-specific antibodies which were diluted 1:1000 in 5% BSA in TBST. Secondary antibodies were diluted 1:2000 in 5% nonfat dry milk in TBST.

Cell signaling and chemical chaperone treatment

For signaling studies, cells were serum starved in EBM-2 media (Lonza) supplemented with 0.1% bovine serum albumin (BSA) for 16 hours and then treated with 10ng/ml BMP2 for 4 hours. EBM-2 is the basal media used to make complete EGM-2MV without addition of supplements, growth factors and FBS. Chemical chaperones were added to confluent monolayers of cells. 4-PBA and TUDCA were dissolved in water and added to cells at the indicated concentrations 48 hours and 5 hours prior to biotinylation, respectively. For functional studies, primary PECs were treated with 4-PBA at 100□M and 1mM for 48 hours. Cells were serum starved for 16 hours, as described above, and treated with 10ng/ml of BMP2 for 4 hours before lysis.

Glycosidase Sensitivity Assay

Cells were lysed in LB and immunoprecipitated using Protein G dynabeads (Life Technologies) conjugated to anti-BMPR2 antibody (Clone 18, BD) at room temperature for 15 minutes, per the manufacturer's directions. Immunoprecipitates were washed 3 times with LB, denatured using de-glycosylation buffer and subjected to Endo-H or PNGase-F digestion for 3 hours in a 37^{o} C before adding sample loading buffer, according to the manufacturer's instructions (New England Biolabs).

Biotinylation of Cell Surface Proteins

Confluent monolayers were washed 2 times with ice-cold PBS and cell surface proteins labeled with 1mg/ml Sulfo-NHS-LC-Biotin in PBS for 30 minutes on ice and at 4^{o}C. Cells were washed 3 times with ice cold PBS and biotin labeling quenched by incubating cells with 100mM glycine in PBS for 5 minutes on ice. After this, cells were carefully washed in ice cold PBS to remove any residual glycine. Cells were then lysed in LB and protein concentration determined. 750□g of lysate protein was incubated for 30 minutes with Streptavidin beads at 4^{o}C, after which the beads were washed 3 times with LB before adding denaturing loading buffer and separating by SDS-PAGE. Supernatant leftover after the streptavidin pull-down was incubated with anti-BMPR2 antibody (Clone 18, BD) overnight at 4^{o}C and then subjected to immunoprecipitation with Protein A/G Plus agarose beads (Santa-Cruz) for 30 minutes. Immunoprecipitates were washed with LB and proteins eluted by adding sample loading buffer.

Statistical Analysis

Statistical analyses were performed using one-way ANOVA with Multiple comparisons between groups and Bonferroni Comparison test correction post hoc with Graphpad Prism 5 software. Significance is indicated if $p<0.05$.

Results

Characterization of the BMPR2ΔEx2 mutant protein product in HPAH patient-derived lymphocytes

To determine if NMD negative *BMPR2* mutations are expressed and incorrectly trafficked to the cell surface in patients with HPAH, we evaluated BMPR2 protein expression in HPAH patient-derived lymphocytes [46,122]. Cultured immortalized lymphocytes were used because these cells are easily isolated and stored. Additionally, we have a repository of frozen, HPAH patient-derived cultured lymphocytes at Vanderbilt from participants in the Vanderbilt Prospective Pulmonary Hypertension Research Cohort study [31,46,47,122-125]. For these studies we evaluated BMPR2 expression in lymphocytes derived from an HPAH patient from Vanderbilt PAH Family 108 (F108) who carry a splice site mutation predicted to result in an in-frame deletion of *BMPR2 EXON2,* which encodes residues 26-82 of the 1038 full length BMPR2 protein[46]. If expressed, the mutant product, BMPR2ΔEx2, would be distinguishable from the wild type allelic product by a mobility shift on western blot resulting from deletion of 56 amino acids encoded by *EXON2*. We obtained lymphocytes from one normal control and one F108 HPAH patient. The anti-BMPR2 antibody, Clone 18, which is a mouse monoclonal antibody raised against a recombinant fragment (residues 803-996) from the cytoplasmic tail of human BMPR2 (Fig. 10A), detected a strong 130-145 kDa wild type BMPR2 band in control and F108 HPAH patient lymphocytes (Fig. 10B). An additional weaker 120 kDa band was detected in F108 HPAH, but not in normal control cells. To determine if the 120 kDa band was the predicted product resulting from in-frame deletion of *BMPR2 EXON2* in F108 HPAH lymphocytes, we generated an affinity purified rabbit polyclonal anti-BMPR2 antibody, ASQ, raised against the peptide sequence of the first 14 amino acids encoded by *BMPR2 EXON2* (Fig.

10A). The 130-145 kDa wild type BMPR2 band was detected in control and F108 lymphocytes, but the 120 kDa BMPR2 band was not detected in F108 cells using this antibody (Fig. 10C). These data indicate that lymphocytes from a F108 HPAH patient express a mutant BMPR2 product resulting from an in-frame deletion of *BMPR2 EXON2* (BMPR2ΔEx2).

We next evaluated if the BMPR2ΔEx2 product was expressed at the cell surface. For this, cell surface proteins were labeled with a membrane impermeable biotin and detected by streptavidin pull-down and western blot for BMPR2 using the Clone 18 anti-BMPR2 antibody. The 130-145 kDa wild type BMPR2 product was detected in the streptavidin pull-down in control and F108 cultured lymphocytes, but the 120 kDa BMPR2ΔEx2 band was not (Fig. 10D, right panel). These data indicate that the BMPR2ΔEx2 mutant product resulting from the in-frame deletion of *BMPR2 EXON2* in the F108 HPAH patient does not correctly traffic to the cell surface in cultured lymphocytes.

Characterization of the Bmpr2ΔEx2 product in pulmonary endothelial cells from $Bmpr2^{\Delta Ex2/+}$ *mice*

To evaluate expression and trafficking of the same, endogenously expressed, BMPR2ΔEx2 mutant product in a more physiologically relevant cell type, we isolated conditionally immortalized pulmonary endothelial cells (ciPECs) from $Bmpr2^{\Delta Ex2/+}$ mice.

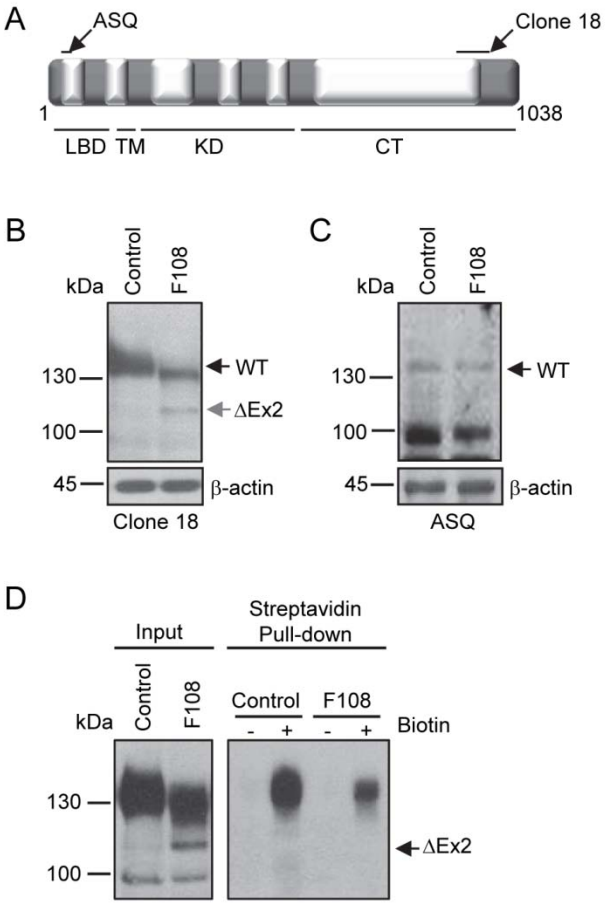

Figure 10. HPAH patient-derived lymphocytes express mutant BMPR2 products. A, Schematic of the BMPR2 protein. Areas recognized by the anti-BMPR2 antibodies clone 18 and ASQ are indicated by black arrows. Exons 1-13 are represented by alternating gray and white boxes, and numbers indicate corresponding amino acids. LBD, represents the ligand binding domain, TM the transmembrane domain, KD the kinase domain and CT the cytoplasmic tail. B, Detection of BMPR2 products in HPAH patient-derived lymphocytes, image representative of three experiments. Western blot using anti-BMPR2 antibody, Clone 18. A 130-145 kDa wild type BMPR2 product (WT) was detected in normal control and Family 108 (F108) HPAH patient-derived lymphoblasts. F108 cells expressed an additional 120 kDa BMPR2 mutant product (ΔEx2). C, Representative western blot from three experiments using the ASQ anti-BMPR2 antibody. The 130-145 kDa product was detected in both control and F108 lymphocytes, but the 120 kDa band was not detected. D, Cell surface expression of BMPR2 in HPAH patient-derived lymphocytes labeled with a membrane impermeable biotin. Experiment replicated three times. Left panel, input cell lysates before the streptavidin pull-down. Right panel, cell surface proteins detected in streptavidin pull-down by Western blot using Clone 18 anti-BMPR2 antibody. A 130-145 kDa wild type BMPR2 product was detected in control and F108 cultured lymphocytes in streptavidin pull-down but not 120kDa BMPR2ΔEx2 mutant product.

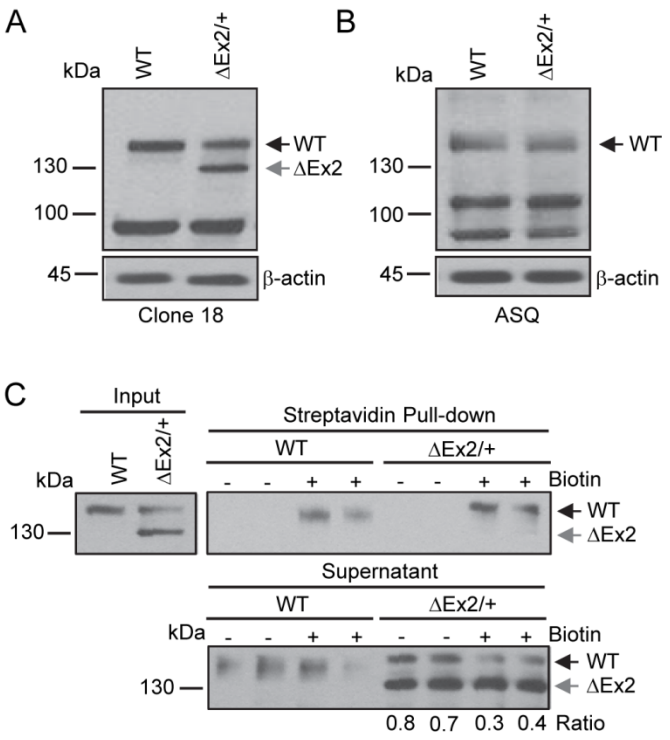

Figure 11. Characterization of the endogenously expressed *Bmpr2* mutant product in pulmonary endothelial cells from *Bmpr2*$^{\Delta Ex2/+}$ mice. Studies were performed using conditionally immortalized PECs (ciPECs) isolated from wild type control and *Bmpr2*$^{\Delta Ex2/+}$ mice and replicated at least three times. A, Western blot using the Clone 18 anti-BMPR2 antibody in wild type (WT) and *Bmpr2*$^{\Delta Ex2/+}$ (ΔEx2/+) ciPEC lysates. Both cell lines expressed a 150 kDa wild type Bmpr2 product (WT). *Bmpr2*$^{\Delta Ex2/+}$ ciPECs also expressed a 130 kDa product (ΔEx2). B, Western blot using ASQ anti-BMPR2 antibody. Wild type control and *Bmpr2*$^{\Delta Ex2/+}$ ciPECs expressed 150 kDa WT Bmpr2, but the 130 kDa product was not detected. C, Cell surface expression of Bmpr2 in ciPECs. ciPECs were labeled with membrane impermeable biotin and cell surface expression of Bmpr2 detected in streptavidin pull-down of cell lysates. Anti-BMPR2 Clone 18 antibody detected the 150 kDa wild type Bmpr2 in control and *Bmpr2*$^{\Delta Ex2/+}$ ciPECs after streptavidin pull-down but not the 130kDa Bmpr2ΔEx2 mutant product. Lower panel, Western blot for Bmpr2 in the supernatant remaining after depletion of cell surface proteins by streptavidin pull-down. The ratios of 150 kDa WT Bmpr2 and the 130 kDa Bmpr2ΔEx2 mutant band intensities in *Bmpr2*$^{\Delta Ex2/+}$ ciPECs supernatants after depletion of cell surface proteins are indicated below the lower panel.

Bmpr2$^{\Delta Ex2/+}$ mice carry the same, heterozygous in-frame deletion of *Exon 2* found in F108 HPAH patients [108]. The anti-BMPR2 antibody Clone 18 detected a 150 kDa band in control (wild type) and *Bmpr2*$^{\Delta Ex2/+}$ ciPECs, but an additional 130 kDa band was only detected in the *Bmpr2*$^{\Delta Ex2/+}$ ciPECs (Fig. 11A). To determine if the 130 kDa band was the predicted product resulting from an in-frame deletion of *Bmpr2 Exon2*, we performed western blot analysis using the anti-BMPR2 antibody ASQ, raised against the peptide sequence in Exon2 (Fig. 10A). The wild type 150kDa Bmpr2 band was detected in both the control and *Bmpr2*$^{\Delta Ex2/+}$ ciPECs, but the 130kDa product was not detectable in the Bmpr2$^{\Delta Ex2/+}$ciPECs using this antibody (Fig. 11B). These data indicate that *Bmpr2*$^{\Delta Ex2/+}$ ciPECs expressed high levels of the Bmpr2ΔEx2 mutant product, which is detected as a 130 kDa band on western blot and is distinct from the 150 kDa wild type Bmpr2 product.

We performed cell surface biotinylation studies to determine whether the BmprΔEx2 mutant product was expressed at the cell surface of *Bmpr2*$^{\Delta Ex2/+}$ciPECs. The 150 kDa wild type product was detected in the streptavidin pull-down in both control and *Bmpr2*$^{\Delta Ex2/+}$ ciPECs (Figure 11C). In contrast, the 130 kDa Bmpr2ΔEx2 mutant product was not detected in the streptavidin pull-down. Additionally, while there was reduced expression of the wild type Bmpr2 protein in control and *Bmpr2*$^{\Delta Ex2/+}$ ciPECs in the supernatant remaining after depletion of cell surface biotinylated proteins by streptavidin pull-down, expression of the 130kDa Bmpr2ΔEx2 mutant product was not reduced (Fig. 11C, lower panel). These data indicate that like the 120 kDa BMPR2ΔEx2 product in F108 HPAH patient cultured lymphocytes, the 130 kDa Bmpr2ΔEx2 mutant product does not traffic to the cell surface in *Bmpr2*$^{\Delta Ex2/+}$ ciPECs.

Differential glycosidase sensitivity of the Bmpr2ΔEx mutant product

We used N-linked glycosidases to determine if the Bmpr2ΔEx2 mutant product was able to traffic correctly through the endoplasmic reticulum (ER) and Golgi apparatus. N-linked glycosylated proteins that are processed in the ER are sensitive to Endo-H glycosidase, but become resistant to Endo-H once the glycoprotein has passed through to the *trans*-Golgi [126]. In contrast, PNGase-F de-glycosylates all N-linked glycosylated proteins irrespective of their maturation state. This sensitivity to glycosidase digestion can be detected by a change in protein mobility resulting from cleavage of glycan moieties. As expected, the 150 kDa wild type Bmpr2 product in control and $Bmpr2^{\Delta Ex2/+}$ ciPECs underwent a mobility shift after treatment with PNGase-F, but was resistant to Endo-H digestion (Fig. 12). In contrast, the 130 kDa Bmpr2ΔEx2 mutant product underwent a mobility shift after digestion with PNGase-F and Endo-H ($\Delta Ex2 > \Delta Ex2^{1}$). This indicates that wild type Bmpr2 is correctly processed through the ER and Golgi but that the 130 kDa Bmpr2ΔEx2 mutant product is likely to be retained in the ER.

Chemical chaperones restore trafficking of the Bmpr2ΔEx2 mutant product to the cell surface

Since the retention of mutant protein in the ER is often a consequence of incorrect protein folding [127], we wanted to evaluate the effects of two chemical chaperones known to aid in protein folding, 4-PBA and TUDCA [119,120,128-133] , on trafficking of the Bmpr2ΔEx2 mutant product to the cell surface. $Bmpr2^{\Delta Ex2/+}$ ciPECs treated with increasing concentrations of 4-PBA show a dose-dependent increase expression of the 130kDa Bmpr2ΔEx2 mutant product in the streptavidin pull-down (Fig 13A/B). Treatment with 4-PBA also increased the cell surface expression of the 150 kDa wild type Bmpr2 protein in $Bmpr2^{\Delta Ex2/+}$ ciPECs, but to a relatively lesser extent than Bmpr2ΔEx2. An aliquot of cell lysates taken before the streptavidin pull-down

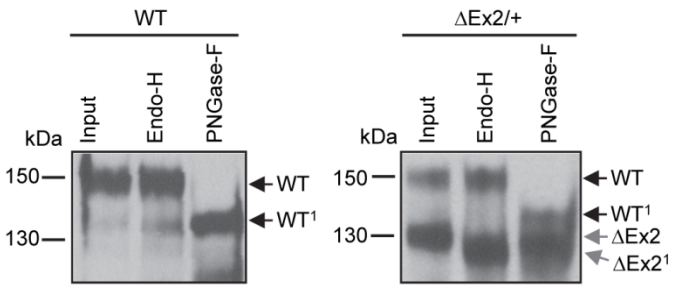

Figure 12. Differential N-linked glycosidase sensitivity of wild type Bmpr2 and Bmpr2ΔEx2 mutant products. Wild type control and *Bmpr2*$^{\Delta Ex2/+}$ ciPEC lysates were immunoprecipitated and digested with N-linked glycosidases Endo-H or PNGase-F. The 150 kDa wild type Bmpr2 bands in both control and *Bmpr2*$^{\Delta Ex2/+}$ ciPECs were sensitive to PNGase-F digestion, determined by a 15 kDa mobility shift (WT>WT^{1}), but were insensitive to Endo-H digestion. Unlike wild type Bmpr2, the 130 kDa Bmpr2ΔEx2 mutant product in *Bmpr2*$^{\Delta Ex2/+}$ ciPECs was sensitive to Endo-H digestion (ΔEx2>ΔEx2^{1}).

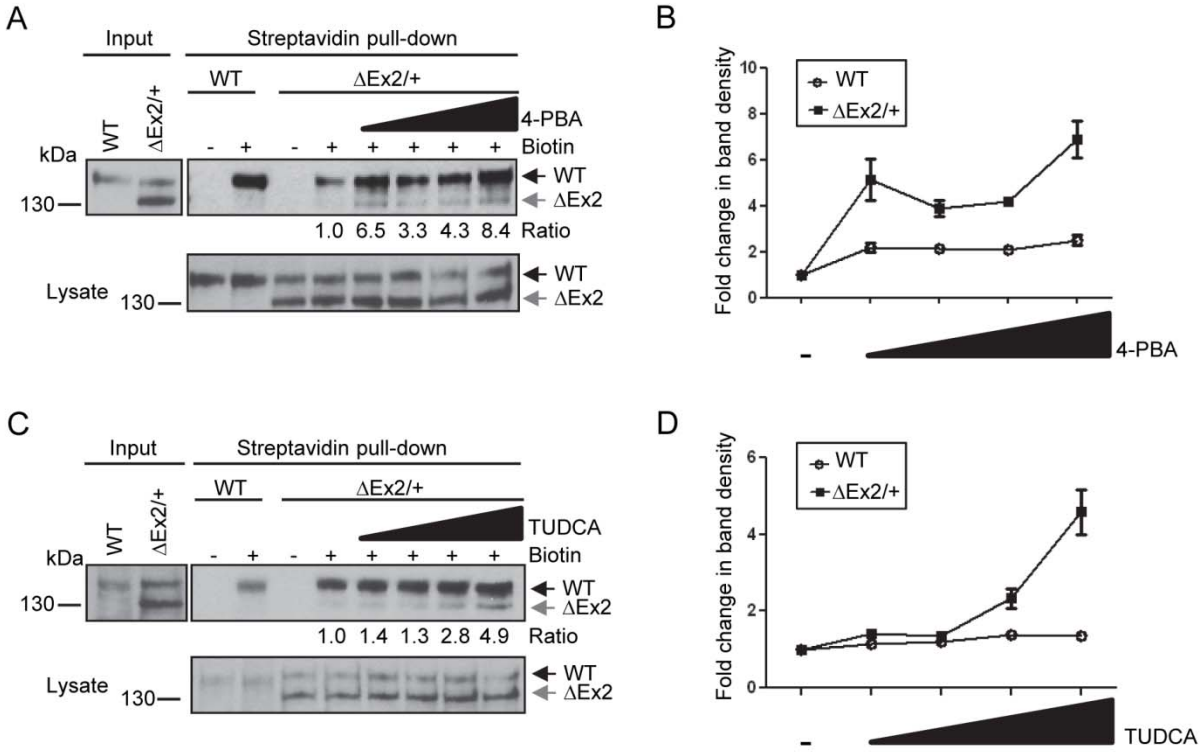
A
Input
Streptavidin pull-down
WT
ΔEx2/+
4-PBA
Biotin
kDa
130
WT
ΔEx2
1.0 6.5 3.3 4.3 8.4 Ratio
Lysate
B
Fold change in band density
4-PBA
C
TUDCA
1.0 1.4 1.3 2.8 4.9 Ratio
D
TUDCA

Figure 13. Chemical chaperones partially restore Bmpr2ΔEx2 mutant product expression at the cell surface. A, Cell surface expression of Bmpr2ΔEx2 in *Bmpr2*$^{\Delta Ex2/+}$ ciPECs treated with 4-PBA. *Bmpr2*$^{\Delta Ex2/+}$ ciPECs were treated for 48 hours with 100uM, 250uM, 500uM or 1mM of 4-PBA. Monolayers were then labeled with membrane impermeable biotin and biotinylated cell surface proteins pulled-down with streptavidin agarose beads. Western Blot was performed with Clone 18 anti-BMPR2 antibody. The 150 kDa wild type Bmpr2 product was detected in the streptavidin pull-down in control and *Bmpr2*$^{\Delta Ex2/+}$ ciPECs, but the 130 kDa Bmpr2ΔEx2 mutant product was not detected. After treating with the chemical chaperone 4-PBA, the 130kDa Bmpr2ΔEx2 mutant product was detected and there was increased expression of the wild type Bmpr2 product in the streptavidin pull-down. Numbers shown below the upper panel indicate the ratio of the 130 kDa Bmpr2ΔEx2 band before and after treatment with 4-PBA. Lower panel, expression of wild type Bmpr2 and Bmpr2ΔEx2 in ciPEC cell lysates with 4-PBA treatment. B, Quantification of wild type Bmpr2 and Bmpr2ΔEx2 band densities after 4-PBA treatment relative to untreated controls from three independent experiments, standard error is indicated. C, Cell surface expression of Bmpr2ΔEx2 in *Bmpr2*$^{\Delta Ex2/+}$ ciPECs treated with TUDCA. Wild type and *Bmpr2*$^{\Delta Ex2/+}$ ciPECs were treated for 5 hours with 50uM 100uM, 250uM or 500uM of TUDCA. Streptavidin pull-down shows that the 130kDa Bmpr2ΔEx2 mutant product was partially restored at the cell surface and there was a slight increase in wild type Bmpr2 with TUDCA treatment (1.4 fold increase with 500μM TUDCA versus untreated cells). Numbers shown below the upper panel indicate the ratio of the 130 kDa Bmpr2ΔEx2 band before and after treatment with TUDCA Lower panel, expression of wild type Bmpr2 and Bmpr2ΔEx2 in ciPEC cell lysates with TUDCA treatment. D, Quantification of wild type Bmpr2 and Bmpr2ΔEx2 band densities after TUDCA treatment relative to untreated controls from three independent experiments.

showed no change in expression of wild type Bmpr2 or Bmpr2ΔEx2 with the addition of 4-PBA (Fig. 13A, lower panel). An additional chemical chaperone, TUDCA added to cells prior to biotinylation also increased cell surface expression of the 130kDa Bmpr2ΔEx2 mutant protein in *Bmpr2*$^{\Delta Ex2/+}$ ciPECs (Fig. 13C/D). There was also a small increase in cell surface expression of wild type Bmpr2 after treatment with TUDCA (a 1.4 fold increase with 500μM TUDCA versus untreated cells). These data indicate that chemical chaperones increase cell surface expression of Bmpr2ΔEx2 in *Bmpr2*$^{\Delta Ex2/+}$ ciPECs, and suggest that ER retention of Bmpr2ΔEx2 results from mis-folding of the mutant protein.

BMP signaling defects in primary pulmonary endothelial cells from Bmpr2$^{\Delta Ex/+}$ *mice*

To determine the functional effects of the *Bmpr2*$^{\Delta Ex2/+}$ mutation on BMP-mediated signaling responses, we evaluated BMP signaling in early passage primary pulmonary endothelial cells (PECs). For this, six separate PEC isolates were prepared from 3 wild type control and 3 *Bmpr2*$^{\Delta Ex2/+}$ mice. There was a significant decrease in BMP-stimulated phospho-Smad1/5/8 expression in *Bmpr2*$^{\Delta Ex2/+}$ PECs associated with reduced basal and BMP-induced Id1 expression (Fig. 14A/B/C). There was also an increase in phospho-Erk1/2 expression in *Bmpr2*$^{\Delta Ex2/+}$ PECs (Fig. 14A/D) but no significant change in phospho-Akt (Fig. 14A/E). These studies indicate that *Bmpr2*$^{\Delta Ex2/+}$ PECs exhibit BMP signaling defects.

Chemical Chaperone 4-PBA restores BMP signaling defects in Bmpr2$^{\Delta Ex2/+}$ *PECs*

To determine whether restoration of cell surface expression of Bmpr2ΔEx2 restores defective BMP signaling in *Bmpr2*$^{\Delta Ex2/+}$ PECs, we evaluated BMP signaling primary PECs isolates obtained from 1 wild type control and 3 *Bmpr2*$^{\Delta Ex2/+}$ mice treated with 4-PBA (Fig. 15A)

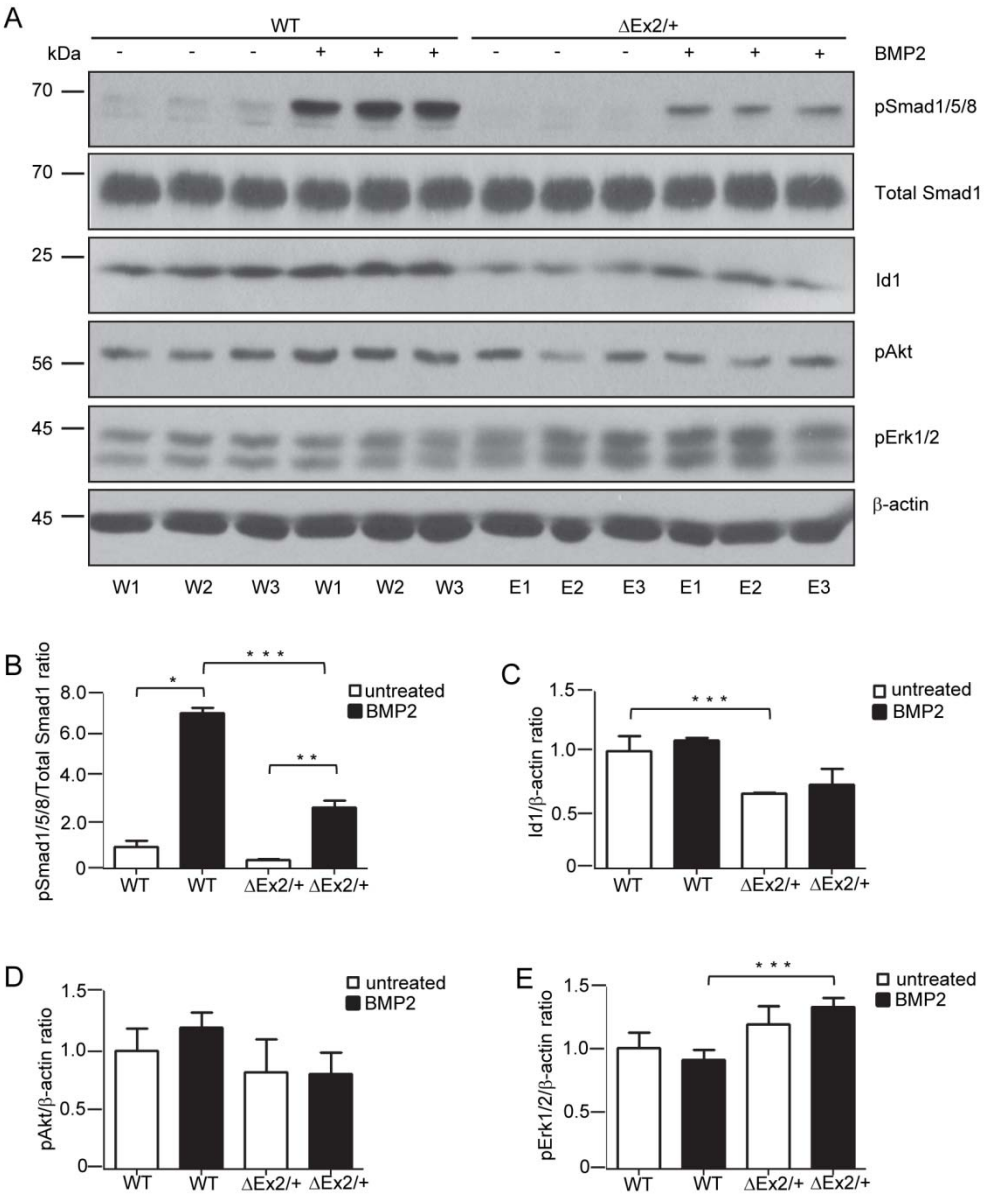

Figure 14. BMP signaling defects in primary pulmonary endothelial cells from *Bmpr2*$^{\Delta Ex2/+}$ mice. Primary PECs were isolated from 3 different wild type control (WT) and 3 *Bmpr2*$^{\Delta Ex2/+}$ mice (ΔEx2). A,Western blot of cell lysates isolated from wild type control (W1-W3) and *Bmpr2*$^{\Delta Ex2/+}$ (E1-E3) PECs treated with 10ng/ml BMP2 for 4 hours. Antibodies indicated on the right. Densitometry for phospho-Smad1/5/8 (B), Id1 (C), pERK1/2 (D) and pAKT bands (E). Results expressed as mean +/- SEM, 3 per group. One-way ANOVA with post hoc Bonferroni correction, $p<0.05$ *WT +/-BMP2; **ΔEx2+/-BMP2; ***WT vs. ΔEx2. Experiment and isolation of primary PECs was replicated four times.

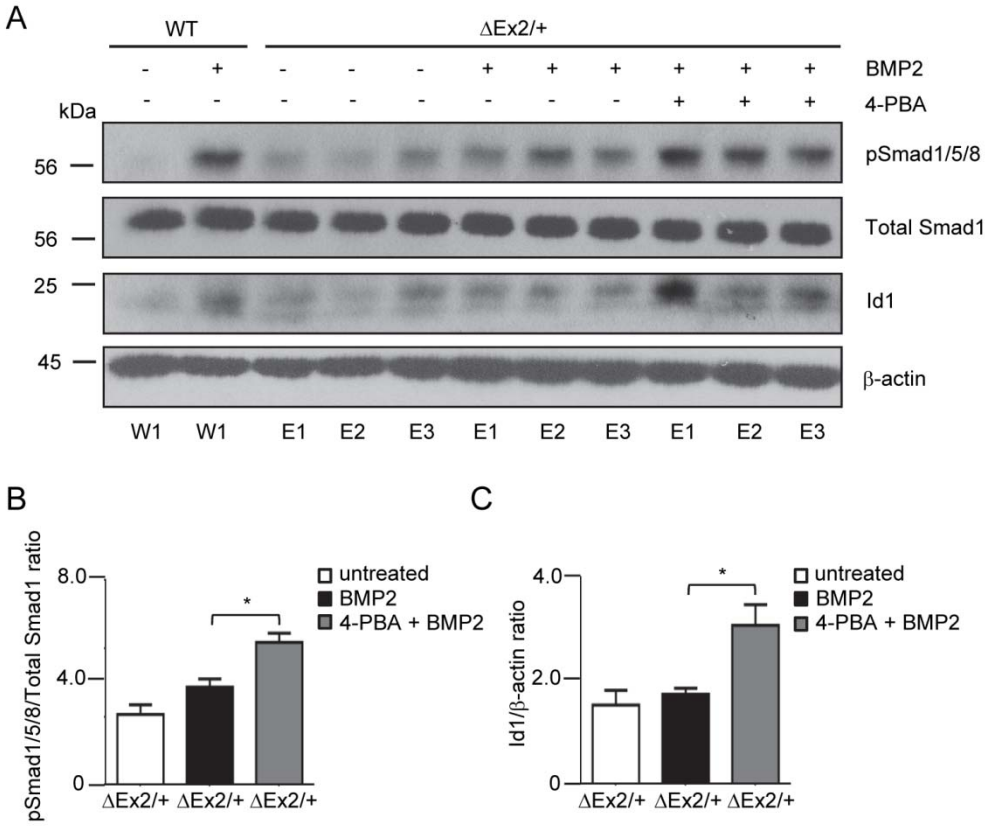

Figure 15. Treatment with 4-PBA rescues signaling defects in *Bmpr2*$^{\Delta Ex2/+}$ pulmonary endothelial cells. Individual primary PECs isolates obtained from 1 wild type control and 3 *Bmpr2*$^{\Delta Ex2/+}$ mice were treated with 1mM 4-PBA for 48 hours followed by BMP2 treatment for 4 hours, as indicated. A. Western blot for phospho-Smad1/5/8 and Id1 shows 4-PBA restores phospho-Smad1/5/8 and Id1 expression in *Bmpr2*$^{\Delta Ex2/+}$ PECs to expression levels similar to BMP-stimulated WT PECs. B. Densitometry for phospho-Smad1/5/8 and C. Id1 expressed as ratio to total Smad1 and β-actin respectively. Results expressed as mean +/- SEM of three individual PEC isolates per group. One-way ANOVA with post hoc Bonferroni correction, $p<0.05$ * ΔEx2/+ +BMP2 vs. ΔEx2/+ +BMP2+4-PBA.

4-PBA restored BMP2 induced Smad1/5/8 phosphorylation (Fig. 15B) and BMP-induced Id1 protein expression in *Bmpr2*$^{\Delta Ex2/+}$ PECs to a level comparable to that seen in wild type PECs treated with BMP2 (Fig. 15C). These data indicate that treatment with the chemical chaperone 4-PBA restores the defective BMP-Smad/Id1 signaling axis in *Bmpr2*$^{\Delta Ex2/+}$ PECs.

Discussion

In these studies, we provide the first evidence that an NMD negative *BMPR2* mutation found in patients with HPAH is expressed endogenously, and that this mutant protein product is mis-folded and incorrectly trafficked to the cell surface. We also show that chemical chaperones partially restore cell surface expression of the same *Bmpr2* mutant product in pulmonary endothelial cells from mice carrying the same heterozygous germ line mutation, and that treatment with chemical chaperones rescues the associated BMP signaling defects in these cells. These data provide the first evidence for the therapeutic use of chemical chaperones to correct endogenous signaling defects resulting from mis-folded *BMPR2* mutant products in patients with HPAH.

Our studies focus on the expression and trafficking of these *BMPR2* mutant products in pulmonary endothelial cells from *Bmpr2*$^{\Delta Ex2/+}$ mice since BMPR2 is highly expressed in endothelial cells in the pulmonary vasculature, and endothelial expression of BMPR2 has been implicated in maintaining normal pulmonary vasculature tone and integrity[44,78,89,99,100,134]. We have also previously shown that mice with heterozygous in-frame deletion of *Bmpr2 Exon2 (Bmpr2*$^{\Delta Ex2/+}$*)* have reduced endothelium-dependent vasodilator responses in the pulmonary vasculature [99], and approximately 30% of mice with conditional ablation of *Bmpr2* in endothelial cells develop spontaneous pulmonary hypertension [100]. These

findings suggest that endothelial BMPR2 plays an important role in the regulating pulmonary vascular function, and suggests strategies to correct BMP signaling in pulmonary endothelial cells may have beneficial effects on the pulmonary vasculature in mice and HPAH patients with *BMPR2* mutations.

We found that the Bmpr2ΔEx2 mutant product was expressed at high levels in pulmonary endothelial cells isolated from $Bmpr2^{\Delta Ex2/+}$ mice. The identity of this band was verified as the in-frame deletion of Exon2 by using an antibody raised against the peptide sequence encoded by *BMPR2 Exon2* (ASQ). This in-frame deletion of Exon2 is also expressed in the F108 HPAH patient-derived lymphocytes. However, there are differences in mobility of both wild type BMPR2 and the BMPR2ΔEx2 products in mouse ciPECs and cultured human lymphocytes. This is likely due to cell-type dependent differences in post-translational modifications/glycosylation of BMPR2. In addition, unlike F108 HPAH patient–derived lymphocytes, the presumed Bmpr2ΔEx2 mutant product in $Bmpr2^{\Delta Ex2/+}$ ciPECs had an expression level similar to the 150 kDa wild type Bmpr2 product. This indicates that there are cell-type dependent differences in expression of the mutant allelic products, and that high levels of Bmpr2ΔEx2 expression in endothelial cells may exert more profound effects on cellular function than in different cell types. Cell surface biotinylation and N-glycosidase sensitivity assays indicate that the Bmpr2ΔEx2 mutant product does not traffic correctly to the cell surface and is retained in the ER. Additionally, chemical chaperones 4-PBA and TUDCA, agents that are known to aid in protein folding [119,120,128-133], partially restore trafficking of the Bmpr2ΔEx2 mutant product to the cell surface. These findings suggest that the Bmpr2ΔEx2 is retained in the ER as a result of mis-folding of the mutant product. Since deletion of *Exon2* in Bmpr2ΔEx2 results in a loss of 3/10 cysteine residues located in the ligand-binding domain of Bmpr2, it is likely that mis-folding

occurs as a result of a breakdown in paired cysteine disulfide bond formation which is required for correct Bmpr2 structure and folding in the ER [135-138].

Our data suggest that chemical chaperones may be used to correct BMP signaling defects in HPAH patients with NMD negative *BMPR2* mutations. Functional studies show that 4-PBA treatment can restore CFTR receptor ΔF508 mutant trafficking and function in cells derived from Cystic Fibrosis (CF) patients [120], and 4-PBA has recently been used in clinical trials as a chemical chaperone to treat CF [139,140]. Treatment with chemical chaperones like 4-PBA aid in protein folding and trafficking to the cell surface; however it is important to note that there are a number of NMD negative *BMPR2* mutations located in regions of the protein that would not benefit from trafficking to the cell surface. For example, mutations located in the kinase domain or cytoplasmic tail domains of BMPR2 in particular may not benefit from chaperone treatment. For this strategy to work in HPAH patients with NMD negative *BMPR2* mutations, the mutations must allow at least partial BMPR2 function when the mutant product is expressed at the cell surface. Correcting a protein-folding defect of an HPAH NMD negative *BMPR2* mutant product that has dominant negative activity when expressed at the cell surface might have adverse effects on BMP signaling. This has been demonstrated with the kinase inactive HPAH *BMPR2 C483R* mutation in in a heterologous over-expression system [116], but still needs to be evaluated endogenously in HPAH patient-derived cells. In the case of Bmpr2ΔEx2, correction of BMP signaling defects by chemical chaperones may be occurring through two non-mutually exclusive mechanisms. While the Bmpr2ΔEx2 mutation interferes with the structure of the ligand-binding domain of the receptor (and presumably therefore interferes with ligand binding to the receptor), Bmpr2ΔEx2 may still participate in functional hetero-tetrameric complexes with wild type BMPR2 and other BMP Type 1 receptors that can independently directly engage BMP ligands at

the cell surface. Interestingly, 11% of NMD negative *BMPR2* mutations are in the ligand-binding domain of BMPR2 [45], and may similarly benefit from corrected trafficking to the cell surface. However, in addition to restoring cell surface expression of the mutant allelic product, our data show that 4-PBA, and to a lesser extent TUDCA, increase cell surface expression of wild type Bmpr2 in *Bmpr2*$^{\Delta Ex2/+}$ ciPECs. Since mis-folding of Bmpr2ΔEx2 may trap some wild type Bmpr2 in the ER, it is possible that this effect is a direct consequence of 4-PBA-dependent correction of the cell surface trafficking defect of the mutant allele. Given that expression levels of Bmpr2 have been shown to be important in maintaining normal signaling function [43,125], this increase in expression of wild type Bmpr2 protein at the cell surface may account for the restoration in BMP signaling in *Bmpr2*$^{\Delta Ex2/+}$ ciPECs after treatment with chemical chaperones. However, irrespective of the mechanisms restoring BMP signaling in *Bmpr2*$^{\Delta Ex2/+}$ ciPECs, our data indicate that there may be a subset of HPAH patients with NMD negative *BMPR2* mutations that show beneficial responses to protein folding agents. Further analysis of endogenous *BMPR2* mutant product folding and signaling defects in HPAH patients carrying different NMD negative *BMPR2* mutations will have to be performed to determine which patients might benefit from this therapy.

Our studies provide the first evidence that chemical chaperones can be used to rescue BMP signaling defects associated with endogenously expressed NMD negative HPAH *BMPR2* mutations in the pulmonary endothelium. Additionally, the chemical chaperones we evaluated, 4-PBA and TUDCA, are FDA-approved drugs and commercially available supplements, respectively, and are in clinical trials for other diseases caused by mis-folded proteins [139-141]. Therefore, while further analysis of endogenous *BMPR2* mutant product folding and signaling defects in HPAH patients will have to be performed to determine which patients might benefit

from this therapy, our data suggest an additional disease modifying therapy that may benefit a subset of HPAH patients with NMD negative *BMPR2* mutations.

CHAPTER IV

GENERATION AND DIFFERENTIATION OF INDUCED PLURIPOTENT STEM CELLS FROM HPAH PATIENT FIBROBLASTS

Introduction

Heritable pulmonary arterial hypertension (HPAH) is a progressive disorder characterized by occlusion of small pulmonary arteries leading to increased mean pulmonary arterial pressure and right heart failure. Over 200 different mutations have been identified throughout the *BMPR2* open reading frame in HPAH patients but despite the commonality of these mutations disease penetrance is relatively low [45,46,104]. A recent study from Vanderbilt suggests that NMD- mutations cause more severe HPAH. Using mRNA isolated from peripheral blood lymphoblasts, they identified 24 NMD- *BMPR2* mutations in 54 HPAH patients with known *BMPR2* mutations. These patients had disease onset and death compared to the NMD+ patients that did not produce a mutant *BMPR2* transcript [104]. This suggests that NMD- *BMPR2* mutant products exert dominant inhibitory effects on vascular target cells.

Evidence of dominant negative effects of an NMD- mutation comes from two independent sources. Studies from Nick Morrell's group show that the NMD- mis-sense *BMPR2* mutation, *BMPR2 C118W* is mis-folded, retained in the ER and exerts inhibitory effects on BMP signaling by sequestrating other BMPR1 receptors in the ER [116]. However, these studies were carried out using transient over-expression systems, so the functional consequences of

endogenous mutations are largely unknown. Studies from our laboratory have shown that mice carrying a heterozygous mutation at the *Bmpr2* locus, *Bmpr2*$^{\Delta Ex2/+}$, which is indistinguishable from an NMD- HPAH mutation Family 108, *BMPR2ΔEXON2*, develop more severe hypoxic PH that mice carrying a heterozygous null *Bmpr2*$^{+/-}$ mutation ([99], Chapter 2). Furthermore, mice carrying the *Bmpr2*$^{\Delta Ex2/+}$ mutation have defects in pulmonary vascular tone with EC dysfunction and reduced Smad phosphorylation. The key question therefore is whether endogenously expressed NMD- *BMPR2* mutant product directly from HPAH patients exert similar dominant inhibitory effects.

HPAH-patient derived cells are rare, difficult to propagate, and usually of end-stage disease. Additionally, it is difficult to get patient cell lines of vascular cells, as this requires a lung biopsy. For these reasons, we decided to generate several iPSC lines from multiple NMD+ and NMD- *BMPR2* mutant patients in order to study the specific effects of mutation type on endothelial cell function. iPSCs are a new technology that offer a noninvasive way to study human genetic diseases. iPSCs are generated by reprogramming differentiated adult cells to a pluripotent, stem cell-like state from which they can be differentiated into a range of different cell types. As such, these cells represent an unlimited pool of cells to study cell differentiation, disease modeling, and drug therapy [142-144]. Given difficulty in obtaining pulmonary ECs from patients with HPAH, this technology provides a unique opportunity to study the biology of endogenously expressed *BMPR2* mutant products in vascular target cells. There are several established methods for reprogramming IPSCs from skin fibroblasts. One of the best characterized systems involves the transduction of cultured skin fibroblasts with three ES-cell factors, *OCT3/4, KLF4, SOX2*, using a sequential lentiviral/retroviral over-expression system [145]. After 3 weeks, iPSC colonies begin to form, providing a large pool of stem cells that can

be used to generate EC. This method was initially used in these studies to generate control lines . After several attempts to use this method to generate iPSCs from HPAH fibroblasts, we changed approaches and utilized a different method which added p53 suppression and nontransforming L-Myc in addition to ES-cell factors *OCT3/4*, *SOX2*, *KLF4*, and *LIN28,* to generate iPSCs [144]. Validation of iPSCs includes RT-PCR to check for the expression of pluripotent markers, karyotype analysis of each line, and teratoma formation[145].

Here we describe the generation of several iPSC lines from HPAH fibroblasts containing NMD+ and NMD- mutations and begin to develop EC differentiation protocols to study endogenous *BMPR2* biology in HPAH. This technology will provide a powerful tool to explore the biology of *BMPR2* mutations in other vascular cell types, and effects of other mutations on vascular cell function in other inherited cardiovascular diseases.

Materials and Methods

Ethics statement

The Vanderbilt University Medical Center Institutional Review Boards approved use of control of HPAH patient-derived fibroblasts obtained by skin biopsy and participants gave informed written consent for use of their fibroblast cultures for study (IRB#9401). Patient fibroblasts were obtained from the Vanderbilt HPAH skin fibroblast repository.

Patient fibroblast cell culture

Cells were maintained in complete media, DMEM media (Life Technologies) supplemented with 20% fetal bovine serum (FBS)(Sigma), 1% pen/strep (Life Technologies), and 1% non-essential amino acids (Sigma). To passage fibroblasts, complete media was

aspirated, cells were rinsed with D-Phosphate Buffered Saline (D-PBS)(Life technologies), and detached from 10cm cell culture dish with 0.05% Trypsin-EDTA (Life technologies). Trypsin was neutralized with the addition of complete media, cells were centrifuged, counted and re-plated as experiment required.

Generation of human iPSCs from HPAH fibroblasts

Methods were adapted from [144,146] (Figure 16). 6 $X10^5$ patient fibroblasts were necessary for transduction. Fibroblasts were trypsinized (see above), and spun in a tabletop centrifuge at 200 x g for 5 minutes at room temperature, counted and re-suspended in Neon tube (Life technologies) with 115µl re-suspension buffer provided in the Neon 100µl kit (Life technologies). 1µg of pCXLE-hOCT3/4-shp53, 1µg of pCXLE-hSK, and 1µg of pCXLE-hUL (plasmids described in [144], Addgene) were added to the fibroblasts in suspension. Cells were electroporated using the Neon transfection system (Life technologies) set to 1,650 volts, 10 ms, 3 time pulses, per plate. Cells were then plated in complete media. Media was changed the next day to remove cell debris and then replenished every other day for 7 days. On day 7, fibroblasts were trypsinized and 1 X 10^5 fibroblasts were plated on 1.8x 10^6 SNL feeder cells (MMRC, UC Davis, CA) per 10cm dish. 24 hours later complete media is changed to hES media: DMEM/F12 (Life technologies), 20% Knockout serum replacement (Life technologies), 0.5% Glutamax (Life technologies), 1% pen/strep (Life technologies), 1% non-essential amino acids (Sigma), rhFGF basic (8ng/ml final concentration, Promega), β-mercapatoethanol (100µM final concentration, Sigma). hES media was replenished daily. 2-4 weeks later, emerging iPS colonies were picked individually, plated in 24-well plates coated with stem cell-grade matrigel (BD), per manufacturer specified dilution. 5 days later, hES media was replaced with 75% hES, 25% mTESR1 (Stemcell technologies). 5 days later, media was transitioned to 50% hES and 50%

mTESR1, and so on until iPS colonies were maintained in 100% mTESR1. Areas of differentiation (assessed visually) were manually scraped away from each iPS colony once every 2-3 days. Media was replaced daily.

Immunofluorescence

Cells were fixed in PBS containing 4% paraformaldehyde (PFA) for 10 minutes at room temperature and then permeabilized in 0.1% Saponin for 15 minutes. Cells were then incubated in 10% donkey serum in PBS for 1 hour, and incubated overnight at 4^{o}C with primary antibodies at the following dilutions: SSEA3 (1:500 Millipore), SSEA4 (1:500 BD Biosciences), TRA1-81 (1:500 Millipore), and OCT4 (1:2000 Millipore) diluted in 10% donkey serum in PBS. Secondary antibodies conjugated to DyLight 488 (1:200), DyLight 549 (1:400) (Jackson ImmunoResearch) were used.

Alkaline phosphatase assay

An alkaline phosphatase kit (Sigma) was used to stain iPS colonies, as per manufacturer's protocol.

Endothelial differentiation

For these experiments the 2 control iPSC lines BG4 and BG6 (a kind gift from Dr. Kevin Ess) were used. Protocol was adapted from [147,148]. Briefly, iPSCs were grown on SNL feeder cells in differentiation media (DM) for 10 days. VEGFR2+; VE-Cadherin+ cells were sorted by a FACS ariaII (BD) and re-cultured onto collagen IV-coated plates without feeder cells and addition of 50ng/ml VEGF.

FACs sorting

Cells were detached and pelleted using a centrifuge at 200 x g for 5 minutes. Cells were resuspended, washed in PBS and recentrifuged. The cell pellet was resuspended in 100µl PBS containing fluorescently conjugated primary antibodies, CD34-PE (abCam) and VEGFR2-APC (BD Pharmigen). Cells were incubated for 20 minutes on ice protected from light. Cells were then pelleted and washed in ice-cold PBS and re-suspended in 200µl of PBS. FACs analysis was performed by the VA FACs CORE.

RT-PCR validation

Total RNA from BG4 and BG6 iPScs was prepared using the RNeasy kit (Qiagen, Valencia, CA) according to the manufacturer's instructions. Isolated mRNA was then reverse transcribed into cDNA on a Thermocycler (Bio-Rad) using SuperScript III (Invitrogen) according to the protocol provided by manufacturer. qRT-PCR was performed with Power SYBR Green Master Mix (Applied Biosystems) on an ABI 7900HT fast real-time PCR detection system (Applied Biosystems)

Results

HPAH fibroblasts with NMD positive and negative BMPR2 mutations

We used 4 different HPAH fibroblast cell lines from the Vanderbilt HPAH Tissue Repository (Table 4) to generate multiple iPSC lines with the aim to create a protocol to differentiate HPAH patient-derived iPSCs into ECs, and to use these ECs to evaluate the NMD pathway in patients with different *BMPR2* mutations in a physiologically relevant environment. Family 14 is a NMD- Cysteine to Tryptophan point mutation occurring at amino acid 118, part

Family	Phenotype	Mutation	NMD Status	Gender
F16	HPAH	C117Y	Negative	Female
F16	Healthy	C117Y	Negative	Male
F29	HPAH	C118W	Negative	Male
F29	Healthy	C118W	Negative	Male
F29	HPAH	C118W	Negative	Female
F14	HPAH	C118W	Negative	Male
F14	HPAH	C118W	Negative	Female
F14	HPAH	C118W	Negative	Male
F14	HPAH	C118W	Negative	Male
*F14	HPAH	C118W	Negative	Female
*F108	HPAH	ΔEX2	Negative	Female
F28	HPAH	R322X	Positive	Female
F28	HPAH	R322X	Positive	Male
F28	HPAH	R322X	Positive	Female
*F173	HPAH	R491W	Pending	Female
*F150	HPAH	835F/S	Positive	Female
F150	Healthy	835F/S	Positive	Female
F146	HPAH	Pending	Pending	Female
S747	SPAH	Pending	Pending	Female
F139	HPAH	Pending	Pending	Female
F48	HPAH	None	None	Male
F48	HPAH	None	None	Female
F48	HPAH	None	None	Male

Table 4. HPAH skin fibroblast repository at Vanderbilt (+3 normal controls, +3 HPAH without mutation). *Skin fibroblasts used to generate iPSCs.

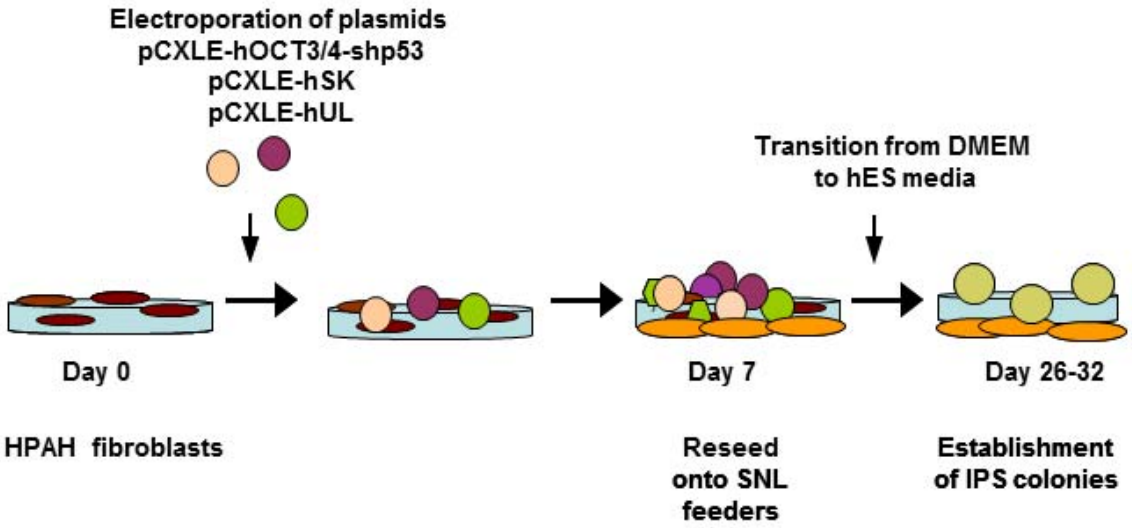

Figure 16. Method of HPAH fibroblast iPS cell induction. HPAH fibroblasts are electorporated with plasmids driving the expression of p53 shRNA and OCT3/4 (pCXL-hOCT3/4-shp53), SOX2 and KLF4 (pCXL-HSK), and L-MYC and LIN28 (pCXLE-hUL). Fibroblasts are then replated onto SNL feeder cells, DMEM is replaced by hES media, and iPS colonies begin to form 2-3 weeks after transduction.

of the ligand binding domain of BMPR2. The *C118W* mutation has been characterized previously using a transient over-expression system, where it was shown that the mutant receptor was unable to traffic to the cell surface [116]. F108 is another NMD- mutation, and results in an in-frame deletion of *BMPR2 EXON2*. We have previously characterized this type of mutation using F108 HPAH lymphocytes, a mouse model, $Bmpr2^{\Delta Ex/+}$ (Chapter II and [99]), and in primary mouse pulmonary endothelial cells derived from the mouse model (Chapter III). F150 is an NMD+ *BMPR2* mutation, a frameshift in the cytoplasmic tail of BMPR2, which is predicted to result in a haploinsufficient phenotype. The final fibroblast line F173 is a predicted NMD- missense point mutation, Arginine 491 to Tryptophan, between the kinase domain and cytoplasmic tail of BMPR2. Although predicted to be an NMD- mutation, it is important to note that this fibroblast line has not been validated at this time.

Generation of iPS cells from HPAH fibroblasts

In order to generate iPS cell lines from the HPAH fibroblasts, we utilized a method reported to have enhanced efficiency of reprogramming with episomal plasmids (Figure 16) [145]. This system features two unique characteristics compared to other methods, the addition of L-MYC as a reprogramming factor in replacement of the more traditional C-MYC, and the suppression of p53 [144]. HPAH fibroblasts were electorporated with plasmids expressing *TP53* shRNA, *OCT3/4, L-MYC, SOX2, KLF4, and LIN28* and then reseeded on SNL feeder cells. Compared to traditional reprogramming mechanisms with *OCT3/4*, *SOX2*, *KLF4*, *c-MYC*, *LIN28* and *NANOG* [142,149], which in our hands yielded less than 5 potential iPS colonies, this method resulted in greater than 50 potential iPS colonies. Potential colonies were expanded based on morphology, characterized by large nuclei and minimal cytoplasm and alkaline phosphatase staining, which is expressed on the cell membrane of stem cells [150] (Figure 17).

Each HPAH fibroblast line produced multiple alkaline positive colonies. Three were selected from each of the original fibroblast lines for further validation; the remaining colonies were frozen and stored for future use. 3 F150 and F173 alkaline phosphatase positive colonies were expanded and then evaluated for the expression of pluripotent stem cell markers SSEA3 and SSEA4 [151], TRA1-81 [152], and OCT4 [153] (Figure 18). Expression of the pluripotent markers varies widely between lines derived from the same HPAH fibroblasts as wells as from lines derived from different HPAH fibroblasts, with expression of OCT4 notably reduced in almost all lines. Further validation of the colonies is required before they can be considered iPS colonies. This includes RT-PCR to detect possible integration of episomal plasmids, which would result in the invalidation of a line, qRT-PCR to detect the expression of pluripotent markers, karyotyping, teratoma formation, and embryoid body formation and differntion.

Preliminary evaluation of endothelial cell differentiation

While we were generating iPSCs from HPAH fibroblasts, we evaluated endothelial differentiation protocols with control iPSCs BG4 and BG6 with the aim of determining the timing of the highest level of expression of endothelial cell markers by using FACs and RT-PCR. We began with the simplest endothelial cell differentiation protocol [147,148] (Figure 19.) We first evaluated the expression of endothelial markers CD-34 and VEGFR2 in BG6 cells by FACs analysis in cells grown for 10 days in differentiation media compared to normal hES media (Figure 20A). There is a subtle but clear population of cells that express CD34 or VEGFR2 after 10 days in differentiation media. We further evaluated the expression of CD34 and VEGFR2 at days 0, 2, 4, 6, 8, and 10 in differentiation media. Cells grown in normal hES media have no marked increase in the expression of either CD34 or VEGFR2 (Figure 20B and C). Conversely, there is an increase in cells expressing CD34 and VEGFR2 grown in

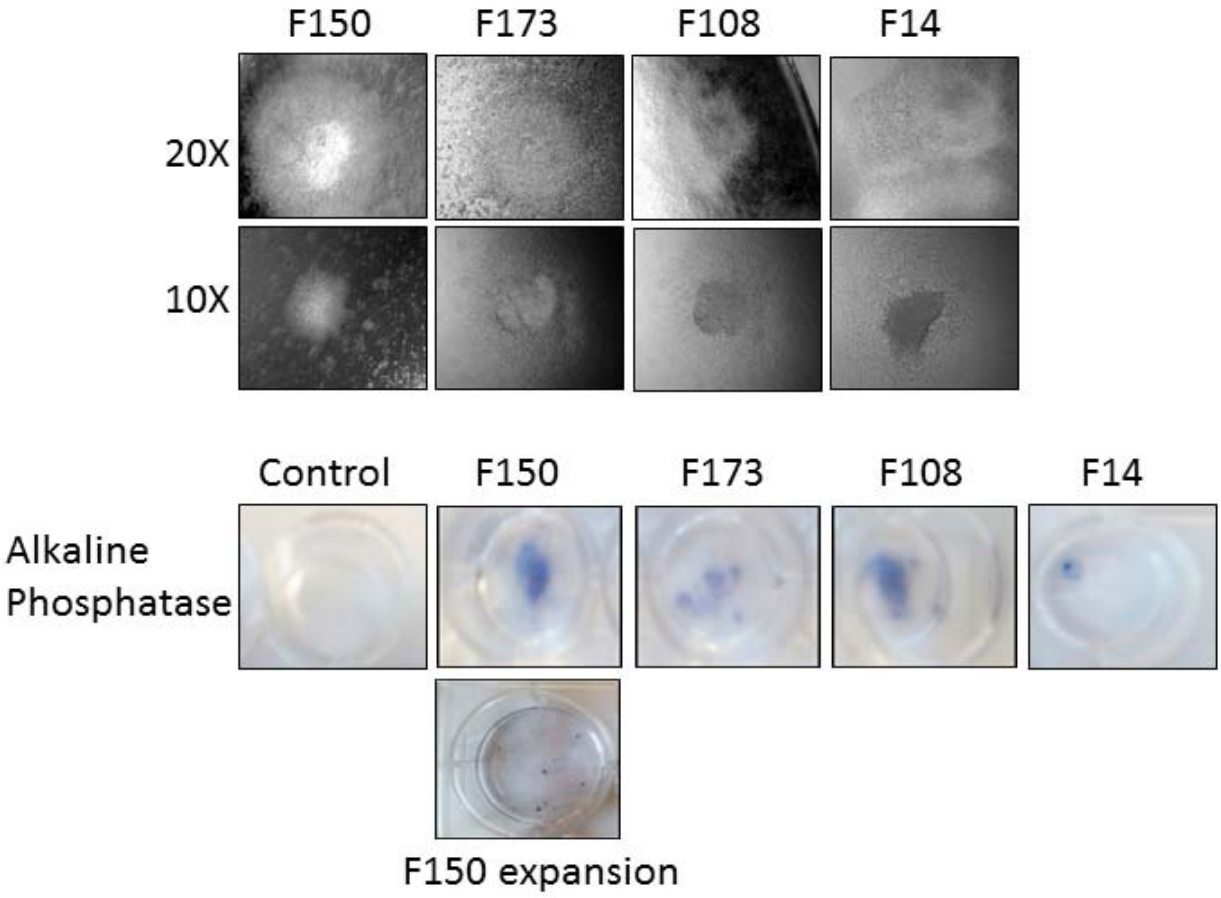

Figure 17. Preliminary validation of HPAH iPS colonies. Top, potential iPS colonies forming 2-3 weeks after the 4 HPAH fibroblast lines, F150 (NMD+), F173 (NMD-), F108 (NMD-), and F14 (NMD-) were transduced with reprogramming factors. Each fibroblast line produced greater than 10 potential iPS colonies. Bottom, positive alkaline phosphatase stain of iPS colonies. Control is HPAH F150 fibroblasts, and are alkaline phosphatase negative. Bottom-most panel is the expansion of a single F150 colony into multiple colonies.

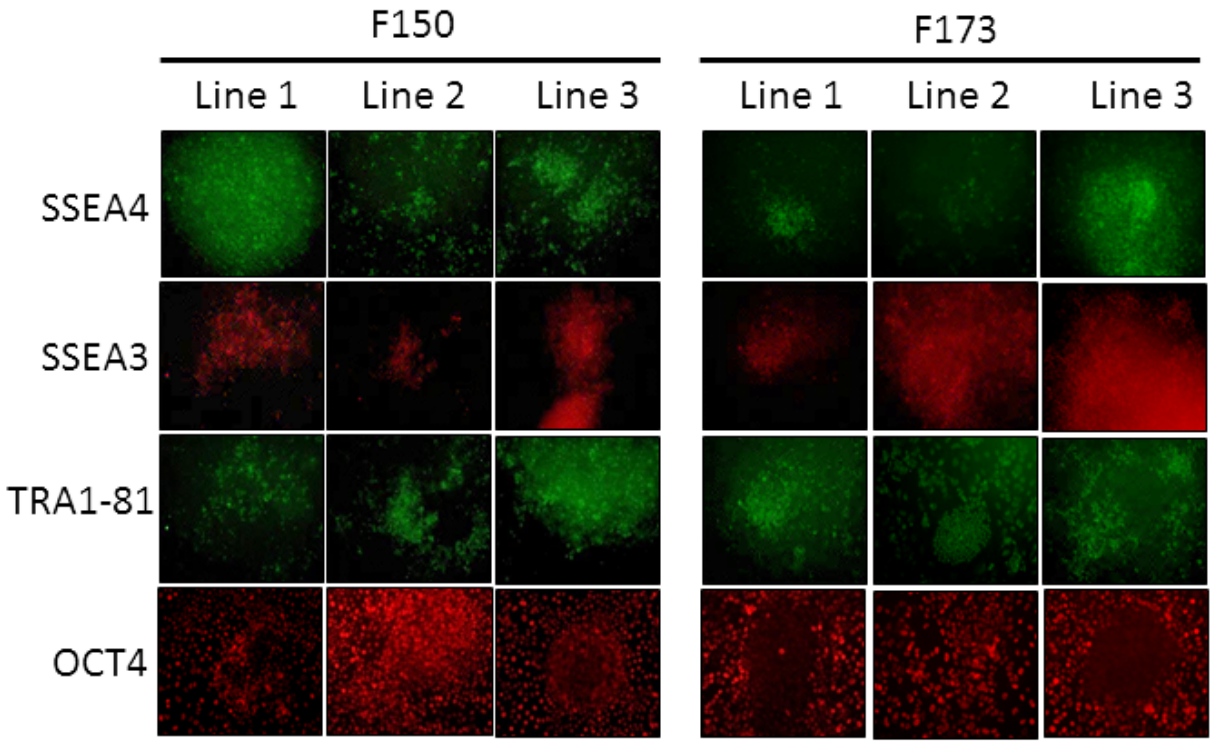

Figure 18. Expression of pluripotent markers in iPS cell lines. Three potential iPS colonies were expanded and evaluated for pluripotent markers from HPAH F150 and F173.

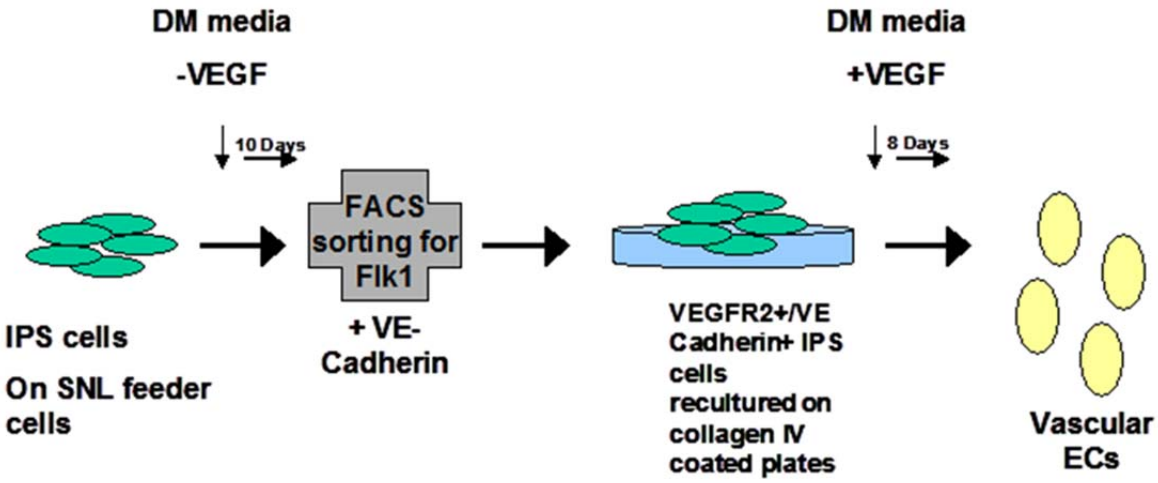

Figure 19. Endothelial cell differentiation strategy. Cells are grown in differentiation media and the FACs sorted for expression of endothelial markers, replated on collagen-coated plates and further differentiated with the addition of VEGF

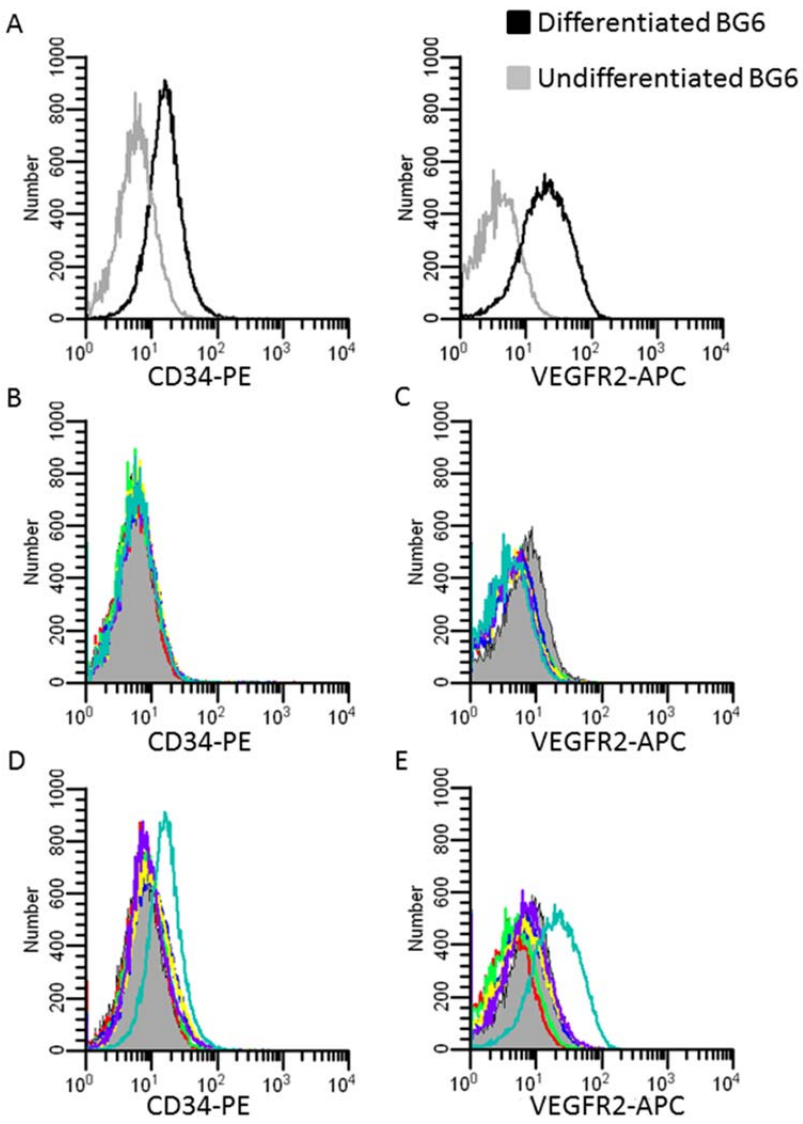

Figure 20. Expression of CD34-PE and VEGFR2-APC in control iPS line BG6. A. Expression of CD34 and VEGFR2 in undifferentiated cells versus differentiated cells at day 10. B. Expression of CD34 in undifferentiated cells at day 0,2,4,6,8, and 10 (day 10 is the blue line). C. Expression of VEGFR2 in undifferentiated cells at day 0,2,4,6,8,10 (day 10 is the blue line). D. Expression of CD34 in cells undergoing differentiation at day 0,2,4,6,8,10 (day 10 is blue). E. Expression of VEGFR2 in cells undergoing differentiation at day0,2,4,6,8,10.

differentiation media, but not until day 10 (Figure 20D and 20E, blue line). These results indicate that the highest level of endothelial marker expression is at 10 days in differentiation media, and that this would be the optimal time to FACs sort the EC marker expressing cells and begin the second part of the differentiation protocol.

Expression of endothelial cell, smooth muscle cell, and pluripotent markers in BG4 and BG6

To validate the expression of endothelial cell markers using a second method, as well as to evaluate the expression of SMC markers and pluripotent markers, we performed RT-PCR in BG4 and BG6 control cells 1, 3, 5, 7, 9, and 11 days after endothelial cell differentiation initiation. We found that BG6 had lower levels of pluripotency markers *OCT3*, *KLF4, NANOG, DNMT3B*, and *SOX2* than BG4 (Figure 21), indicating that those these control cells may be harder to maintain as iPS cells, they may demonstrate a greater capacity of differentiation into endothelial cells. This was partially confirmed by evaluation of EC markers (Figure 22). While BG6 cells expressed higher levels of *VEGFR2* transcripts, BG4 expressed higher levels of *VE-CADHERIN*. Neither BG6 nor BG4 expressed significant levels of *PECAM*. SMC markers were more similarly expressed in both control lines.

Taken together, these results represent a beginning. Further validation of HPAH iPS cells is required before they can be used experimentally. Additionally, further optimization of endothelial differentiation protocols is needed. However, these findings demonstrate that there is variability between iPS lines, and these differences may affect the ability of a cell line to self-renew and remain pluripotent as well as the lines ability to differentiation into a specific cell type. For example, BG6 expresses EC markers with stimulation and may be easier to push down an endothelial lineage than BG4.

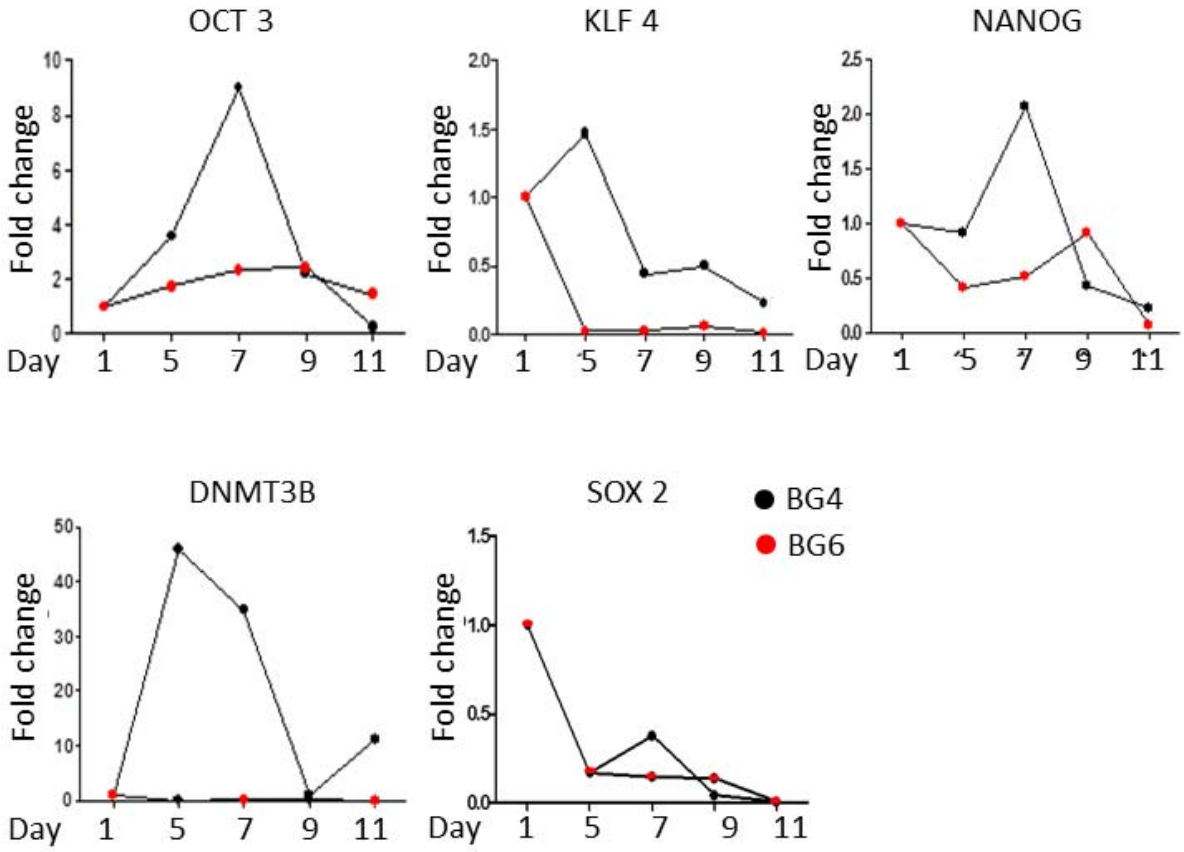

Figure 21. Evaluation of pluripotent markers in BG4 and BG6 cells undergoing differentiation. BG6 has less expression of *OCT3, KLF4, NANOG, DNMT3B*, and *SOX2* compared to BG4 except on day 9 of differentiation.

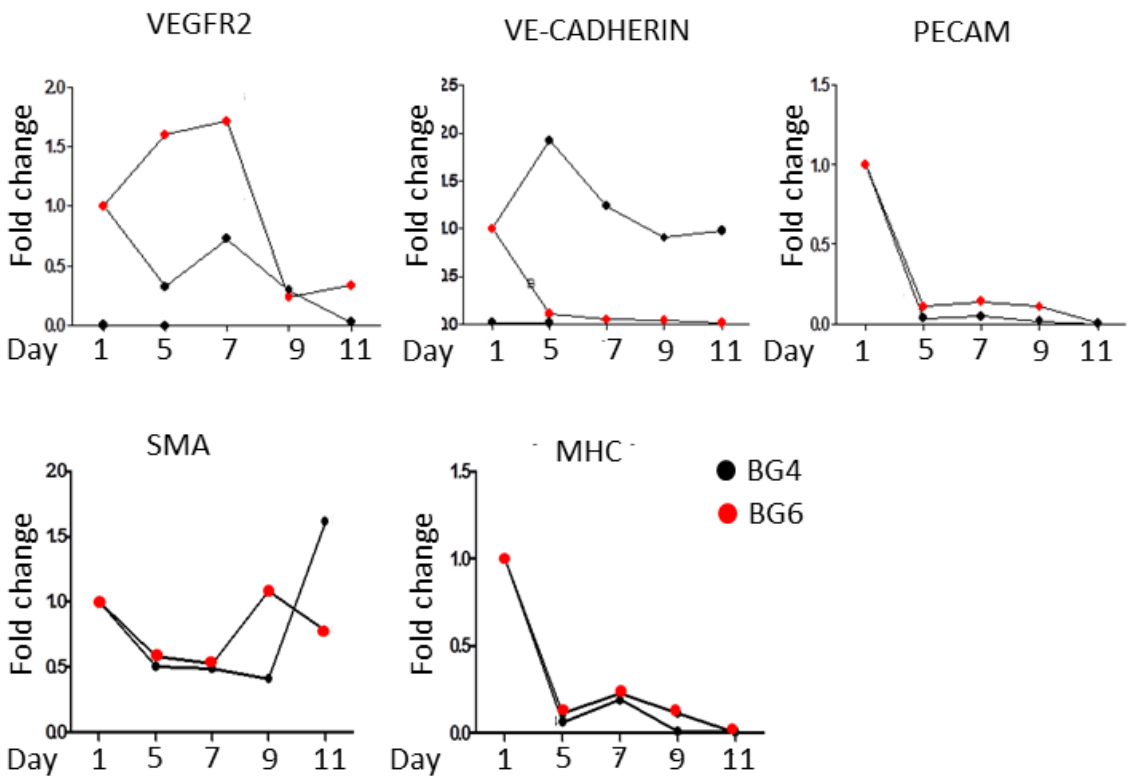

Figure 22. Evaluation of markers of endothelial cells and smooth muscle cells in BG4 and BG6 cells undergoing differentiation. BG6 has less expression of endothelial marker *VEGFR2* and reduced expression of endothelial marker *VE-CADHERIN* compared to BG4. Neither strongly express endothelial marker *PECAM*. BG6 and BG4 express similar levels of smooth muscle cell markers smooth muscle alpha (*SMA*) and myosin heavy chain (*MHC*).

Discussion

The recent advancements in iPS cell generation provides an exciting opportunity to evaluate patient-specific responses in a *BMPR2* mutation-type and cell-type specific way. The role of BMPR2 signaling in vascular cells isolated from experimental models of PH and from patients (often deceased or in end-stage disease) is convoluted and unclear [80,86,95,154]. iPSCs would provide a limitless source of patient-derived endothelial cells that would otherwise be difficult to obtain.

Additionally, current treatments for PAH mostly target the vasodilatory response and have little effect on vascular remodeling or hemodynamics [36,38-40]. This is compounded in HPAH where very few patients respond to current vasodilatory therapies [2]. 5 year survival rates among these patients are significantly lower than in patients without *BMPR2* mutations or with other forms of PH [35]. Patient-derived iPSCs could be adapted to a high-throughput system that could be used to evaluate patient-specific and mutation-specific responses to drugs, aid in drug-discovery, or aid in the identification of new pathways that could be used for more targeted for therapies.

The differentiation protocol reported here is outdated, and more recent protocols offer more detailed and better characterized approaches that result in a larger percentage of cells undergoing differentiation [155,156]. That said, there are differences in signaling function and protein expression in the vascular endothelium based on where it is localized (proximal or distal) and whether it is vascular endothelium or pulmonary vascular endothelium [82,157]. This in part leads to the confusion of the role of the endothelium in HPAH. To date, current differentiation

protocols are not detailed enough distinguish between vascular endothelial cell types. This could cause further signaling discrepancies in future studies.

In conclusion, this work demonstrates a highly effective system for generating iPS cells from patient fibroblasts and provides a preliminary evaluation of HPAH-derived iPS cells, and of endothelial differentiation pathways. Interestingly, BMPR2 signaling has been shown to be a necessary component in the differentiation of stem cells and progenitors, usually by promoting differentiation [158,159]. It is unclear how the reported HPAH *BMPR2* mutations will affect the ability of iPS lines to undergo differentiation.

CHAPTER V

DISCUSSION AND FUTURE DIRECTIONS

The studies reported in this dissertation were designed to address conflicting clinical data that described HPAH patients with NMD+ and NMD- *BMPR2* mutations [104,106]. One study found a link in a PAH patient cohort between mutant *BMPR2* NMD status and severity of disease [104], but the other did not find a connection [106]. We used *in vivo* and *in vitro* techniques to examine this controversy and evaluate the biology of *Bmpr2* mutation type in experimental models of disease. We identified key physiological and pulmonary vascular structure differences between *Bmpr2* NMD+ and NMD- mutations. We continued the characterization of the *Bmpr2* NMD- mutant using biochemical techniques and identified trafficking and signaling defects. Finally, we began to address the limitations of current HPAH patient-derived cells by generating HPAH-patient iPS cell lines expressing *BMPR2* NMD+ and NMD- mutations. This chapter will focus on the major conclusions of this dissertation, indicate likely avenues of future investigation, and place the key findings of this work in context with the current knowledge of HPAH and BMPR2 receptor biology.

The effect of NMD status in Bmpr2 mutants *in vivo* and *in vitro*

Chapter II describes studies using 3 models of experimental PH: chronic hypoxia, serotonin infusion + chronic hypoxia, and VEGFR2 inhibitor SU5416 + chronic hypoxia [96,98,99,110] to evaluate the impact of *Bmpr2* mutation type in severity of disease. We found

that NMD- *Bmpr2* mutant mice, *Bmpr2*$^{\Delta Ex2/+}$, have basal signaling defects in phospho-eNOS in whole lungs, and in the SU5416 + chronic hypoxia model of PH have increased RVSP and number of vascular lesions.

The reduction in phospho-eNOS we observed in untreated *Bmpr2*$^{\Delta Ex2/+}$ mice warrants further investigation. An increase in eNOS expression and activity generates the production of NO and under normal conditions a vasodilatory response [160]. This leads to the question of do these mice have vasocontractility defects basally? Phospho-eNOS is increased at 1 week, but decreased (although not significantly) again at 3 weeks. The *Bmpr2*$^{\Delta Ex2/+}$ mice had reduced expression of eNOS at 5 weeks in a chronic hypoxia model of PH [99], so it is possible that instead of global down-regulation of phospho-eNOS, we are observing mis-regulation of eNOS or a feedback loop that regulates eNOS. For example, it has been shown previously that Bmpr2 and Caveolin-1 interact [161], and we have shown that the Bmpr2ΔEx2 mutant product is mis-localized to the ER. We hypothesized that sequestration of Bmpr2ΔEx2 to the ER could alter the regulation and localization of other proteins including Caveolin-1 In fact, we have observed that Caveolin-1 is mis-localized from the plasma membrane in *Bmpr2*$^{\Delta Ex2/+}$ PECs (unpublished data). This could be one mechanism for the mis-regulation of eNOS in these cells because eNOS directly interacts with Caveolin-1, and is dependent on Caveolin-1 for proper regulation and localization [162-164].

The decrease in phospho-eNOS could contribute to the increased RVSP we observed in the SU5416 + chronic hypoxia model. We have shown previously that *Bmpr2*$^{\Delta Ex2/+}$ mice have reduced eNOS expression in a PH model of 5 weeks of chronic hypoxia [99], and have endothelial-cell dependent vasodilatory defects in intra-pulmonary arteries isolated from mice

[99]. PECs isolated from these mice also have decreased Bmp2-stimulated induction of eNOS activity compared to WT cells [80]. Therefore, future studies should characterize contractility responses in the *Bmpr2*$^{\Delta Ex2/+}$ mice treated with and without SU5416 and hypoxia. We should also determine if phospho-eNOS is significantly reduced at 5 weeks in the SU5416 + hypoxia model - this could indicate that the increased levels of phospho-eNOS at 1 week were transient and likely an emergency response of the endothelium to regulate vascular tone. Myography studies in intra-pulmonary arteries from *Bmpr2*$^{\Delta Ex2/+}$ mice would be useful 1) to determine if the mutant mice have basal contractility defects and 2) because it could be used to determine if the SU5416 +hypoxia model caused similar contractility defects to those observed in the chronic hypoxia model. Additionally, inhaled NO could be introduced to catheterized mice and changes to RVSP monitored. This approach would provide real-time data to contractility responses in mice [165].

In addition to eNOS regulation in the *Bmpr2*$^{\Delta Ex2/+}$ mice and in the SU5416+ hypoxia model, we also need to further characterize the vascular lesions we observed in this model. One of the strengths of the SU5416 + hypoxia model is that it recapitulates as best as currently possible the vascular lesions that are characteristic of severe cases of PAH. One of our key findings was the increase in number of lesions in the *Bmpr2*$^{\Delta Ex2/+}$ mice in the SU5416 + hypoxia model. Our next step should be to characterize the cell types that make up the lesions in observed in SU5416 + hypoxia treated WT, *Bmpr2+/-,* and *Bmpr2*$^{\Delta Ex2/+}$ mice. In addition to vWF and α-SMA immunofluorescence to characterize if the lesions are made up of EC and SMC, respectively, we should also evaluate the expression of markers for macrophages (CD68), T-cells (CD3), and pan-leukocytes (CD45). Once the cell types making up the lesions have been

classified, it will be of interest to determine if the *Bmpr2* mutant and WT mice have the same types of lesions.

In Chapter III we further characterized the *Bmpr2* NMD- mutant *in vitro*, providing the first evidence of the endogenous expression of the predicted NMD- *BMPR2* mutant protein product in two HPAH-relevant cell lines: lymphocytes derived from HPAH patients [47,122-124], and mouse primary pulmonary arterial endothelial cells [51,78,81,91,97,100,166]. We show that the mutant has trafficking and signaling defects that can be partially restored with chemical chaperone 4-PBA treatment.

The next step in this project would be to characterize the effect of 4-PBA treatment on WT, *Bmpr2+/-,* and $Bmpr2^{\Delta Ex2/+}$ mice in the SU5416 + hypoxia model of PH. 4-PBA has already been used *in vivo* in other experimental models of disease [128,132,133,167,168]. For our studies, we would evaluate if *in vivo* treatment of 4-PBA, and if the restoration of the mutant receptor to the cell surface, has any ameliorating effect on susceptibility to PH. If there is an effect in susceptibility, measured by RVSP, it may be challenging, but necessary to show that this is definitively caused by restoration of receptor trafficking to the cell surface. 4-PBA, in addition to being a chemical chaperone, is also an HDAC inhibitor, which is why it is important to validate that any changes to susceptibility in vivo were due to its function as a chemical chaperone and not an HDAC (which can be evaluated by histone acetylation) [169,170]. Dosage regimes and timing would need to be optimized. Phospho-Smad1/5/8 could be used as an assessment of the restoration of receptor signaling function with chemical chaperone treatment *in vivo*, however based on our studies in chapter 2, this would need to be assessed after 1 week of SU5416+Hypoxia, which was the only time-point where phospho-Smad1/5/8 was significantly reduced.

In addition to *in vivo* studies of chemical chaperone treatment on mutant receptor function, it would also be of interest to identify and validate *in vitro* interacting partners of the Bmpr2ΔEx2 mutant product. It has been shown that certain NMD- mutants may lead to increased severity of disease by acting as dominant-negative proteins [116]; this was, however, using FLAG-tagged proteins in an artificial expression system. If possible, it would be more impactful and biologically relevant to identify endogenous protein interactions with the mutant *Bmpr2* receptor. Unfortunately, these studies are limited because of the quality of antibodies. A likely interaction of the mutant receptor would be with the Type I Bmp receptors. However, these studies are hampered by the lack of a suitable Type I receptor antibody to use in immunoprecipitation-type studies. Still, there are other protein interactions that could be assessed. We have already observed the mislocalization of Caveolin-1 in these cells. This mislocalization of Caveolin-1 could be due to dominant negative effects of the Bmpr2ΔEx2 receptor. Bmpr2 can also form homodimers, which if this occurred in the ER with the mutant receptor, would restrict the availability of the WT receptor at the cell surface-altering Bmpr receptor complex formation and modulating downstream signaling function[60,61].

Another future direction of research is the characterization of protein turnover in the Bmpr2ΔEx2 receptor, specifically caused by activation of the ER associated degradation pathway (reviewed in [171-173]). Preliminary data from ciECs show that when cells are treated with BMP2, the expression of the WT receptor is decreased, indicating that the receptor is likely internalized and degraded. In contrast, in *Bmpr2*$^{\Delta Ex2+/-}$ ciECs stimulated with BMP2, the mutant ΔEx2 receptor is maintained at high levels while the WT receptor is decreased. The mutant Bmpr2 may have decreased turnover due to the ΔEx2 mutation. *Exon2* contains 3 cysteine residues important for disulfide bond formation and proper protein folding in the ER [135]. The

missing cysteine residues led us to hypothesize that the *Bmpr2* mutant product was likely unstable, misfolded, and mislocalized. In addition to the cysteine residues, *Exon2* also contains an asparagine residue in a potential N-linked glycosylation motif [174]. The identification of the missing asparagine residue as crucial for proper processing of the Bmpr2 protein in the ER would be a novel finding. Because of the ΔEx2 mutation, it is possible that the missing asparagine residue prevents proper glycosylation in the ER, and possibly prevents proper recognition by the ER quality control machinery [126,136]. If the mutant product is not recognized, or not efficiently recognized by the ERAD machinery, it would result in the buildup of Bmpr2 mutant protein in the ER [175]. That said, there is likely some turnover of the mutant protein because it is not expressed in massive amounts. To assess this properly, rate of protein synthesis should also be determined, but this represents a novel area of research that would link to oxidative stress generation in the ER, ER stress, and UPR responses. Initial assessment did not detect activation of ER stress, but more stringent characterization could yield different results.

Generation and preliminary validation of HPAH patient-derived IPS cells

In Chapter IV, we begin to address the limitations of current HPAH patient-derived cells. Currently available HPAH patient cells are usually from end-stage disease, are likely altered because of the various patient treatment regimes, and are not the cell type of interest. For example, they are patient fibroblasts or lymphocytes instead of pulmonary vascular endothelial cells or smooth muscle cells. We attempt to address the lack of endothelial or smooth muscle HPAH patient cells in chapter IV by generating and beginning validation of HPAH-patient iPS cell lines expressing *BMPR2* NMD+ and NMD- mutations.

To be able to use the generated iPS cells experimentally, a number of validation assays must first be completed. To do this, we need to first use PCR to confirm that the plasmids used to generate the cell lines did not genomically integrate into the iPS lines. While iPS lines with integrated plasmids can be used experimentally, they increase the risk of tumor formation in mice and absolutely could not be reintroduced into patients because the expression of reprogramming factors used to derive the iPS cells would be uncontrolled, driven by a constitutively active promoter [144]. Additionally, integration of plasmids driving the expression of reprogramming factors will likely affect the ability of an iPSC line to undergo differentiation. We would then need to perform RT-PCR analysis of pluripotent markers using human embryonic stem cells as a positive control to confirm expression levels were similar. Additionally, DNA methylation status of the *NANOG* promoter region in the patient fibroblasts, iPS lines, and human stem cell lines would be needed to show that the iPS cells were more like stem cells and less like the patient fibroblasts from which they were derived. Next, the iPS lines would need to be karyotyped to assure there are no gross chromosomal abnormalities from the change from fibroblasts to iPS cells. And finally, the iPS cell lines would need to be evaluated for the formation of all three germ layers, assessed either by embryoid body formation *in vitro* or teratoma formation in mice [142,144]

Once the iPSC are validated, the ultimate goal is to generate highly efficient and directed differentiation protocols to pulmonary vascular cell types. At the time, we were limited by the number of established protocols to generate endothelial cells [147,148]. Therefore, we began our differentiation studies with the most basic protocol with the intention of advancing from there. Because of time and financial constraints, further optimization never occurred. Now, however, there are more practical and efficient vascular endothelial differentiation protocols [155,156].

One important caveat is that although there are protocols available for vascular endothelial cells, vascular endothelial cells are not the same cell type as pulmonary vascular endothelial cells, or even pulmonary microvascular endothelial cells [82]. We and others have already shown that Bmpr2-mediated signaling effects are cell-type specific [51,80,176], so it will be important to establish exactly what type of endothelial cell you are differentiating your HPAH-derived iPSCs. Once efficient endothelial cell differentiation has been achieved, other vascular cell types should be investigated, specifically pulmonary vascular smooth muscle cells.

The generation of HPAH patient-derived iPSCs began as a side project. We quickly realized that the generation of iPSCs was in fact a main project with both demands on time and expense. Because of this, we froze our iPSCs once they were generated, but before they were completely validated. Instead we turned our attention to an alternate source of HPAH patient cells- endothelial progenitor cells (EPCs), reviewed in [177-180]. These cells can be easily isolated from patient blood, and exhibit characteristic expression patterns and signaling function to endothelial cells. In fact, late outgrowth EPCs display most characteristics of endothelial cells, so may be the more biologically relevant, easily accessible EPC population for our studies [179]. Studies are underway in our lab to determine signaling capabilities in these cells, and to evaluate the effects of NMD+ and NMD- *BMPR2* mutations on those pathways.

In conclusion, the studies reported in this dissertation examine the role of *BMPR2* mutation type in HPAH. Over 70% of HPAH patients have a mutation in *BMPR2,* and with over 200 different mutations identified throughout the reading frame of the gene [45,47], it is challenging to determine the definitive role of *BMPR2* mutation in disease pathogenesis. In fact, it is likely that mutations located in different regions of the gene result in different disease phenotypes. A mutation that is expressed (NMD-) could behave as a dominant negative, with

evidence supporting this in over-expression systems [79,116], or mutations could be recognized by RNA surveillance machinery and degraded (NMD+) and result in a haploinsufficient effect [125]. It is also likely that mutants of the NMD- type do not contribute the same way to disease. For example a cysteine point mutation in the ligand binding domain is mis-trafficked, leading to signaling defects [103,116]. Conversely, a mutation in the cytoplasmic tail domain of Bmpr2 would likely result in disrupting protein interactions but not alter the Smad pathway [103,181]. Taken together, the studies reported in this dissertation provide key information on biological principles underlying clinical data, basic Bmpr2 receptor and mutant receptor biology, offer proof of principle for a potential therapeutic for certain types of Bmpr2 mutation, and begin to generate HPAH patient iPS cell lines to address the lack of available HPAH cell lines that are biologically relevant to disease pathogenesis.

REFERENCES

1. Rosenzweig EB, Morse JH, Knowles JA, Chada KK, Khan AM, et al. (2008) Clinical implications of determining BMPR2 mutation status in a large cohort of children and adults with pulmonary arterial hypertension. J Heart Lung Transplant 27: 668-674.

2. Elliott CG, Glissmeyer EW, Havlena GT, Carlquist J, McKinney JT, et al. (2006) Relationship of BMPR2 mutations to vasoreactivity in pulmonary arterial hypertension. Circulation 113: 2509-2515.

3. Galie N, Hoeper MM, Humbert M, Torbicki A, Vachiery JL, et al. (2009) Guidelines for the diagnosis and treatment of pulmonary hypertension. Eur Respir J 34: 1219-1263.

4. Kovacs G, Berghold A, Scheidl S, Olschewski H (2009) Pulmonary arterial pressure during rest and exercise in healthy subjects: a systematic review. Eur Respir J 34: 888-894.

5. Whyte K, Hoette S, Herve P, Montani D, Jais X, et al. (2012) The association between resting and mild-to-moderate exercise pulmonary artery pressure. Eur Respir J 39: 313-318.

6. Simonneau G, Robbins IM, Beghetti M, Channick RN, Delcroix M, et al. (2009) Updated clinical classification of pulmonary hypertension. J Am Coll Cardiol 54: S43-54.

7. Hatano S ST (1975) Primary pulmonary hypertension. Report on a WHO meeting.

8. Brenot F, Herve P, Petitpretz P, Parent F, Duroux P, et al. (1993) Primary pulmonary hypertension and fenfluramine use. Br Heart J 70: 537-541.

9. Abenhaim L, Moride Y, Brenot F, Rich S, Benichou J, et al. (1996) Appetite-suppressant drugs and the risk of primary pulmonary hypertension. International Primary Pulmonary Hypertension Study Group. N Engl J Med 335: 609-616.

10. Hachulla E, Gressin V, Guillevin L, Carpentier P, Diot E, et al. (2005) Early detection of pulmonary arterial hypertension in systemic sclerosis: a French nationwide prospective multicenter study. Arthritis Rheum 52: 3792-3800.

11. Tanaka E, Harigai M, Tanaka M, Kawaguchi Y, Hara M, et al. (2002) Pulmonary hypertension in systemic lupus erythematosus: evaluation of clinical characteristics and response to immunosuppressive treatment. J Rheumatol 29: 282-287.

12. Degano B, Guillaume M, Savale L, Montani D, Jais X, et al. (2010) HIV-associated pulmonary arterial hypertension: survival and prognostic factors in the modern therapeutic era. AIDS 24: 67-75.

13. Rodriguez-Roisin R, Krowka MJ, Herve P, Fallon MB (2004) Pulmonary-Hepatic vascular Disorders (PHD). Eur Respir J 24: 861-880.

14. Teixeira-Mendonca C, Henriques-Coelho T (2013) Pathophysiology of pulmonary hypertension in newborns: Therapeutic indications. Rev Port Cardiol.

15. Montani D, Achouh L, Dorfmuller P, Le Pavec J, Sztrymf B, et al. (2008) Pulmonary veno-occlusive disease: clinical, functional, radiologic, and hemodynamic characteristics and outcome of 24 cases confirmed by histology. Medicine (Baltimore) 87: 220-233.

16. Gaine SP, Rubin LJ (1998) Primary pulmonary hypertension. Lancet 352: 719-725.

17. Sztrymf B, Coulet F, Girerd B, Yaici A, Jais X, et al. (2008) Clinical outcomes of pulmonary arterial hypertension in carriers of BMPR2 mutation. Am J Respir Crit Care Med 177: 1377-1383.

18. Girerd B, Montani D, Coulet F, Sztrymf B, Yaici A, et al. (2010) Clinical outcomes of pulmonary arterial hypertension in patients carrying an ACVRL1 (ALK1) mutation. Am J Respir Crit Care Med 181: 851-861.

19. Austin ED, Ma L, LeDuc C, Berman Rosenzweig E, Borczuk A, et al. (2012) Whole exome sequencing to identify a novel gene (caveolin-1) associated with human pulmonary arterial hypertension. Circ Cardiovasc Genet 5: 336-343.

20. Deng Z, Morse JH, Slager SL, Cuervo N, Moore KJ, et al. (2000) Familial primary pulmonary hypertension (gene PPH1) is caused by mutations in the bone morphogenetic protein receptor-II gene. Am J Hum Genet 67: 737-744.

21. Frost AE, Badesch DB, Barst RJ, Benza RL, Elliott CG, et al. (2011) The changing picture of patients with pulmonary arterial hypertension in the United States: how REVEAL differs from historic and non-US Contemporary Registries. Chest 139: 128-137.

22. Oudiz RJ (2007) Pulmonary hypertension associated with left-sided heart disease. Clin Chest Med 28: 233-241, x.

23. Cottin V, Nunes H, Brillet PY, Delaval P, Devouassoux G, et al. (2005) Combined pulmonary fibrosis and emphysema: a distinct underrecognised entity. Eur Respir J 26: 586-593.

24. Chaouat A, Bugnet AS, Kadaoui N, Schott R, Enache I, et al. (2005) Severe pulmonary hypertension and chronic obstructive pulmonary disease. Am J Respir Crit Care Med 172: 189-194.

25. Pengo V, Lensing AW, Prins MH, Marchiori A, Davidson BL, et al. (2004) Incidence of chronic thromboembolic pulmonary hypertension after pulmonary embolism. N Engl J Med 350: 2257-2264.

26. Nunes H, Humbert M, Capron F, Brauner M, Sitbon O, et al. (2006) Pulmonary hypertension associated with sarcoidosis: mechanisms, haemodynamics and prognosis. Thorax 61: 68-74.

27. Loyd JE, Tillman BF, Atkinson JB, Des Prez RM (1988) Mediastinal fibrosis complicating histoplasmosis. Medicine (Baltimore) 67: 295-310.

28. Yigla M, Nakhoul F, Sabag A, Tov N, Gorevich B, et al. (2003) Pulmonary hypertension in patients with end-stage renal disease. Chest 123: 1577-1582.

29. Li JH, Safford RE, Aduen JF, Heckman MG, Crook JE, et al. (2007) Pulmonary hypertension and thyroid disease. Chest 132: 793-797.

30. Hamaoka K, Nakagawa M, Furukawa N, Sawada T (1990) Pulmonary hypertension in type I glycogen storage disease. Pediatr Cardiol 11: 54-56.

31. Austin ED, Loyd JE, Phillips JA, 3rd (2009) Genetics of pulmonary arterial hypertension. Semin Respir Crit Care Med 30: 386-398.

32. Farber HW, Loscalzo J (2004) Pulmonary arterial hypertension. N Engl J Med 351: 1655-1665.

33. Abe K, Toba M, Alzoubi A, Ito M, Fagan KA, et al. (2010) Formation of plexiform lesions in experimental severe pulmonary arterial hypertension. Circulation 121: 2747-2754.

34. Jonigk D, Golpon H, Bockmeyer CL, Maegel L, Hoeper MM, et al. (2011) Plexiform lesions in pulmonary arterial hypertension composition, architecture, and microenvironment. Am J Pathol 179: 167-179.

35. Humbert M, Sitbon O, Chaouat A, Bertocchi M, Habib G, et al. (2006) Pulmonary arterial hypertension in France: results from a national registry. Am J Respir Crit Care Med 173: 1023-1030.

36. Thenappan T, Shah SJ, Rich S, Tian L, Archer SL, et al. (2010) Survival in pulmonary arterial hypertension: a reappraisal of the NIH risk stratification equation. Eur Respir J 35: 1079-1087.

37. Gomberg-Maitland M, Olschewski H (2008) Prostacyclin therapies for the treatment of pulmonary arterial hypertension. Eur Respir J 31: 891-901.

38. Sitbon O, Humbert M, Jais X, Ioos V, Hamid AM, et al. (2005) Long-term response to calcium channel blockers in idiopathic pulmonary arterial hypertension. Circulation 111: 3105-3111.

39. Tilton RG, Munsch CL, Sherwood SJ, Chen SJ, Chen YF, et al. (2000) Attenuation of pulmonary vascular hypertension and cardiac hypertrophy with sitaxsentan sodium, an orally active ET(A) receptor antagonist. Pulm Pharmacol Ther 13: 87-97.

40. Zeng WJ, Sun YJ, Gu Q, Xiong CM, Li JJ, et al. (2012) Impact of sildenafil on survival of patients with idiopathic pulmonary arterial hypertension. J Clin Pharmacol 52: 1357-1364.

41. Sitbon O, McLaughlin VV, Badesch DB, Barst RJ, Black C, et al. (2005) Survival in patients with class III idiopathic pulmonary arterial hypertension treated with first line oral bosentan compared with an historical cohort of patients started on intravenous epoprostenol. Thorax 60: 1025-1030.

42. Lane KB, Machado RD, Pauciulo MW, Thomson JR, Phillips JA, 3rd, et al. (2000) Heterozygous germline mutations in BMPR2, encoding a TGF-beta receptor, cause familial primary pulmonary hypertension. Nat Genet 26: 81-84.

43. Machado RD, Pauciulo MW, Thomson JR, Lane KB, Morgan NV, et al. (2001) BMPR2 haploinsufficiency as the inherited molecular mechanism for primary pulmonary hypertension. Am J Hum Genet 68: 92-102.

44. Atkinson C, Stewart S, Upton PD, Machado R, Thomson JR, et al. (2002) Primary pulmonary hypertension is associated with reduced pulmonary vascular expression of type II bone morphogenetic protein receptor. Circulation 105: 1672-1678.

45. Machado RD, Aldred MA, James V, Harrison RE, Patel B, et al. (2006) Mutations of the TGF-beta type II receptor BMPR2 in pulmonary arterial hypertension. Hum Mutat 27: 121-132.

46. Cogan JD, Pauciulo MW, Batchman AP, Prince MA, Robbins IM, et al. (2006) High frequency of BMPR2 exonic deletions/duplications in familial pulmonary arterial hypertension. Am J Respir Crit Care Med 174: 590-598.

47. Cogan JD, Vnencak-Jones CL, Phillips JA, 3rd, Lane KB, Wheeler LA, et al. (2005) Gross BMPR2 gene rearrangements constitute a new cause for primary pulmonary hypertension. Genet Med 7: 169-174.

48. De Caestecker M, Meyrick B (2001) Bone morphogenetic proteins, genetics and the pathophysiology of primary pulmonary hypertension. Respir Res 2: 193-197.

49. Shi Y, Massague J (2003) Mechanisms of TGF-beta signaling from cell membrane to the nucleus. Cell 113: 685-700.

50. Miyazono K, Kamiya Y, Morikawa M (2010) Bone morphogenetic protein receptors and signal transduction. J Biochem 147: 35-51.

51. Lowery JW, de Caestecker MP (2010) BMP signaling in vascular development and disease. Cytokine Growth Factor Rev 21: 287-298.

52. Urist MR, Strates BS (1971) Bone morphogenetic protein. J Dent Res 50: 1392-1406.

53. Affolter M, Basler K (2007) The Decapentaplegic morphogen gradient: from pattern formation to growth regulation. Nat Rev Genet 8: 663-674.

54. De Robertis EM, Kuroda H (2004) DORSAL-VENTRAL PATTERNING AND NEURAL INDUCTION IN XENOPUS EMBRYOS. Annual Review of Cell and Developmental Biology 20: 285-308.

55. Moustakas A, Heldin CH (2009) The regulation of TGFbeta signal transduction. Development 136: 3699-3714.

56. Kishigami S, Mishina Y (2005) BMP signaling and early embryonic patterning. Cytokine Growth Factor Rev 16: 265-278.

57. Wrana JL, Attisano L, Wieser R, Ventura F, Massague J (1994) Mechanism of activation of the TGF-beta receptor. Nature 370: 341-347.

58. Poorgholi Belverdi M, Krause C, Guzman A, Knaus P (2012) Comprehensive analysis of TGF-beta and BMP receptor interactomes. Eur J Cell Biol 91: 287-293.

59. Rosenzweig BL, Imamura T, Okadome T, Cox GN, Yamashita H, et al. (1995) Cloning and characterization of a human type II receptor for bone morphogenetic proteins. Proc Natl Acad Sci U S A 92: 7632-7636.

60. Ehrlich M, Horbelt D, Marom B, Knaus P, Henis YI (2011) Homomeric and heteromeric complexes among TGF-beta and BMP receptors and their roles in signaling. Cell Signal 23: 1424-1432.

61. Ehrlich M, Gutman O, Knaus P, Henis YI (2012) Oligomeric interactions of TGF-beta and BMP receptors. FEBS Lett 586: 1885-1896.

62. Zhang YE (2009) Non-Smad pathways in TGF-beta signaling. Cell Res 19: 128-139.

63. Yamaji N, Celeste AJ, Thies RS, Song JJ, Bernier SM, et al. (1994) A mammalian serine/threonine kinase receptor specifically binds BMP-2 and BMP-4. Biochem Biophys Res Commun 205: 1944-1951.

64. Koenig BB, Cook JS, Wolsing DH, Ting J, Tiesman JP, et al. (1994) Characterization and cloning of a receptor for BMP-2 and BMP-4 from NIH 3T3 cells. Mol Cell Biol 14: 5961-5974.

65. ten Dijke P, Yamashita H, Sampath TK, Reddi AH, Estevez M, et al. (1994) Identification of type I receptors for osteogenic protein-1 and bone morphogenetic protein-4. J Biol Chem 269: 16985-16988.

66. Ebisawa T, Tada K, Kitajima I, Tojo K, Sampath TK, et al. (1999) Characterization of bone morphogenetic protein-6 signaling pathways in osteoblast differentiation. J Cell Sci 112 (Pt 20): 3519-3527.

67. Macias-Silva M, Hoodless PA, Tang SJ, Buchwald M, Wrana JL (1998) Specific activation of Smad1 signaling pathways by the BMP7 type I receptor, ALK2. J Biol Chem 273: 25628-25636.

68. Brown MA, Zhao Q, Baker KA, Naik C, Chen C, et al. (2005) Crystal structure of BMP-9 and functional interactions with pro-region and receptors. J Biol Chem 280: 25111-25118.

69. David L, Mallet C, Mazerbourg S, Feige JJ, Bailly S (2007) Identification of BMP9 and BMP10 as functional activators of the orphan activin receptor-like kinase 1 (ALK1) in endothelial cells. Blood 109: 1953-1961.

70. Kotzsch A, Nickel J, Seher A, Sebald W, Muller TD (2009) Crystal structure analysis reveals a spring-loaded latch as molecular mechanism for GDF-5-type I receptor specificity. EMBO J 28: 937-947.

71. Erlacher L, McCartney J, Piek E, ten Dijke P, Yanagishita M, et al. (1998) Cartilage-derived morphogenetic proteins and osteogenic protein-1 differentially regulate osteogenesis. J Bone Miner Res 13: 383-392.

72. Vitt UA, Mazerbourg S, Klein C, Hsueh AJ (2002) Bone morphogenetic protein receptor type II is a receptor for growth differentiation factor-9. Biol Reprod 67: 473-480.

73. Moore RK, Otsuka F, Shimasaki S (2003) Molecular basis of bone morphogenetic protein-15 signaling in granulosa cells. J Biol Chem 278: 304-310.

74. Nasim MT, Ogo T, Ahmed M, Randall R, Chowdhury HM, et al. (2011) Molecular genetic characterization of SMAD signaling molecules in pulmonary arterial hypertension. Hum Mutat 32: 1385-1389.

75. Shintani M, Yagi H, Nakayama T, Saji T, Matsuoka R (2009) A new nonsense mutation of SMAD8 associated with pulmonary arterial hypertension. J Med Genet 46: 331-337.

76. McDonald J, Bayrak-Toydemir P, Pyeritz RE (2011) Hereditary hemorrhagic telangiectasia: an overview of diagnosis, management, and pathogenesis. Genet Med 13: 607-616.

77. Gallione CJ, Richards JA, Letteboer TG, Rushlow D, Prigoda NL, et al. (2006) SMAD4 mutations found in unselected HHT patients. J Med Genet 43: 793-797.

78. Burton VJ, Ciuclan LI, Holmes AM, Rodman DM, Walker C, et al. (2011) Bone morphogenetic protein receptor II regulates pulmonary artery endothelial cell barrier function. Blood 117: 333-341.

79. Nishihara A, Watabe T, Imamura T, Miyazono K (2002) Functional Heterogeneity of Bone Morphogenetic Protein Receptor-II Mutants Found in Patients with Primary Pulmonary Hypertension. Molecular Biology of the Cell 13: 3055-3063.

80. Anderson L, Lowery JW, Frank DB, Novitskaya T, Jones M, et al. (2010) Bmp2 and Bmp4 exert opposing effects in hypoxic pulmonary hypertension. Am J Physiol Regul Integr Comp Physiol 298: R833-842.

81. Frank DB, Abtahi A, Yamaguchi DJ, Manning S, Shyr Y, et al. (2005) Bone morphogenetic protein 4 promotes pulmonary vascular remodeling in hypoxic pulmonary hypertension. Circ Res 97: 496-504.

82. Stevens T, Rosenberg R, Aird W, Quertermous T, Johnson FL, et al. (2001) NHLBI workshop report: endothelial cell phenotypes in heart, lung, and blood diseases. Am J Physiol Cell Physiol 281: C1422-1433.

83. deMello DE, Reid LM (2000) Embryonic and early fetal development of human lung vasculature and its functional implications. Pediatr Dev Pathol 3: 439-449.

84. Nishihara A, Watabe T, Imamura T, Miyazono K (2002) Functional heterogeneity of bone morphogenetic protein receptor-II mutants found in patients with primary pulmonary hypertension. Mol Biol Cell 13: 3055-3063.

85. Morrell NW, Yang X, Upton PD, Jourdan KB, Morgan N, et al. (2001) Altered growth responses of pulmonary artery smooth muscle cells from patients with primary

pulmonary hypertension to transforming growth factor-beta(1) and bone morphogenetic proteins. Circulation 104: 790-795.

86. Yang X, Long L, Southwood M, Rudarakanchana N, Upton PD, et al. (2005) Dysfunctional Smad signaling contributes to abnormal smooth muscle cell proliferation in familial pulmonary arterial hypertension. Circ Res 96: 1053-1063.

87. Zhang S, Fantozzi I, Tigno DD, Yi ES, Platoshyn O, et al. (2003) Bone morphogenetic proteins induce apoptosis in human pulmonary vascular smooth muscle cells. Am J Physiol Lung Cell Mol Physiol 285: L740-754.

88. Wagner DO, Sieber C, Bhushan R, Borgermann JH, Graf D, et al. (2010) BMPs: from bone to body morphogenetic proteins. Sci Signal 3: mr1.

89. Ramos M, Lame MW, Segall HJ, Wilson DW (2006) The BMP type II receptor is located in lipid rafts, including caveolae, of pulmonary endothelium in vivo and in vitro. Vascul Pharmacol 44: 50-59.

90. Gangopahyay A, Oran M, Bauer EM, Wertz JW, Comhair SA, et al. (2011) Bone morphogenetic protein receptor II is a novel mediator of endothelial nitric-oxide synthase activation. J Biol Chem 286: 33134-33140.

91. Gangopahyay A, Oran M, Bauer EM, Wertz JW, Comhair SA, et al. (2011) Bone Morphogenetic Protein Receptor II Is a Novel Mediator of Endothelial Nitric-oxide Synthase Activation. Journal of Biological Chemistry 286: 33134-33140.

92. Alastalo TP, Li M, Perez Vde J, Pham D, Sawada H, et al. (2011) Disruption of PPARgamma/beta-catenin-mediated regulation of apelin impairs BMP-induced mouse and human pulmonary arterial EC survival. J Clin Invest 121: 3735-3746.

93. Dorai H, Vukicevic S, Sampath TK (2000) Bone morphogenetic protein-7 (osteogenic protein-1) inhibits smooth muscle cell proliferation and stimulates the expression of markers that are characteristic of SMC phenotype in vitro. J Cell Physiol 184: 37-45.

94. Nakaoka T, Gonda K, Ogita T, Otawara-Hamamoto Y, Okabe F, et al. (1997) Inhibition of rat vascular smooth muscle proliferation in vitro and in vivo by bone morphogenetic protein-2. J Clin Invest 100: 2824-2832.

95. Dewachter L, Adnot S, Guignabert C, Tu L, Marcos E, et al. (2009) Bone morphogenetic protein signalling in heritable versus idiopathic pulmonary hypertension. Eur Respir J 34: 1100-1110.

96. Beppu H, Ichinose F, Kawai N, Jones RC, Yu PB, et al. (2004) BMPR-II heterozygous mice have mild pulmonary hypertension and an impaired pulmonary vascular remodeling response to prolonged hypoxia. Am J Physiol Lung Cell Mol Physiol 287: L1241-1247.

97. Song Y, Coleman L, Shi J, Beppu H, Sato K, et al. (2008) Inflammation, endothelial injury, and persistent pulmonary hypertension in heterozygous BMPR2-mutant mice. Am J Physiol Heart Circ Physiol 295: H677-690.

98. Long L, MacLean MR, Jeffery TK, Morecroft I, Yang X, et al. (2006) Serotonin increases susceptibility to pulmonary hypertension in BMPR2-deficient mice. Circ Res 98: 818-827.

99. Frank DB, Lowery J, Anderson L, Brink M, Reese J, et al. (2008) Increased susceptibility to hypoxic pulmonary hypertension in Bmpr2 mutant mice is associated with endothelial dysfunction in the pulmonary vasculature. Am J Physiol Lung Cell Mol Physiol 294: L98-109.

100. Hong KH, Lee YJ, Lee E, Park SO, Han C, et al. (2008) Genetic ablation of the BMPR2 gene in pulmonary endothelium is sufficient to predispose to pulmonary arterial hypertension. Circulation 118: 722-730.

101. West J, Fagan K, Steudel W, Fouty B, Lane K, et al. (2004) Pulmonary hypertension in transgenic mice expressing a dominant-negative BMPRII gene in smooth muscle. Circ Res 94: 1109-1114.

102. Sztrymf B, Yaici A, Girerd B, Humbert M (2007) Genes and pulmonary arterial hypertension. Respiration 74: 123-132.

103. Waite KA, Eng C (2003) From developmental disorder to heritable cancer: it's all in the BMP/TGF-beta family. Nat Rev Genet 4: 763-773.

104. Austin ED, Phillips JA, Cogan JD, Hamid R, Yu C, et al. (2009) Truncating and missense BMPR2 mutations differentially affect the severity of heritable pulmonary arterial hypertension. Respir Res 10: 87.

105. Muhlemann O, Eberle AB, Stalder L, Zamudio Orozco R (2008) Recognition and elimination of nonsense mRNA. Biochim Biophys Acta 1779: 538-549.

106. Girerd B, Montani D, Eyries M, Yaici A, Sztrymf B, et al. (2010) Absence of influence of gender and BMPR2 mutation type on clinical phenotypes of pulmonary arterial hypertension. Respir Res 11: 73.

107. Beppu H, Kawabata M, Hamamoto T, Chytil A, Minowa O, et al. (2000) BMP Type II Receptor Is Required for Gastrulation and Early Development of Mouse Embryos. Developmental Biology 221: 249-258.

108. Delot EC, Bahamonde ME, Zhao M, Lyons KM (2003) BMP signaling is required for septation of the outflow tract of the mammalian heart. Development 130: 209-220.

109. Sakao S, Taraseviciene-Stewart L, Lee JD, Wood K, Cool CD, et al. (2005) Initial apoptosis is followed by increased proliferation of apoptosis-resistant endothelial cells. FASEB J 19: 1178-1180.

110. Ciuclan L, Bonneau O, Hussey M, Duggan N, Holmes AM, et al. (2011) A Novel Murine Model of Severe Pulmonary Arterial Hypertension. American Journal of Respiratory and Critical Care Medicine 184: 1171-1182.

111. Taraseviciene-Stewart L, Kasahara Y, Alger L, Hirth P, Mc Mahon G, et al. (2001) Inhibition of the VEGF receptor 2 combined with chronic hypoxia causes cell death-dependent pulmonary endothelial cell proliferation and severe pulmonary hypertension. FASEB J 15: 427-438.

112. Austin ED, Lahm T, West J, Tofovic SP, Johansen AK, et al. (2013) Gender, sex hormones and pulmonary hypertension. Pulm Circ 3: 294-314.

113. Kolb TM, Hassoun PM (2012) Right ventricular dysfunction in chronic lung disease. Cardiol Clin 30: 243-256.

114. Lowery JW, Frump AL, Anderson L, DiCarlo GE, Jones MT, et al. (2010) ID family protein expression and regulation in hypoxic pulmonary hypertension. Am J Physiol Regul Integr Comp Physiol 299: R1463-1477.

115. Frump AL, Lowery JW, Hamid R, Austin ED, de Caestecker M (2013) Abnormal trafficking of endogenously expressed BMPR2 mutant allelic products in patients with heritable pulmonary arterial hypertension. PLoS One 8: e80319.

116. Sobolewski A, Rudarakanchana N, Upton PD, Yang J, Crilley TK, et al. (2008) Failure of bone morphogenetic protein receptor trafficking in pulmonary arterial hypertension: potential for rescue. Hum Mol Genet 17: 3180-3190.

117. Flynn C, Zheng S, Yan L, Hedges L, Womack B, et al. (2012) Connectivity map analysis of nonsense-mediated decay-positive BMPR2-related hereditary pulmonary arterial hypertension provides insights into disease penetrance. Am J Respir Cell Mol Biol 47: 20-27.

118. Rudarakanchana N, Flanagan JA, Chen H, Upton PD, Machado R, et al. (2002) Functional analysis of bone morphogenetic protein type II receptor mutations underlying primary pulmonary hypertension. Hum Mol Genet 11: 1517-1525.

119. Pruliere-Escabasse V, Planes C, Escudier E, Fanen P, Coste A, et al. (2007) Modulation of epithelial sodium channel trafficking and function by sodium 4-phenylbutyrate in human nasal epithelial cells. J Biol Chem 282: 34048-34057.

120. Lim M, McKenzie K, Floyd AD, Kwon E, Zeitlin PL (2004) Modulation of deltaF508 cystic fibrosis transmembrane regulator trafficking and function with 4-phenylbutyrate and flavonoids. Am J Respir Cell Mol Biol 31: 351-357.

121. Whitehead RH, VanEeden PE, Noble MD, Ataliotis P, Jat PS (1993) Establishment of conditionally immortalized epithelial cell lines from both colon and small intestine of adult H-2Kb-tsA58 transgenic mice. Proc Natl Acad Sci U S A 90: 587-591.

122. Hamid R, Hedges LK, Austin E, Phillips JA, 3rd, Loyd JE, et al. (2010) Transcripts from a novel BMPR2 termination mutation escape nonsense mediated decay by downstream translation re-initiation: implications for treating pulmonary hypertension. Clin Genet 77: 280-286.

123. West J, Cogan J, Geraci M, Robinson L, Newman J, et al. (2008) Gene expression in BMPR2 mutation carriers with and without evidence of pulmonary arterial hypertension suggests pathways relevant to disease penetrance. BMC Med Genomics 1: 45.

124. Austin ED, Menon S, Hemnes AR, Robinson LR, Talati M, et al. (2011) Idiopathic and heritable PAH perturb common molecular pathways, correlated with increased MSX1 expression. Pulm Circ 1: 389-398.

125. Hamid R, Cogan JD, Hedges LK, Austin E, Phillips JA, 3rd, et al. (2009) Penetrance of pulmonary arterial hypertension is modulated by the expression of normal BMPR2 allele. Hum Mutat 30: 649-654.

126. Freeze HH, Kranz C (2008) Endoglycosidase and glycoamidase release of N-linked glycans. Curr Protoc Immunol Chapter 8: Unit 8 15.

127. Lodish HF (1988) Transport of secretory and membrane glycoproteins from the rough endoplasmic reticulum to the Golgi. A rate-limiting step in protein maturation and secretion. J Biol Chem 263: 2107-2110.

128. Sorrenson B, Suetani RJ, Williams MJ, Bickley VM, George PM, et al. (2013) Functional rescue of mutant ABCA1 proteins by sodium 4-phenylbutyrate. J Lipid Res 54: 55-62.

129. Roque T, Boncoeur E, Saint-Criq V, Bonvin E, Clement A, et al. (2008) Proinflammatory effect of sodium 4-phenylbutyrate in deltaF508-cystic fibrosis transmembrane conductance regulator lung epithelial cells: involvement of extracellular signal-regulated protein kinase 1/2 and c-Jun-NH2-terminal kinase signaling. J Pharmacol Exp Ther 326: 949-956.

130. Duricka DL, Brown RL, Varnum MD (2012) Defective trafficking of cone photoreceptor CNG channels induces the unfolded protein response and ER-stress-associated cell death. Biochem J 441: 685-696.

131. Hua Y, Kandadi MR, Zhu M, Ren J, Sreejayan N (2010) Tauroursodeoxycholic acid attenuates lipid accumulation in endoplasmic reticulum-stressed macrophages. J Cardiovasc Pharmacol 55: 49-55.

132. da-Silva WS, Ribich S, Arrojo e Drigo R, Castillo M, Patti ME, et al. (2011) The chemical chaperones tauroursodeoxycholic and 4-phenylbutyric acid accelerate thyroid hormone activation and energy expenditure. FEBS Lett 585: 539-544.

133. Cao SS, Zimmermann EM, Chuang BM, Song B, Nwokoye A, et al. (2013) The unfolded protein response and chemical chaperones reduce protein misfolding and colitis in mice. Gastroenterology 144: 989-1000 e1006.

134. Liu D, Wang J, Kinzel B, Mueller M, Mao X, et al. (2007) Dosage-dependent requirement of BMP type II receptor for maintenance of vascular integrity. Blood 110: 1502-1510.

135. Bulleid NJ (2012) Disulfide bond formation in the mammalian endoplasmic reticulum. Cold Spring Harb Perspect Biol 4.

136. Hebert DN, Garman SC, Molinari M (2005) The glycan code of the endoplasmic reticulum: asparagine-linked carbohydrates as protein maturation and quality-control tags. Trends Cell Biol 15: 364-370.

137. Yin H, Yeh LC, Hinck AP, Lee JC (2008) Characterization of ligand-binding properties of the human BMP type II receptor extracellular domain. J Mol Biol 378: 191-203.

138. Yeh LC, Falcon WE, Garces A, Lee JC, Lee JC (2012) A host-guest relationship in bone morphogenetic protein receptor-II defines specificity in ligand-receptor recognition. Biochemistry 51: 6968-6980.

139. Rubenstein RC, Zeitlin PL (1998) A pilot clinical trial of oral sodium 4-phenylbutyrate (Buphenyl) in deltaF508-homozygous cystic fibrosis patients: partial restoration of nasal epithelial CFTR function. Am J Respir Crit Care Med 157: 484-490.

140. Zeitlin PL, Diener-West M, Rubenstein RC, Boyle MP, Lee CK, et al. (2002) Evidence of CFTR function in cystic fibrosis after systemic administration of 4-phenylbutyrate. Mol Ther 6: 119-126.

141. Obici L, Cortese A, Lozza A, Lucchetti J, Gobbi M, et al. (2012) Doxycycline plus tauroursodeoxycholic acid for transthyretin amyloidosis: a phase II study. Amyloid 19 Suppl 1: 34-36.

142. Takahashi K, Tanabe K, Ohnuki M, Narita M, Ichisaka T, et al. (2007) Induction of pluripotent stem cells from adult human fibroblasts by defined factors. Cell 131: 861-872.

143. Yamanaka S (2009) A fresh look at iPS cells. Cell 137: 13-17.

144. Okita K, Matsumura Y, Sato Y, Okada A, Morizane A, et al. (2011) A more efficient method to generate integration-free human iPS cells. Nat Methods 8: 409-412.

145. Ohnuki M, Takahashi K, Yamanaka S (2009) Generation and characterization of human induced pluripotent stem cells. Curr Protoc Stem Cell Biol Chapter 4: Unit 4A 2.

146. Neely M. D. TAM, Aboud A. A., Ess K. C., and Bowman A. B. ((2011)) Induced Pluripotent Stem Cells (iPSCs): An Emerging Model System for the Study of Human Neurotoxicology, in Cell Culture Techniques Springer, New York: pp 27–62.

147. Taura D, Sone M, Homma K, Oyamada N, Takahashi K, et al. (2009) Induction and isolation of vascular cells from human induced pluripotent stem cells--brief report. Arterioscler Thromb Vasc Biol 29: 1100-1103.

148. Sone M, Itoh H, Yamahara K, Yamashita JK, Yurugi-Kobayashi T, et al. (2007) Pathway for differentiation of human embryonic stem cells to vascular cell components and their potential for vascular regeneration. Arterioscler Thromb Vasc Biol 27: 2127-2134.

149. Yu J, Vodyanik MA, Smuga-Otto K, Antosiewicz-Bourget J, Frane JL, et al. (2007) Induced pluripotent stem cell lines derived from human somatic cells. Science 318: 1917-1920.

150. O'Connor MD, Kardel MD, Iosfina I, Youssef D, Lu M, et al. (2008) Alkaline phosphatase-positive colony formation is a sensitive, specific, and quantitative indicator of undifferentiated human embryonic stem cells. Stem Cells 26: 1109-1116.

151. Lanctot PM, Gage FH, Varki AP (2007) The glycans of stem cells. Curr Opin Chem Biol 11: 373-380.

152. Schopperle WM, DeWolf WC (2007) The TRA-1-60 and TRA-1-81 human pluripotent stem cell markers are expressed on podocalyxin in embryonal carcinoma. Stem Cells 25: 723-730.

153. Radzisheuskaya A, Chia Gle B, dos Santos RL, Theunissen TW, Castro LF, et al. (2013) A defined Oct4 level governs cell state transitions of pluripotency entry and differentiation into all embryonic lineages. Nat Cell Biol 15: 579-590.

154. Teichert-Kuliszewska K, Kutryk MJ, Kuliszewski MA, Karoubi G, Courtman DW, et al. (2006) Bone morphogenetic protein receptor-2 signaling promotes pulmonary arterial endothelial cell survival: implications for loss-of-function mutations in the pathogenesis of pulmonary hypertension. Circ Res 98: 209-217.

155. Rufaihah AJ, Huang NF, Jame S, Lee JC, Nguyen HN, et al. (2011) Endothelial cells derived from human iPSCS increase capillary density and improve perfusion in a mouse model of peripheral arterial disease. Arterioscler Thromb Vasc Biol 31: e72-79.

156. Rufaihah AJ, Huang NF, Kim J, Herold J, Volz KS, et al. (2013) Human induced pluripotent stem cell-derived endothelial cells exhibit functional heterogeneity. Am J Transl Res 5: 21-35.

157. Frid MG, Aldashev AA, Crossno JT, Jorgensen JM, Kale VA, et al. (2004) Yin and Yang of an endothelial cell: from normal to the extreme in growth, secretion, and transdifferentiation capabilities. Paediatr Respir Rev 5 Suppl A: S253-257.

158. Watabe T, Miyazono K (2009) Roles of TGF-beta family signaling in stem cell renewal and differentiation. Cell Res 19: 103-115.

159. Suzuki A, Raya A, Kawakami Y, Morita M, Matsui T, et al. (2006) Nanog binds to Smad1 and blocks bone morphogenetic protein-induced differentiation of embryonic stem cells. Proc Natl Acad Sci U S A 103: 10294-10299.

160. Levine AB, Punihaole D, Levine TB (2012) Characterization of the role of nitric oxide and its clinical applications. Cardiology 122: 55-68.

161. Nohe A, Keating E, Underhill TM, Knaus P, Petersen NO (2005) Dynamics and interaction of caveolin-1 isoforms with BMP-receptors. Journal of Cell Science 118: 643-650.

162. Zhao YY, Malik AB (2009) A novel insight into the mechanism of pulmonary hypertension involving caveolin-1 deficiency and endothelial nitric oxide synthase activation. Trends Cardiovasc Med 19: 238-242.

163. Rath G, Dessy C, Feron O (2009) Caveolae, caveolin and control of vascular tone: nitric oxide (NO) and endothelium derived hyperpolarizing factor (EDHF) regulation. J Physiol Pharmacol 60 Suppl 4: 105-109.

164. Dessy C, Feron O, Balligand JL (2010) The regulation of endothelial nitric oxide synthase by caveolin: a paradigm validated in vivo and shared by the 'endothelium-derived hyperpolarizing factor'. Pflugers Arch 459: 817-827.

165. Totzeck M, Hendgen-Cotta UB, Luedike P, Berenbrink M, Klare JP, et al. (2012) Nitrite Regulates Hypoxic Vasodilation via Myoglobin-Dependent Nitric Oxide Generation. Circulation 126: 325-334.

166. Majka S, Hagen M, Blackwell T, Harral J, Johnson JA, et al. (2011) Physiologic and molecular consequences of endothelial Bmpr2 mutation. Respir Res 12: 84.

167. Kuliawat R, Ramos-Castaneda J, Liu Y, Arvan P (2005) Intracellular trafficking of thyroid peroxidase to the cell surface. J Biol Chem 280: 27713-27718.

168. Liang B, Wang S, Wang Q, Zhang W, Viollet B, et al. (2013) Aberrant endoplasmic reticulum stress in vascular smooth muscle increases vascular contractility and blood pressure in mice deficient of AMP-activated protein kinase-alpha2 in vivo. Arterioscler Thromb Vasc Biol 33: 595-604.

169. Steckert AV, Valvassori SS, Varela RB, Mina F, Resende WR, et al. (2013) Effects of sodium butyrate on oxidative stress and behavioral changes induced by administration of D-AMPH. Neurochem Int 62: 425-432.

170. Resende WR, Valvassori SS, Reus GZ, Varela RB, Arent CO, et al. (2013) Effects of sodium butyrate in animal models of mania and depression: implications as a new mood stabilizer. Behav Pharmacol.

171. Brodsky JL (2012) Cleaning up: ER-associated degradation to the rescue. Cell 151: 1163-1167.

172. Guerriero CJ, Brodsky JL (2012) The delicate balance between secreted protein folding and endoplasmic reticulum-associated degradation in human physiology. Physiol Rev 92: 537-576.

173. Tamura T, Sunryd JC, Hebert DN (2010) Sorting things out through endoplasmic reticulum quality control. Mol Membr Biol 27: 412-427.

174. Helenius A, Aebi M (2001) Intracellular functions of N-linked glycans. Science 291: 2364-2369.

175. Bernon C, Carre Y, Kuokkanen E, Slomianny MC, Mir AM, et al. (2011) Overexpression of Man2C1 leads to protein underglycosylation and upregulation of endoplasmic reticulum-associated degradation pathway. Glycobiology 21: 363-375.

176. Southwood M, Jeffery TK, Yang X, Upton PD, Hall SM, et al. (2008) Regulation of bone morphogenetic protein signalling in human pulmonary vascular development. J Pathol 214: 85-95.

177. Yoder MC (2013) Endothelial progenitor cell: a blood cell by many other names may serve similar functions. J Mol Med (Berl) 91: 285-295.

178. Richardson MR, Yoder MC (2011) Endothelial progenitor cells: quo vadis? J Mol Cell Cardiol 50: 266-272.

179. Toshner M, Morrell NW (2010) Endothelial progenitor cells in pulmonary hypertension - dawn of cell-based therapy? Int J Clin Pract Suppl: 7-12.

180. Yang JX, Pan YY, Zhao YY, Wang XX (2013) Endothelial progenitor cell-based therapy for pulmonary arterial hypertension. Cell Transplant 22: 1325-1336.

181. West J, Harral J, Lane K, Deng Y, Ickes B, et al. (2008) Mice expressing BMPR2R899X transgene in smooth muscle develop pulmonary vascular lesions. Am J Physiol Lung Cell Mol Physiol 295: L744-755.